Design and Modeling of Superconducting Fault Current Limiter for a High Voltage Substation
A Case study: AkAki substation II (400KV to 230KV)

A thesis presented to School of electrical and computer engineering, Addis Ababa Institute of Technology, Addis Ababa University in partial fulfilment of Master of Science in electrical power engineering.

By

Dereje Nigussie

Advisor: Getachew Bekele (Ph.D.)

ADDIS ABABA UNIVERSITY

ADDIS ABABA INSTITUTE OF TECHNOLOGY

School of Electrical and Computer Engineering

October 2017

Submitted by:

Dereje Nigussie (GSR/2256/07)	_____	_____
Student name	**Signature**	**Date**

Approved by:

1. Mr. Amare Assefa (MSc.)	_____	_____
Chairman, Department of Graduate Committee	**Signature**	**Date**
2. Getachew Bekele (Ph.D.)	_____	_____
Advisor name	**Signature**	**Date**
3. Prof. N.P. Singh	_____	_____
Internal Examiner	**Signature**	**Date**
4. Dr. Ing. Getachew Biru	_____	_____
External Examiner	**Signature**	**Date**

Dedication

…to

All people who are academicians

And

...to the following school and universities

AkAki Adventist School, Addis Ababa University (Addis Ababa Institute of Technology) and Mettu University.

Acknowledgment

First of all the author thanks God for all His support in every steps of this thesis research work.

I take this chance to thank my advisor, Dr. Getachew Bekele, for his necessary guidance of this thesis work from the early beginning up to the end, follow up and proof reading during the progress of the work.

At the end of the work, Dr. In. Getachew Biru and Pro. N.P. Singh played a great role for better accomplishment of documentation work.

And, again, he wants to thank K. Alemayew, in-charge person at Gellan substation of EEP, for his excellence support to collect all related data in the substation.

I would like to thank my family and friends for keeping me in the research work and for their help. In particular, I would like to thank W/ro Wednesh Hailu, Ato Nigussie Shawel, Ato G/MikAel G/Meskel.

Abstract

Modern electric power systems are becoming more complex in order to meet high load demand with good quality. So, the increasing amount of on-site generation should be integrated into the power grid. This translates to more sophisticated electric network with intrinsically high short circuit current capacity.

A superconducting fault current limiter (SFCL) is proposed as a solution in order to increase safety margin of circuit breakers (CBs) by reducing the maximum short-circuit current below the breaking capacity of the substation. SFCL is a device with negligible impedance under normal operating conditions that immediately switches to a high impedance state in case of over-current. This advantage makes SFCL a key component in this regard.

At AkAki II substation, 230 kV bus-bar, ***a hybrid-resistive SFCL*** *is designed. The design procedure encompasses collection of the substation data, short-circuit analysis of the substation and designing of all parts of the SFCL. The short-circuit analysis is done using ETAP simulation software. Then, a hybrid-resistive SFCL is designed to have a current-limiting-resistor with* ***143.2 MW*** *rating at* ***4.111 kA*** *and* ***8.476 Ω, 5.832 cm*** *width and* ***721.76 m*** *length of selected (*Yttrium, bismuth, strontium, copper and oxygen*)YBCO coated-conductor, fast-switch interrupting* ***9.35 kA*** *within* ***48 ms****, and a cooling requiring* ***80 liters*** *of liquid nitrogen and* ***256 kW*** *condenser.*

This designed SFCL is modeled using Matlab/Simulink and the result showed that the SFCL can minimize the maximum short-circuit current from ***44 kA*** *to* ***35 kA*** *and enables the substation to clear the fault without problem. This means that the substation can be integrated to additional power coming from a generation having short-circuit rating of* **3585 MVA** *with the previous safety margin still.*

To implement the SFCL system, the whole system components cost **$320,000/phase** and *require* ***10m × 20m*** *area by* ***1.8m*** *height space of the substation.*

Key words: SFCL design, SFCL model using Matlab, short-circuit analysis using ETAP, AkAki II substation, and fault current limiter.

Table of Content

List of Figures

List of Tables

Nomenclatures

AC	Alternative current
ANSI	
BSCCO	Compounds containing bismuth, strontium, calcium, copper and oxygen
CB	Circuit breaker
CLR	Current limiter resistor
CT	Current transformer
CVT	Capacitive voltage transformer
DC	Direct current
EEP	Ethiopia electric power
EEPCo	Ethiopian electric power corporation
ETAP	Electrical transient analyzer program
FCL	Fault current limiter
GERD	Grand Ethiopian Renaissance dam
HTS	High temperature superconductor
I	Current
IEC	
LN_2	Sub-cooled nitrogen
LTS	Low temperature superconductor
M	Mass
NPS	Negative phase sequence
R	Resistance
RMS	Root-mean-square
RRRV	Rate rise of recovery voltage
ρ	Resistivity
ρ_d	density
OFAF	Cooling system of transformer to mean oil-forced-air-forced
ONAF	Cooling system of transformer to mean oil-normal-air-forced
ONAN	Cooling system of transformer to mean oil-normal-air-normal
PPS	Positive phase sequence

Q	Heat
SC	Short circuit
SFCL	Superconductor fault current limiter
Sp	Space
SuC	Superconductor
V	Voltage
$\mathbb{V}$	Volume
YBCO	Compounds containing Yttrium, bismuth, strontium, copper and oxygen
Z	Impedance
ZPS	Zero phase sequence

1. INTRODUCTION

1.1. Background

The research focused area, AkAki II substation is the largest of all currently functional Ethiopian secondary substations (i.e. primary step-down distribution system) by its power delivering capacity. It is located at 25Km southern from Addis Ababa. This substation is mainly built related with the project of Gibe III power generation plant for the accomplishment of power delivery up to load center and connection into the grid.

The construction was started on 7-October, 2011 by EEPCo (now it is called EEP) and Shanghai Electric Group Co. LTD companies contract. At the end of 2015, some phases of civil and electrical work has been finished and the substation begun to distribute around 500MW electric power.

The substation has four voltage levels resulting from three voltage transformations. The primary conversion is from 400kV to 230kV using 9x166.67MVA single-phase autotransformers in three bays. Then, the second phase is from 230KV to 132kV by 3x125MVA three-phase autotransformers. Finally, there is also one three phase two-winding transformer having rating of 50MVA, 132kV/15kV.

Ethiopian electric power is using an interconnected transmission system. All primary distribution substations are connected to the grid for sharing the national load demand. So, AkAki substation is also interconnected with different substation. The substation mainly receives power from Wollayta Sodo (Gibe-III step up substation) and is connected to Sebeta II substation (for power coming from Gibe-II generation) so that it is connected to the grid to form ring system in 400kV side. In addition, there is also already installed line to be connected with Holleta substation for the upcoming generation from Grand-Ethiopian-Renaissance-Dam (GERD).

The main power flow of the substation, during time of the study, comes through Sodo-II L2 line through which around 800MVA apparent power flows to the substation from Gibe-III generation plant. The power flow through the ring line between Sebeta substation and AkAki

II (Gellan substation) varies its magnitude and direction according to the load of the grid system.

The substation has a number of incoming/outgoing lines from 230kV, 132kV and 15kV bus-bars. The following one line diagrams describe detail information about the connection of the substation.

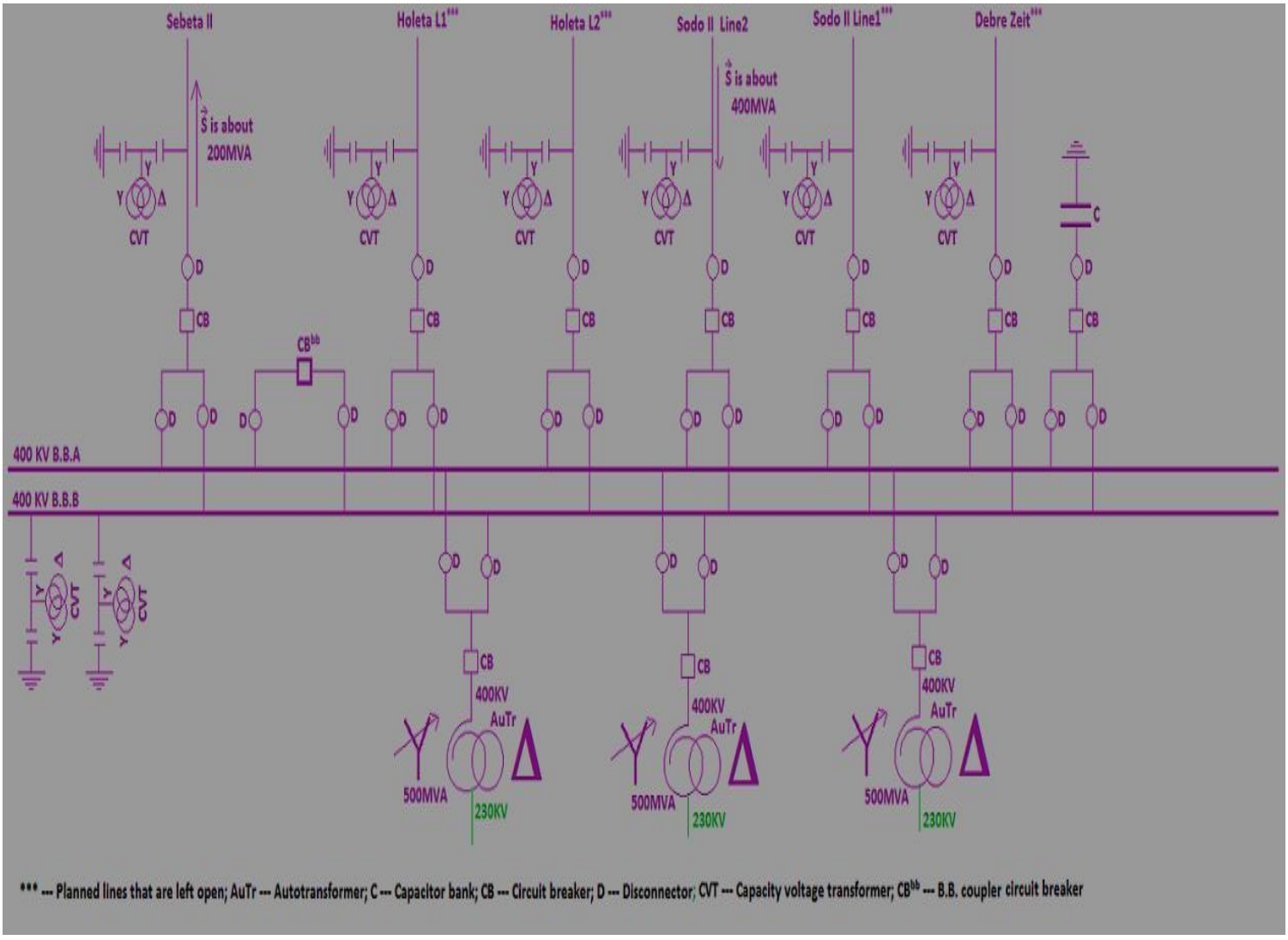

Figure 1-1: One line diagram of 400kV switchyard components of the substation

(Conventionally, 400kV circuit is depicted in violet color)

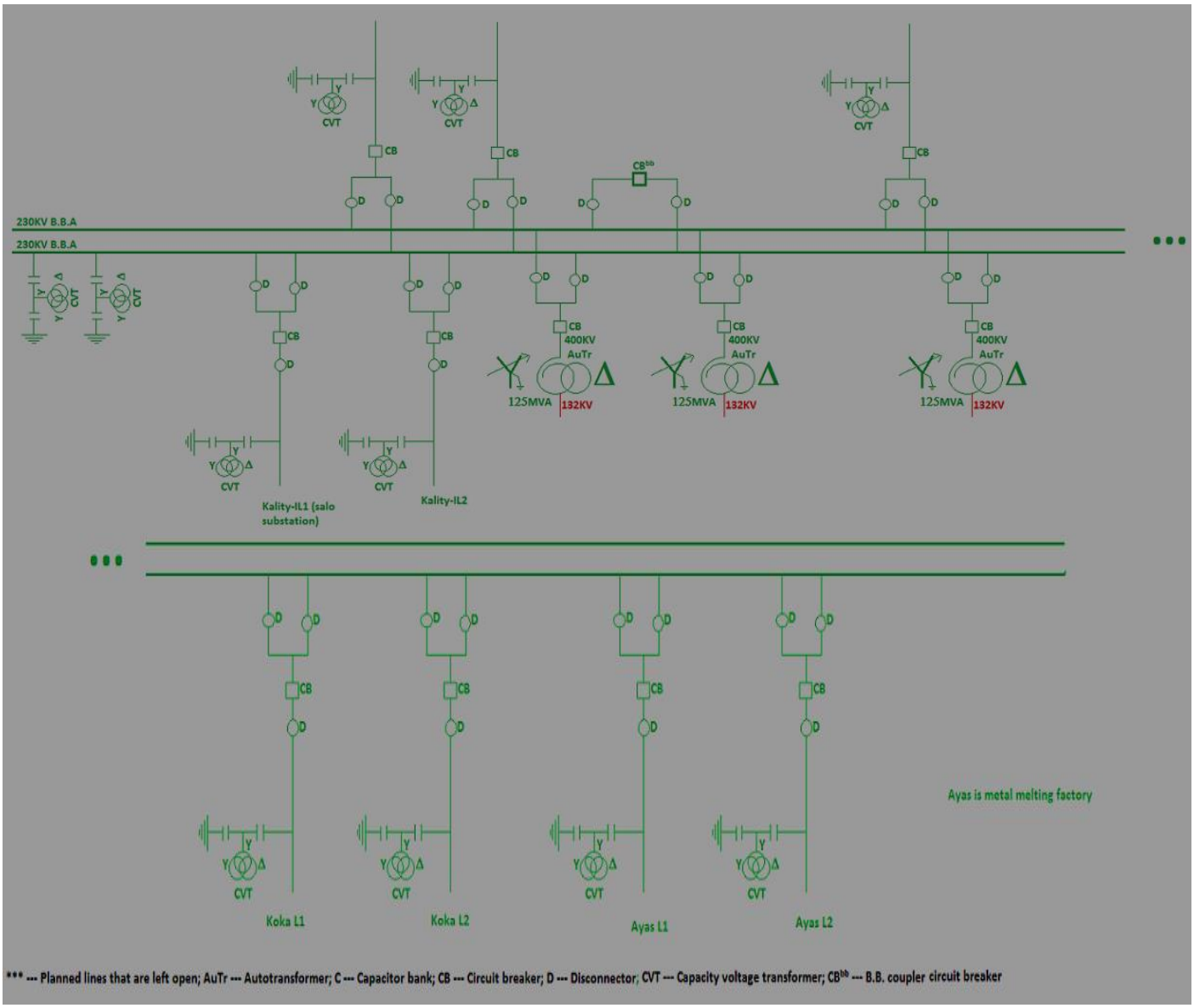

Figure 1-2: One line diagram of 230kV switchyard components of the substation (Conventionally, 230kV circuit is depicted in Green color)

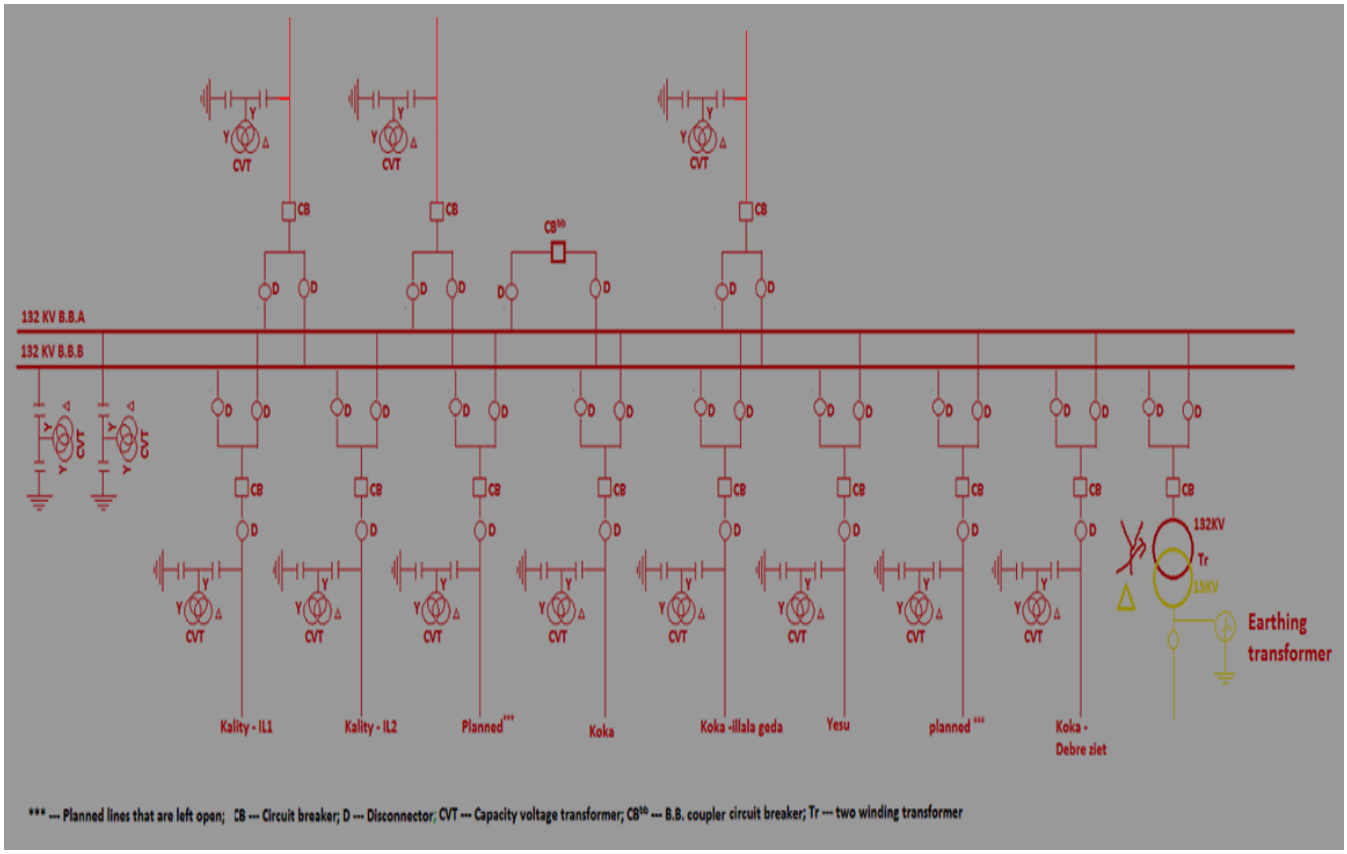

Figure 1-3: 132kV switchyard components of the substation

(Conventionally, 132kV circuit is depicted in Red color)

All the substation components' specifications are given in Appendix B. The components of bay that are found in the substation are mentioned as follow.

- **Lightning arrestor:** The lightning arrestor is a station type that has two gaps filled with high pressured gas. When surge occurs through the incoming line, it gets shorted and diverts the high charging surge current not to pass into the distribution network. It has a surge counter and an ammeter to measure leakage current during normal condition.
- **Voltage transformer:** A capacitive voltage transformer (CVT) is available in the substation. It uses for measurement and protection purposes.
- **Disconnector with earthing switch:** It has both remote and local switch. The type of disconnector used is called pantograph type central lock disconnector.
- **Current transformer (CT):** It is for the use of protection and measurement.

- **Circuit breaker (CB):** T-type circuit breaker is used there. This CB has two chambers. It is called T-type because it has a T arrangement of two fixed parts and one vertically movable part. There are also four chambers CB for line-bay from Holeta.
- **Supportive structure:** It is also known as post insulator. Its purpose is only for physical support of the line but have no electrical application.
- **Bus-bar:** There are two bus-bars with a coupler switch.
- **Line shunt reactor:** It is connected, before the system bus-bar, in shunt with the incoming line 'Sodo II line 2' coming from Gibe III generation plant. That is why it is named line reactor. It reduces the line voltage increment because of Ferranti's effect after about 267 km of transmission.
- **Capacitor bank:** The capacitor bank is a set of 64 single capacitors cells per-phase connected in series and parallel combination. The bank is shunted at 400kV system bus-bar. It compensates the lagging reactive power of the system. The three-phase connection has a star neutral grounding.

As it is discussed, the substation can transform 400kV to 15kV in three different stages. In the first stage, as shown in Figure 1-1, to change 400kV to 230kV, single-phase Y-connected autotransformers with delta tertiary winding are used. Auto-Transformers have several advantages over 2-winding transformers of the same outputs, such as lower weight and cost; lower losses (hence higher efficiency); better regulation as lower impedance; smaller exciting current as lower core weight and smaller overall size; which is especially important for the large power units or for units where shipping size and weight is of importance.

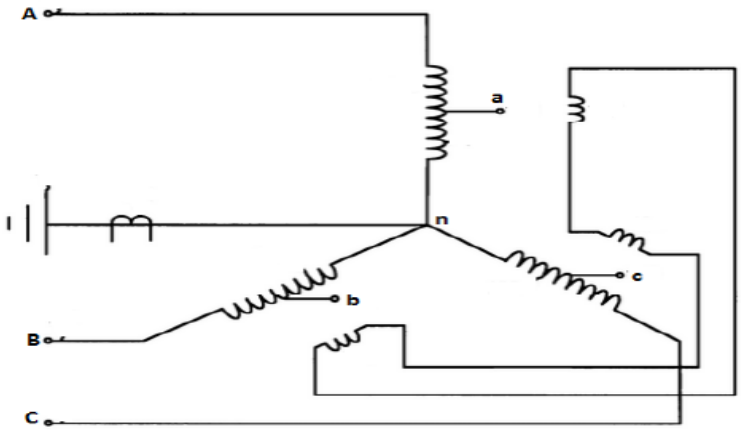

Figure 1-4: YNa0-connected three-phase auto-transformer with tertiary windings

Generally, connecting tertiary winding in Y-connected autotransformer has the following advantages: to supply auxiliary load, to suppress the third harmonic currents and voltages in lines and to stabilize the neutral point of the fundamental frequency voltages. But, in Gellan substation, there is no case of auxiliary load case that is supplied from the autotransformer.

In the second stage, to change 230kV to 132kV, three-phase Y-connected autotransformers with delta tertiary winding are used. The only difference that the 230kV/132kV transformers have is they have one core instead of three separate cores as the case in the previous 400kV/230kV transformers.

For the third stage, there is a two winding three-phase transformer. It has Y-Δ winding connection. And, in its secondary side, earthing transformer is connected in parallel to create neutral point for the distribution network.

1.2. Statement of the Problem

Before detail investigation in the substation to find out research problem, the fact that the substation is huge and built in modern way is the main motivation for the researcher to go through this thesis research work over AkAki II (Gellan) substation.

To the best information that the author has got from direct visit and the substations' installation drawings, there is no any method applied to limit short circuit current occurring at 400kV, 230kV and 132kV buses. Both the autotransformers (400kV/230kV and 230kV/132kV) are YNa0 connected. I.e., the neutral point of these transformers is solidly grounded. Even though the secondary winding of current transformer (CT) is wound on the neutral wire the autotransformers, it is for ground fault detection.

The other transformer is the two winding three-phase winding to change voltage from 132kV to 15kV. This transformer has Y-Δ connection with earthing transformer for creation of artificial neutral point. The earthing transformer has zero sequence impedance of 87Ω. This impedance can limit line-to-ground fault. The earthing wire is rounded by secondary winding of CT for ground fault detection.

Therefore, because of lacking any SC current limiting method, there is a possibility of SC current about the maximum breaking capacity of the relevant CB, 50kA after GERD-Holeta-to-AkAki incoming line is energized.

Because, as indicated in the Figure 1-5 below, when a substation is connected to a number of generation units for sake of increasing reliability, expected fault current would increase. As a result, the circuit breaker might be unable to interrupt this large expected SC current in limited cycles. This causes electromechanical stress and heating up of power system main components like transformers, circuit breakers, busbars, isolators and others. The heat reduces the expected life span of each component.

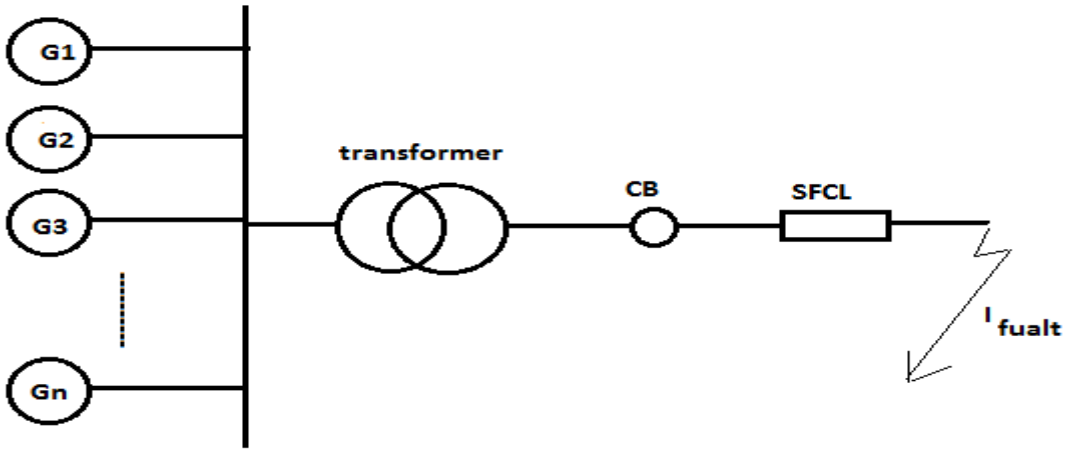

Figure 1-5: A distribution substation connected to a number generation units

The main problem addressed in this thesis is to increase the safety margin of CB of the substation by reducing the maximum SC current using super conductor fault current limiter.

Specifically, at 230kV busbar of the substation, the maximum expected symmetric SC current occurrence is to 47 kA (as shown in Figure 4-13 & Figure 4-14) and out of this, about 44 kA flows through the 230kV CB while the CBs' rated SC current breaking is 50 kA.

It is preferred that CBs ought to work with large safety margin from short-with-stand-current rating (i.e. 40 kA for 1 sec for the 230 kV CB) to interrupt maximum expected fault current.

Under this condition, the 230 kV CBs are in marginally trouble condition. The CB may not be safe to break 44 kA current due to the following reasons.

- Tolerance rating of the CB
- If the fault point is close to generators and motors, breaking capacity will be less than sub-transient symmetrical SC current (IEC 60909)
- Large delay to clear the fault that again affects stability of the system
- Overvoltage conditions decreases current breaking capacity of the CB
- 44 kA breaking current means it may have 2.5 times magnitude of making current (I.e. >100 kA which is greater than the CB making current rating, 80 kA).

The other major problem is the substation cannot be connected for purpose of load sharing and reliability with other power generations after GERD, because it is designed with no safety margin of the CB breaking capacity.

1.3. Objectives

General objective: - The general objective of this thesis is to explore the potential of superconductor fault current limiter to increase the safety margin of substations' CBs by reducing the maximum expected SC current below the breaking capacity of the CBs. As the result, the stability of power system is improved.

The specific objectives:

- To develop model of components of Akaki-II substation in software
- To simulate SC analysis of Akaki-II substation with the SFCL
- To study switching transient characteristic YBCO superconductor material
- To design components of appropriate type of SFCL
- To develop appropriate model of SFCL system
- Simulating Akaki-II substation with the appropriate model
- To estimate overall cost of implementation of SFCL

1.4. Literature Review of Related Research Papers

The paper entitled as “Theoretical expression of rate of rise of recovery voltage across a circuit breaker connected with fault current limiter” is written by E. Calixte and his group [1]. It derives the mathematical expression of the rate of rise of recovery voltage (rrrv) across a circuit breaker connected with fault current limiter (FCL) as a function of the limiting impedance and the limited current when a fault occurs at a distance near the load-side terminals of the FCL. It considers two types of SFCL: resistive SFCL and general inductive SFCL (assuming a constant inductance value). Finally, the mathematical expressions are compared with software simulation output results.

S. W. Yim and et al. also have written a paper with the title of “Improvement in operational characteristics of KEPCO’s line-commutation-type superconducting hybrid fault current limiter” [2]. A hybrid SFCL can be designed to meet the following requirements: maximum impedance in limited space, minimum voltage difference between current paths, uniform magnetic field, easy replacement of defective parts, ease of use, first peak current limitation, and compatibility with the existing hybrid FCL and improvement of its operational properties. The research includes fabrication of the designed hybrid SFCL and laboratory testing.

“Short Circuit Analysis of 220/132 kV Substation by Using Electrical Transient Analyzer Program (ETAP)” [3] deals with the simulation of 220/132 kV substation fault current calculation. It is a volume of international journal of advanced technologies in engineering and science. The analysis of the paper is done by using advance software ETAP with detailed SC analysis. All the data used for analysis is real time and collected from a 220/132 kV substation under. This research work highlights the effective use of ETAP software for SC studies.

S. Lee and his group developed a first peak non limiting hybrid SFCL analysis model using the PSCAD/EMTDC program, which is commonly used in the transient analysis of power systems [4]. The paper also conducts a technical analysis using the model and proposes specifications for the Current Limiting Resistor/ Reactor (CLR) used for applying the SFCL to a real distribution power system in Korea. The researchers of this paper believe that this hybrid SFCL does not fit for this work.

Jennifer Kincaid and et al. consider an existing medium voltage network in the UK, which incorporates distributed generation capacity. The performance of inverse-definite-minimum-time (IDMT) overcurrent and distance relays' protection schemes will be examined when an SFCL is installed in this network. A variety of network operational scenarios including SFCL placement and fault conditions will be considered and compared. [5]

J. Wen and et al., experimentally, show the value of different manufacturer YBCO coated-conductors' maximum permissible voltage. YBCO coated conductors test in the experiment are from American super-conductor (AMSC) and Shanghai Jiao Tong University (SJTU). Based on the results of samples, the whole length of CCs used in the design of a SFCL can be determined. [6]

1.5. Scope

This research project confines the study specifically at the case study substation. Starting from investigating the problem, and selecting most preferable solution. It goes up to finding all specification and characteristics of SFCL for the substation. And, finally, it presents designed device with the result of simulation test. But, it does not embrace the implementing phase tasks.

1.6. Methodology

The Figure 1-6 shows the over-all path of the research. As usual, the research initiation is from finding problem to be eradicated. After the motivation of the research area, the problem SC breaking capacity is stated.

Then, different traditional and modern solutions are investigated to select the appropriate solution fitting the case study scenario. As indicated section-2.4, a hybrid-resistive type SFCL using YBCO 2G (second generation) superconductor is selected to limit the fault current including the first peak.

By, using all necessary data showed in selection-2.1, are used as inputs in the short-circuit analysis of the substation with ETAP software to get the basic SFCL design parameter that is the maximum symmetrical SC current expected at each CBs of the substation.

Not only a SC analysis is an input for determination of the SFCL design parameter, transient behavior of system should be taken under consideration. The transient electro-thermal behavior of the superconductor is necessary for determination of length of superconductor material and the cooling system parameters, as shown in section 3.2. Rate-of-rise-recovery (RRRV) voltage is one of basic transient behavior that must be considered to analysis operations related to CBs.

Installing a resistive SFCL (with small conductance to earth) in series to a CB can decrease rate of rise recovery voltage imposing to the CB to reclose. This concept is elaborated detail in reference [1].

In this regard, the SFCL does not require the CB to further capability against transient recovery voltage.

To the effect of the designed SFCL, it has to be modeled by equivalent components and simulate the substation using it. Therefore, as shown in section-3.3, the SFCL is model in Matlab/Simulink.

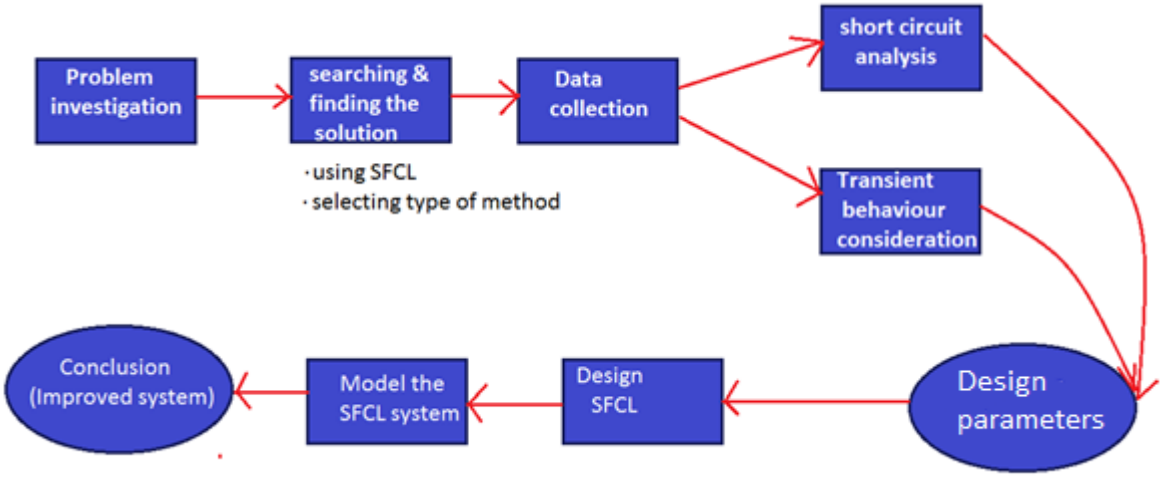

Figure 1-6: The overall tasks of the project

Instead of inserting SFCL in series each CBS, it is economical to use the SFCL between the double bus-bar conductors as shown in Figure 1-7.

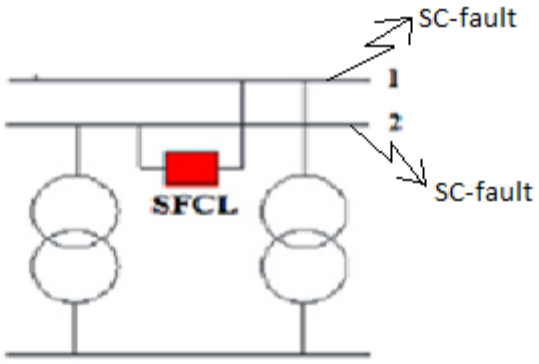

Figure 1-7: SFCL inserted between the bus-bars to reduce the maximum SC current

1.7. Organization of the Thesis

Chapter one is about motivation and statement of the problem, objective of the study, review of related works, scope, methodology and overview of the study area.

Chapter two presents conceptual background of power system short circuit analysis and SFCL. About the power system SC circuit analysis, every type of SC faults are considered how their fault current is calculated using symmetrical networks. Next, starting from defining basic properties of superconductor, types of SFCL are listed with compare and contrast points among them.

Chapter three includes two models in the thesis. These are representation of the substation and related components in ETAP software to carry out SC analysis and the model of SFCL in Matlab/Simulink for simulation of SC current with/without using of the designed SFCL in substation.

Chapter four is simulation studies with results and discussion. Implementation cost of the designed SFCL device is also included.

Chapter five contains short concluding remarks and recommendations are made based on the research basic findings. Also, future works that are planned by the researcher are presented.

2. SHORT CIRCUIT ANALYSIS OF POWER SYSTEM AND SUPERCONDUCTING FAULT CURRENT LIMITERS

2.1. Introduction

This chapter deals with theoretical background of techniques to calculate SC currents for different cases. And, it also presents comparison and contrast among different types of superconductor fault current limiters.

2.2. Short Circuit Analysis of Power System

In electrical power system, unintentional short circuits are usually caused when a wire's insulation breaks down, or when another conducting material is introduced, allowing charge to flow along a different path than the one intended.

A SC fault current can, within milliseconds, be thousands of times larger than the normal operating current of the system in wide electrical network. Therefore, obviously, damage from the SC current is going to be severe.

With power demand rise and addition of new power generation sources, the grid network becomes overcrowded and stressed. As it gets crowded and stressed, faults and power blackouts increase in frequency and severity.

In SC current calculations; an equivalent voltage source at the fault location replaces all voltage sources. A voltage factor ‘c’ is applied to adjust the value of the equivalent voltage source for minimum and maximum current calculations. All machines are represented by their internal impedances. Transformer taps can be set at either the nominal position or at an operating position, and different schemes are available to correct transformer impedance and system voltages if off-nominal tap setting exists. System impedances are assumed to be balanced 3-phase, and the method of symmetrical components is used for unbalanced fault calculations. Zero sequence capacitances of transmission lines, cables and shunt admittances can be considered for unbalanced fault calculations (LG and LLG) if the option in the study case is selected to include branch Y and static load. This means that the capacitances of static

loads and branches are considered based on IEC 60909-0 2001. Calculations consider electrical distance from the fault location to synchronous generators. For a far-from-generator fault, calculations assume that the steady-state value of the SC current is equal to the initial symmetrical SC current and only the DC component decays to zero. However, for a near-to-generator fault, calculations count for decaying in both AC and DC components. The equivalent R/X ratios determine the rates of decay of both components, and different values are taken for generators and loads near the fault. [7]

Detail analyses of balanced and unbalanced Faults in the sequence reference frame are shown in Nasser D. Tleis's book "Power Systems Modelling and Fault Analysis". [7]

2.1.1. Balanced three-phase to earth short-circuit faults analysis

Figure 2-1 (a) shows the representation of this fault. F_R, F_Y and F_B are points in the three-phase system where the three-phase fault is assumed to occur through the balanced fault impedances Z_F, and F'_R, F'_Y and F'_B are the true points of fault. Figure 2-1 (b) shows the connections of the Thévenin's PPS, NPS and ZPS equivalent circuits.

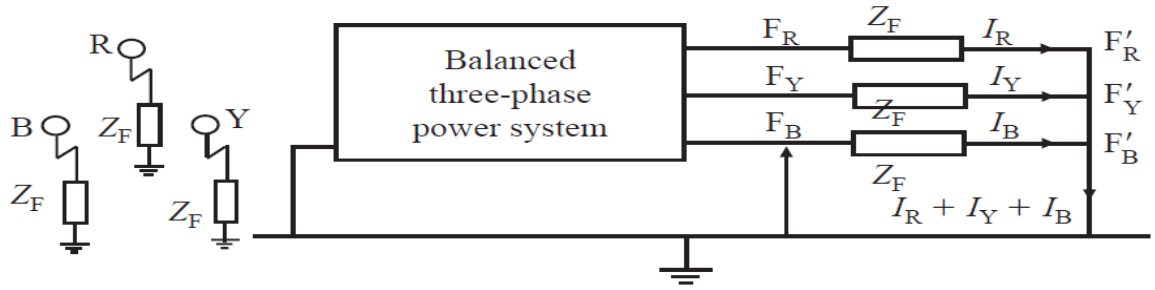

(a) Equivalent circuit diagram of the system after the fault

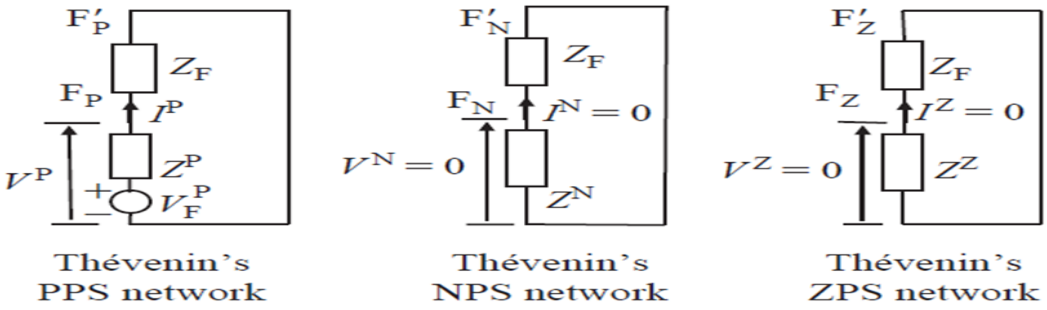

(b) Sequence network Thevenin's equivalent circuit from the fault point

Figure 2-1: Balanced three-phase to earth short-circuit fault through fault impedance Z_F

The voltages at the fault point are given by:

$$\boldsymbol{V_R = Z_F I_R,\ V_Y = Z_F I_Y,\ and\ V_B = Z_F I_B} \quad \textbf{(2.1)}$$

Using phasor system to sequence system representation transformation matrix 'h', it can be shown that the sequence voltages and currents at the fault point are given by,

$$\boldsymbol{V_R^P = Z_F I_R^P = V_F^P - Z^P I_R^P,\ V_R^N = 0,\ and\ V_R^Z = 0} \quad \textbf{(2.2)}$$

And

$$\boldsymbol{I_R^P = \frac{V_F^P}{Z^P + Z_F},\ I_R^N = 0,\ and\ I_R^Z = 0} \quad \textbf{(2.3)}$$

Therefore, the three-phase power system remains balanced and symmetrical after the occurrence of such a fault because the fault impedances are equal in the three phases. Therefore, only positive phase sequence (PPS) voltages exist and only PPS currents can flow.

Since phase R is used as the reference, it is convenient from now on to drop the R notation in the PPS, negative phase sequence (NPS) and zero phase sequence (ZPS) voltage and current equations whilst always remembering that these sequence quantities are those of phase R.

The phasor quantities become:

$$\boldsymbol{I_R = I^P = \frac{V_F^P}{Z^P + Z_F}, I_y = h^2 I^P = \frac{h^2 V_F^P}{Z^P + Z_F}, and\ I_B = hI^P = \frac{hV_F^P}{Z^P + Z_F}} \quad \textbf{(2.4)}$$

And

$$\boldsymbol{V_R = I^P Z_F = \frac{V_F^P}{Z^P + Z_F} Z_F, V_y = h^2 V_R = \frac{h^2 V_F^P}{Z^P + Z_F} Z_F, and\ V_B = hV_R = \frac{hV_F^P}{Z^P + Z_F} Z_F} \quad \textbf{(2.5)}$$

As expected for a balanced and symmetrical SC fault, the sum of the three phase currents $I_R + I_Y + I_B$ is equal to zero hence the net fault current flowing in to earth is zero. Similarly, the sum of the three-phase voltages $V_R + V_Y + V_B$ is equal to zero.

The case of a solid or bolted three-phase to earth SC fault is obtained by setting $Z_F = 0$.

2.1.2. Balanced three-phase clear of earth short-circuit faults

A three-phase SC fault clear of earth at a point F in a three-phase system is represented by connecting an equal fault impedance between each pair of phases as shown in Figure 2-2 (a), i.e., as a delta connection.

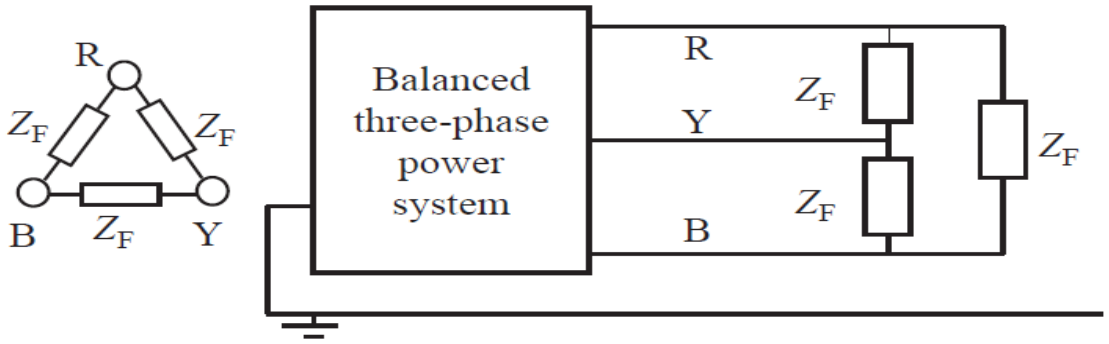

(a)Equivalent circuit diagram of the system after the fault

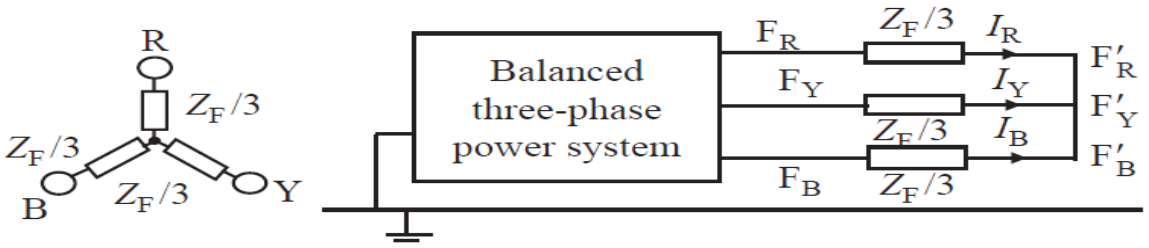

(b) Equivalent Y connected Z_F of the fault impedance

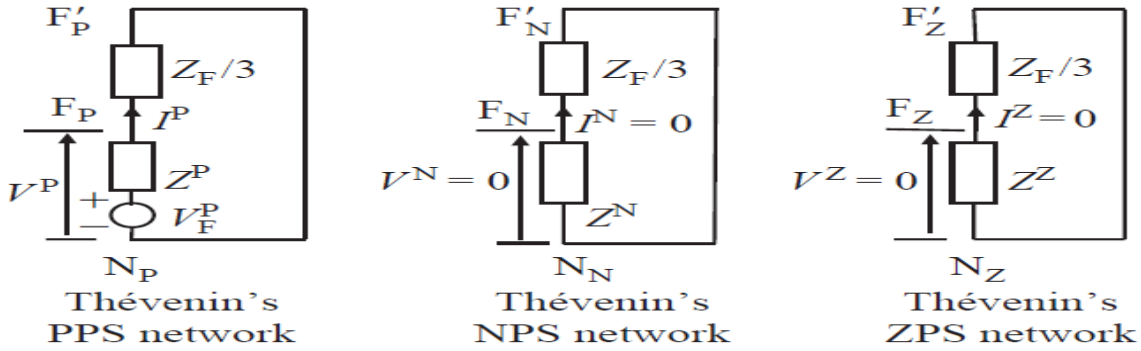

(c) Sequence network Thevenin's equivalent circuit from the fault point

Figure 2-2: Balanced three-phase SC fault clear of earth through fault impedance Z_F [7]

In order to calculate the equivalent fault impedance 'seen' in each phase, a transformation of delta to star with isolated neutral is needed as follows:

$$\boldsymbol{Z_R = Z_Y = Z_B = \frac{Z_F \times Z_F}{Z_F + Z_F + Z_F} = \frac{1}{3} Z_F} \quad \textbf{(2.6)}$$

The phase fault currents and voltages are given by:

$$\boldsymbol{I_R + I_Y + I_B = 0 \quad and\, V_R = V_Y = V_B = 0 \;\; at\; point\; F'} \quad \textbf{(2.7)}$$

$$\boldsymbol{So, V_R = \frac{1}{3} Z_F I_R, \;\; V_Y = \frac{1}{3} Z_F I_Y and\, V_B = \frac{1}{3} Z_F I_B} \quad \textbf{(2.8)}$$

By phasor to sequence quantities transformation, the sequence quantities are as follow:

$$\boldsymbol{V^P = \frac{1}{3} Z_F I^P = V_F^P - Z^P I^P, \;\; V^N = 0 \;\; and\, V^Z = 0} \quad \textbf{(2.9)}$$

$$\boldsymbol{I^P = \frac{V_F^P}{Z^P + \frac{1}{3} Z_F}, \;\; I^N = 0 \;\; and\; I^Z = 0} \quad \textbf{(2.10)}$$

The phase fault currents are given by:

$$\boldsymbol{I_R = I^P = \frac{V_F^P}{Z^P + \frac{1}{3} Z_F}, \; I_Y = h^2 I_R = \frac{h^2 V_F^P}{Z^P + \frac{1}{3} Z_F} \; and \;\; I_Y = h I_R = \frac{h V_F^P}{Z^P + \frac{1}{3} Z_F}} \quad \textbf{(2.11)}$$

The case of a solid of bolted three-phase clear of earth SC fault is obtained by setting $Z_F = 0$.

2.1.3. Unbalanced one-phase to earth short-circuit faults

During one-phase to earth SC fault, the sequence networks become in series connection at the fault point.

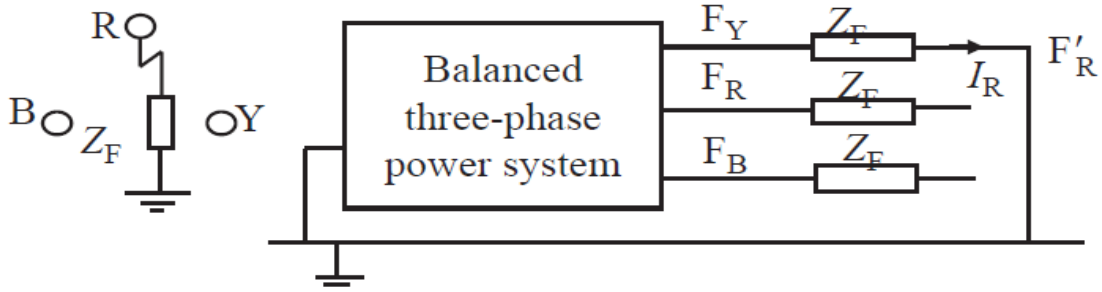

(a) Circuit representation of one-line to earth short circuit faults

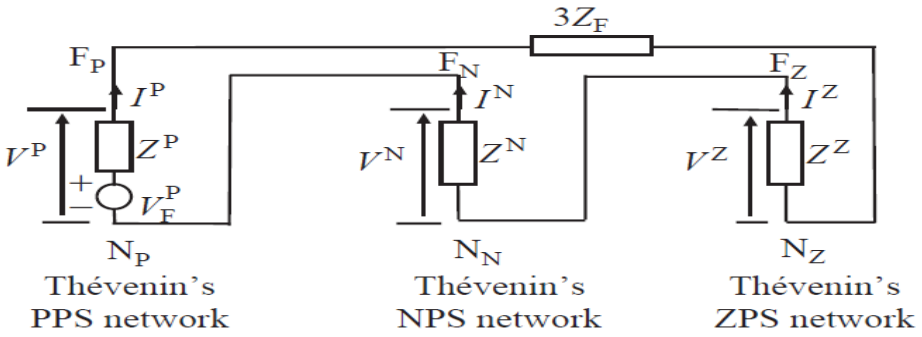

(b) Connections of sequence networks at the fault point

Figure 2-3: Unbalanced 1-phase to earth short-circuit fault through fault impedance Z_F [7]

The sequence currents are:

$$\boldsymbol{I^P = I^N = I^Z = \frac{1}{3} \times I^Z} \quad \textbf{(2.12)}$$

As indicated in Figure 2-3, the sequence fault currents and voltages can be expressed:

$$\boldsymbol{I^P = I^N = I^Z = \frac{V_F}{Z^P + Z^N + Z^Z + 3V_F}} \quad \textbf{(2.13)}$$

And,

$$\boldsymbol{V^P = \frac{Z^N + Z^Z + 3V_F}{Z^P + Z^N + Z^Z + 3V_F} V_F, V^N = \frac{-Z^N}{Z^P + Z^N + Z^Z + 3V_F} V_F \& V^Z = \frac{-Z^Z}{Z^P + Z^N + Z^Z + 3V_F} V_F} \quad \textbf{(2.14)}$$

The phase fault current and voltage are calculated using phase quantity to sequence quantity transformation.

$$\boldsymbol{I_R = \frac{3V_F}{Z^P + Z^N + Z^Z + 3V_F} \ and \ I_R = \frac{3Z_F}{Z^P + Z^N + Z^Z + 3V_F} V_F} \quad \textbf{(2.15)}$$

2.1.4. Unbalanced phase-to-phase or two-phase short-circuit faults

Figure 2-4 (a) shows a representation of an unbalanced two-phase fault on phases Y and B through fault impedance Z_F.

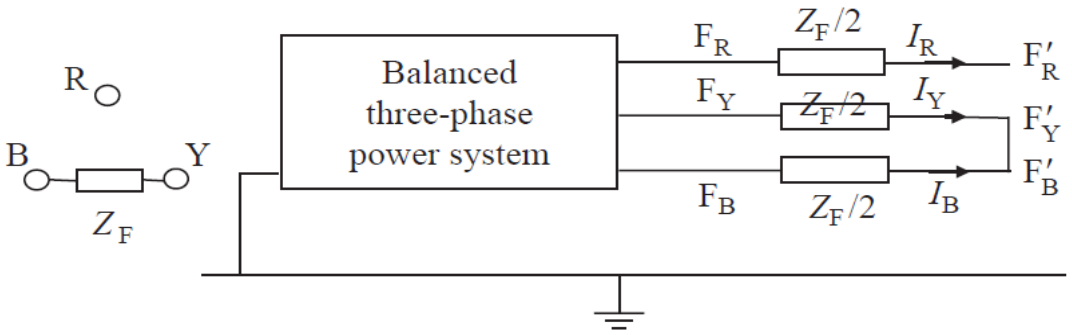

(a) Representation of line-to-line fault

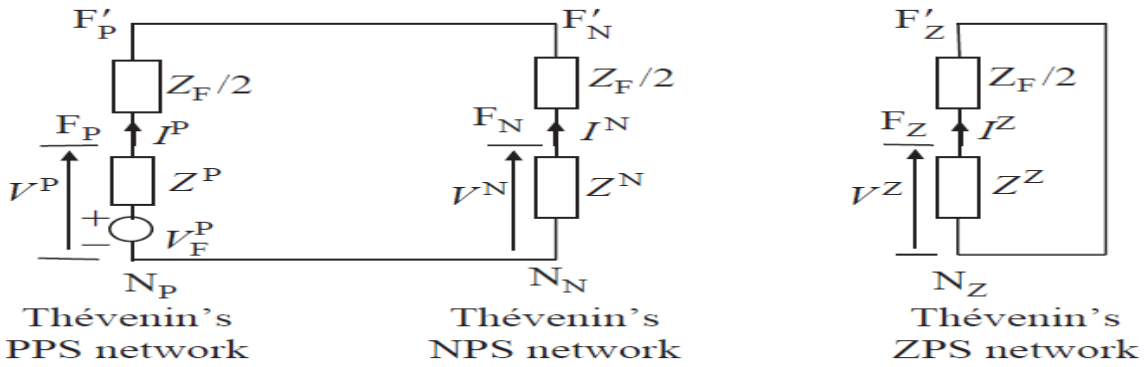

(b) Connection of phase sequence networks at the fault point

Figure 2-4: Unbalanced two-phase short-circuit fault through fault impedance Z $_F$ [7]

The conditions at the point of fault are:

$$\boldsymbol{I_R = 0,\ I_Y = -I_B \quad and\ V_Y - V_B = Z_F I_Y} \tag{2.16}$$

Using the above initial conditions, the sequence currents will be:

$$\boldsymbol{I^Z = 0 \Rightarrow V^Z = 0\ \ and\ I^P = -I^N} \tag{2.17}$$

The sequence fault currents are calculated as:

$$\boldsymbol{I^P = -I^N = \frac{V_F}{Z^P+Z^N+Z_F}} \quad \textbf{(2.18)}$$

The phase fault currents are calculated using the following equations.

$$\boldsymbol{I_Y = -I_B = -j\sqrt{3}I^P = \frac{-j\sqrt{3}V_F}{Z^P+Z^N+Z_F}} \quad \textbf{(2.19)}$$

The phase voltages at the fault location are calculated from the sequence voltages obtained from the sequence networks connection shown in Figure 2-4 (b) after the sequence currents are obtained.

The case of a solid or bolted two-phase SC fault is obtained by setting Z_F=0.

2.1.5. Unbalanced two-phase to earth short-circuit faults

Figure 2-5 (a) &Figure 2-5 (b) show a representation of an unbalanced two-phase to earth fault on phases Y and B through fault impedance Z_F and Z_E.

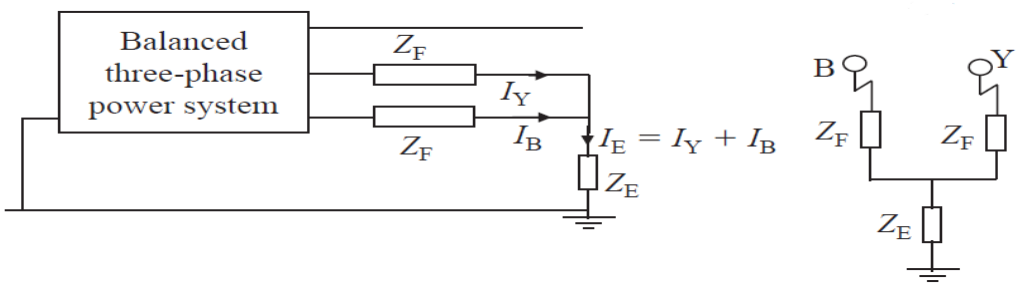

(a) Unbalanced two-phase to earth fault on two phases with finite impedance earthing

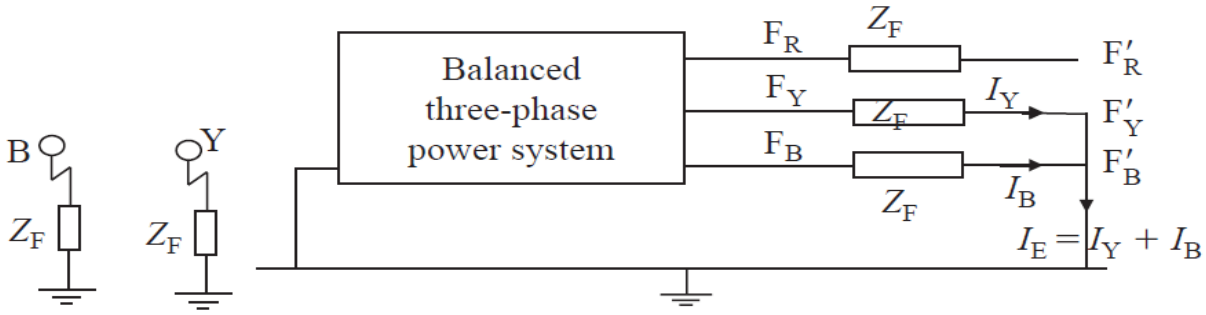

(b) Unbalanced two-phase to earth fault on two phases with bolted earthing

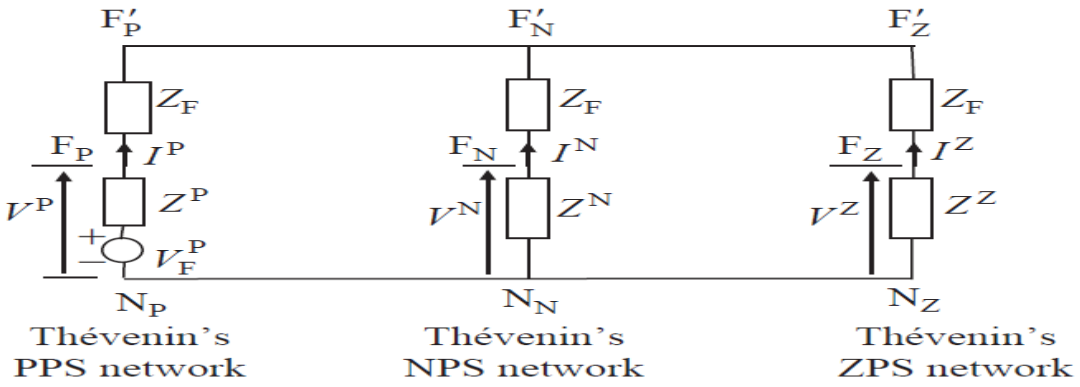

(c) Connection of sequence networks at the fault location

Figure 2-5: Unbalanced two-phase to earth short-circuit fault through fault impedance Z_F

It is easy to start from defining fault conditions of the simpler case of Figure 2-5 (b) and proceed to case in Figure 2-5 (a).

The conditions at the point of fault in Figure 2-5 (b) are given by:

$$\boldsymbol{I_R = 0,\ V_Y = Z_F I_Y \quad and\ V_B = Z_F I_B} \tag{2.20}$$

By using sequence quantities relation in Figure 2-5 (b), the sequence currents will be:

$$\boldsymbol{I^P = \frac{[(Z^N+Z_F)+(Z^Z+Z_F)]V_F}{(Z^N+Z_F)(Z^Z+Z_F)+(Z^N+Z_F)(Z^P+Z_F)+(Z^P+Z_F)(Z^Z+Z_F)}} \tag{2.21-a}$$

$$\boldsymbol{I^N = \frac{-(Z^Z+Z_F)V_F}{(Z^N+Z_F)(Z^Z+Z_F)+(Z^N+Z_F)(Z^P+Z_F)+(Z^P+Z_F)(Z^Z+Z_F)}} \tag{2.22-b}$$

$$\boldsymbol{I^N = \frac{-(Z^N+Z_F)V_F}{(Z^N+Z_F)(Z^Z+Z_F)+(Z^N+Z_F)(Z^P+Z_F)+(Z^P+Z_F)(Z^Z+Z_F)}} \tag{2.23-c}$$

Then, the phase fault currents and voltages are calculated using phasor to sequence quantities.

In the case where earth impedance Z_E presents in the common connection to earth, as shown Figure 2-5 (a), it can be shown that Z^Z on Equation 2.21-a, Equation 2.21-b & Equation 2.21-c for case of Figure 2-5 (b) must be replaced by $Z^Z + 3Z_E$.

2.2. Superconducting Fault Current Limiters

As risks of SC fault have been increasing with growth of electric power networks; engineers also have been discovering various and time-to-time improving methods to overcome the problems.

One conventional solution to these problems is to use higher rated circuit breakers. Schemes are used to detect fault currents and activate isolation devices (circuit breakers) that interrupt the over-current sufficiently rapidly to avoid damage to parts of the power grid.

Connecting a reactor to the neutral points of transformers can limit zero sequence current flow so that it can limit line-to-ground SC fault current. This conventional method is also applicable in secondary distribution systems, currently.

These traditional fault current limiting methods are becoming non effective. Because, the ever-increasing levels of fault current will soon exceed the interruption capabilities of existing devices. In this case, large capital costs are incurred to upgrade not only the circuit breaker but the entire substation equipment.

Therefore, it had become important electrical engineers and scientist to find another method of fault current mitigation with minimum cost, power loss and controlling complexity. Primarily, they aimed to realize fault current limiters (FCLs) with the capability of rapidly increasing their impedance, and thus limiting high fault currents are being developed.

By using superconducting materials, FCLs can be realized. These devices have the promise of controlling fault currents to levels where conventional protection equipment can operate safely. In the first time, Low temperature superconductors (LTSs) were discovered to work under lower temperature near to home temperature ($300K^0$). But, these superconductors could not be implemented in fault current limiting application because of economical factor. LTSs need high cooling energy to keep them under low temperature after quenching.

In particular, an LTS Nb–Tiis available since several years at competitive cost. They are largely used in MRI magnets operating in DC. However, the very low operating temperature makes it unpractical to the use of this material for fault current limiter.

The discovery of high-temperature superconductivity (HTS) in 1986 drastically improved the potential for economic operation of many superconducting devices. This improvement is due to the ability of HTS materials to operate at temperatures around $70K^0$ instead of near $40K^0$, which is required by conventional superconductors. [8]

The advantage is that the refrigeration associated with operating at the higher temperature is about 20 times less costly in terms of both initial capital cost and operational and maintenance (O&M) costs.

Concerning the high temperature superconductors, first generation HT-SFCLs are also available since more than one decade. They consist of BSCCO filaments immersed in a silver matrix and can operate conveniently at the liquid nitrogen temperature (66–77 K^0). Nevertheless the cost of this material is high due to the silver and their use in fault current limiters is difficult due to the large amount of material needed (which implies both high operating costs due to AC losses and high capital costs). [9]

Second generation HTS SFCL based on YBCO (ceramic compounds containing Yttrium, bismuth, strontium, copper and oxygen, $YBa_2Cu_3O_{6+X}$) material are under development worldwide. They have good performance at the liquid nitrogen temperature and are suitable for fault current limiters. At the moment they are still not available at the industrial level ad their cost is still high but their progress in the last 10 years have been impressive. This material has potential to become one of the most suitable candidates in the medium term. Another material which can be considered for fault current limiters is the magnesium di boride (MgB2). This compound has a critical temperature of 39 K^0 and show good performance at 25 K^0. It is available since a few years in industrial length at competitive costs. Despite the relatively low temperature makes not trivial the use of MgB2 for fault current limiters to due AC loss some encouraging prospects for this material can be achieved by means of an innovative device concept. [9]

For the SC material three choices are possible: BSCCO, YBCO andMgB2. The development of new materials known collectively as BSCCO (ceramic compounds containing bismuth, strontium, calcium, copper and oxygen) has initiated a large number of research programs around the world, aimed at creating superconducting devices for electrical power

applications. The BSCCO appears now less attractive than YBCO Coated Conductors (CC), available today in lengths suitable for SCFCL and with high performances. The YBCO CC cost remains high but with perspectives of strong reduction in the future. One main advantage compared to BSCCO is certainly the much lower AC losses with direct cost consequence for cryogenics (investment and operation).

MgB2 presents a cost significantly reduced compared to YBCOCC but should operate at much lower temperature, typically 20 K^0. The cryogenic cost (cost to remove the losses dissipated at the operating temperature) is considerably higher; Carnot's formula shows an increase of 480% and 370% at 20 K^0 compared to 77 K^0 and 65 K^0 respectively. Due to the geometry of MgB2 conductors compared to YBCO CC, MgB2 shows inherently stronger AC losses. [9]

This Higher AC losses and larger cost removal hardly makes MgB2 ACFCL viable compared to YBCO one. MgB2 FCL could be possible for DC grids.

Superconductors' current limiting behavior depends on their nonlinear response to temperature, current and magnetic field variations. Increasing any of these three parameters can cause a transition between the superconducting and the normal conducting regime.

SFCLs act like powerful surge protectors, preventing harmful faults from taking down substation equipment by reducing the fault current to a safer level (20 – 50% reduction) so that the existing switchgear can still protect the grid.

During the 1990s and 2000s the United States was a world leader in both the development of superconducting wire and in the demonstration of power delivery applications. That position has now changed. Germany, Russia, China, Korea, and Japan all have national, government--supported superconductivity development programs which are now equaling or surpassing the level of activity that has been known in the U.S. These countries are carrying out projects to implement SFCL system after 2008 G.C. Project HYDRA: Fault-Current-Limiting HTS Power Cable at Manhattan, New York City in 2009; 138 kV SFCL Demonstration Project at Southern California Edison in 2009-2020; 22.9 kV Hybrid SFCL Development in Korea in 2008; Zenergy Saturable-Core SFCL Demonstrated at SCE at San Bernardino, California in 2009, and 35 kV Saturable-Core FCL Installed in China at Puji substation in 2007 are some best examples [10].

2.3. Types of Superconductor Fault Current Limiters

2.3.1. Resistive SFCL

The current increase due to fault can cause a section of superconductor to become so resistive that the heat generated cannot be removed locally. This excess heat is transferred along the conductor, causing the temperature of adjacent sections to increase. Also this rapid increase in resistance produces a voltage across the superconductor and causes the current to transfer to the shunt resistor which is mostly called Current Limiter Resistor (CLR). The shunt limits the voltage increase across the superconductor during a quench.

The term “quench” is commonly used to describe the transition of a superconductor from superconductive to normal (metallic) zone.

The next curve is a conventional normalized plot showing the non-linear relation between current flow in a superconductor and its resistance [10]. The curve is obtained while the superconductor is in a constant magnetic field and a constant temperature but changing load current. Similar curves can be produced for changes in temperature and magnetic field.

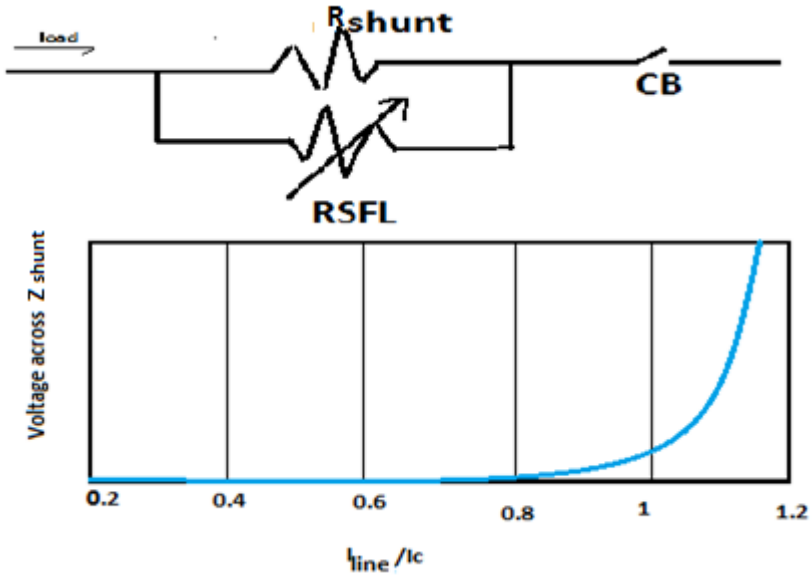

Figure 2-6: Transition behavior of an SFCL

Early resistive SFCL designs experienced issues with “hot spots”, or non-uniform heating of the superconductor during the quench. This is a potential failure mode that occurs when

excessive heat damages the HTS material. Recent advances in procedures for manufacturing HTS materials coupled with some creative equipment designs have reduced the hot-spot issue.

The grid characteristic of the resistive SFCL after a quench is determined by the shunt element. Thus, because the shunt is typically quite reactive, a resistive SFCL typically introduces significant resistance into the power system during a fault. During the transition period when current is being transferred from the superconductor to the shunt, the voltage across the combined element shown in the above Figure 2-6 is typically higher than it is before the current has transitioned into the shunt. The quench process in resistive SFCLs results in heat that must be carried away from the superconducting element by the cryogenic cooling system. Typically, there is a momentary temperature rise in the superconducting element that causes a loss of superconductivity until the cryogenic system can restore the operating temperature. This period of time, known as the *recovery time,* is a critical parameter for utility systems (which may see multiple fault events occurring close together in time) and is a key distinguishing characteristic among various SFCL designs.

To reduce the *recovery time* and protecting the superconductor from "hot spots", a hybrid resistive SFCL is that utilizes a fast operating switch to remove the superconductor from the circuit during quench, leaving an air-core reactor in line with the fault current. The superconducting module allows for fast reduction of the fault current (< 1 cycle). [10]

2.3.2. Inductive SFCL

To implement an SFCL having inductive property, majorly there are two technologies.

I. Shielded-Core SFCL

One of the first SFCL designs developed for grid deployment was the shielded-core design. Basically, the device resembles a transformer with the secondary side shunted by a high temperature switch (HTS) element. During a fault, increased current on the secondary causes the HTS element to quench, resulting in a voltage increase across L1 that opposes the fault current.

This type of SFCL allows the HTS cryogenic environment to remain mechanically isolated from the rest of the circuit. An electrical connection is made between the line and the HTS element through mutual coupling of AC coils via a magnetic field.

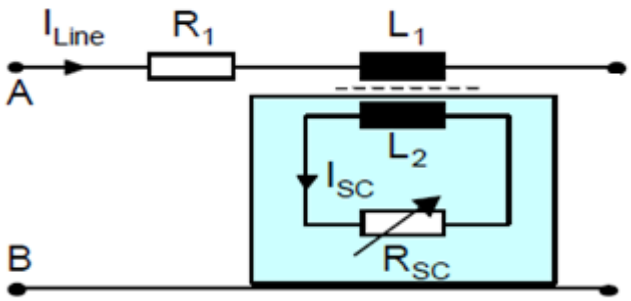

Figure 2-7: Equivalent circuit of shielded core SFCL [10]

Although the superconductor in the shielded-core design has to re-cool after a limiting action just like the resistive type, non-uniform heating of the superconductor (hot spots) is easier to avoid through optimization of the turns ratio. A major drawback of the shielded-core technology is that it is, almost, four times the size and weight of purely resistive SFCLs. [10]

II. Saturable-Core SFCL

Unlike resistive and shielded-core SFCLs, which rely on the quenching of superconductors to achieve increased impedance, saturable-core SFCLs utilize the dynamic behavior of the magnetic properties of iron to change the inductive reactance on the AC line.

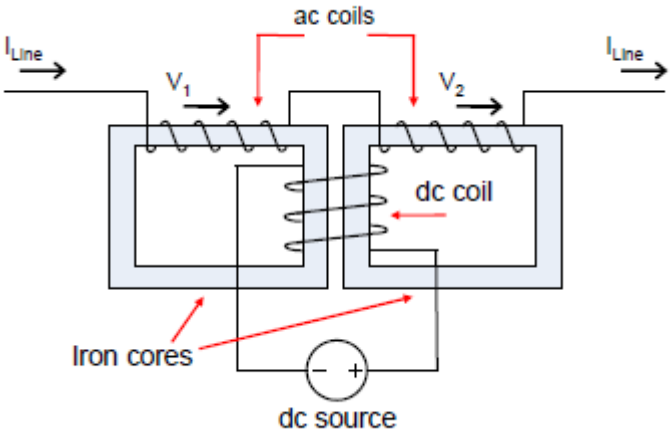

Figure 2-8: Internal circuit of saturable-core SFCL [10]

Under nominal grid conditions (when the AC current does not exceed the maximum rating for the local system), the HTS coil fully saturates the iron so that it has a relative permeability of one. To the AC coils, the iron acts like air, so the AC impedance (inductive reactance) is similar to that of an air-core reactor. Therefore, we do not have core loss due to the load current. Under this conditions, the voltage and current waveforms are basically unaffected by the saturable- core SFCL.

Under fault conditions, the negative and positive current peaks force the core out of saturation, resulting in increased line voltage drop of the line coil in each half cycle. The result is a considerable reduction in peak fault current. During a limiting action, the dynamic action of the core moving instantaneously in and out of saturation produces harmonics in the current waveform.

Unlike resistive SFCLs, which may require time between limiting actions to cool the superconducting components, the saturable-core approach can manage several actions in succession because the superconductor does not quench. And, the high temperature superconductor is used only for the purpose of deduction in operating loss and to get compact size of the winding. In fact, as a principle of operation, the superconductor has no role.

A major drawback of saturable-core SFCL technology is the volume and weight associated with the heavy iron core; however, manufacturers hope to improve this issue in future prototypes.

Table 2-1: Comparison in general characteristics of SFCL [10]

Technology	Losses	Triggering	Recovery	Size/weight	Distortion
Purely resistive SFCL	Hysteretic (dependent on HTS material)	Passive	HTS conductor must be re-cooled	Potential to be small. Because HTS performs limiting action	Only during first cycle
Hybrid resistive SFCL	Hysteretic (amount depends on HTS material)	Passive or active	Much faster than the purely resistive because less energy is deposited in the HTS	Potential to be small, but additional components may increase size	Only during first cycle
Saturable-core SFCL	DC power required to saturate the iron core and joule heating in conventional conductors	Passive	Immediate	Large and heavy due to iron core and conventional windings	Some caused by nonlinear magnetic characteristic
Shielded-core SFCL	Hysteretic (amount depends on HTS materials)	Passive	Faster than purely resistive, but re-cooling required	Large and heavy due to iron core and windings	Only during first cycle

2.4. Selection of Type of Superconductor Fault Current Limiter

Various SFCL types and technologies are being considered, but technology stakeholders have focused on hybrid resistive and saturable-core designs for technical and economic reasons [4]. The technology toward using resistive SFCL is carrying out majorly in two ways. These are hybrid resistive SFCL cable and hybrid resistive SFCL module. Resistive superconducting cable

needs a long area to be installed and so it is installed outside of substation. Therefore, it is mostly used to connect two substations or a substation to a long transmission line.

Therefore, to use SFCL for the substation, hybrid resistive module and saturable-core will be the best choices of this research.

From the comparison data given in Appendix A from EPRI 2012 Technology Watch [11], it can be observed the following important comparative points between the two technologies. The comparison is done between typical recently installed hybrid-resistive SFCL and saturable-core SFCL.

Hybrid resistive SFCL

- Applies full of superconductor principle of operation.
- Since, it requires larger length of superconductor material, extra fast switching device and shunt reactor, by estimation, it is costlier.
- Requires smaller area and weight for a given current rating.
- Additional task to cooperate the fast responding switch.

Saturable-core SFCL

- As principle of operation, it does not have superconductivity application in fault current limiting. The superconductor works only to saturate core of the transformer
- In addition to coil of superconductor, it has two coils for a single line and totally six coils in spider arrangement. These all coils make it with a larger area requirement to be installed.

Since this research titled and intended to be deal with direct application of superconductor for current limiting, the researcher decides to design and model a hybrid resistive SFCL rather than a saturable-core SFCL.

Hybrid SFCLs have two types. The first type of SFCL is a first peak non-limiting type used to limit a fault current after a half cycle of the fault current. This type is reliable enough to meet the reclosing operation requirement for power systems [8]. This type also has an advantage in that an overcurrent relay of a power line with an SFCL operates rapidly in a power fault

condition because the SFCL does not limit the first peak of the fault currents and no need of new protection setting.

The mechanism of operation of a first peak non-limiting hybrid SFCL can be explained by explaining the different fault current paths shown in Figure 2-9. Load current flow through Path-1 under normal state. During normal state, Contact-1 and Contact-2 of the Fast switch are closed and open respectively.

When a fault occurs in the power system, then the fault current flows through the HTS. Immediately, the HTS is quenched because the HTS current is higher than a critical current of the HTS. The resistance of the HTS increases in the quenching state. Currents of over 90% (the maximum SC current is almost ten times of the maximum load current with consideration of 20% initial current increment) of the total current detour through the Driving coil. So, at this instant, the current follow Path-2 in Figure 2-9 that is starting from the source, then passing through Driving coil and HTS, and finally trough Contact-1.

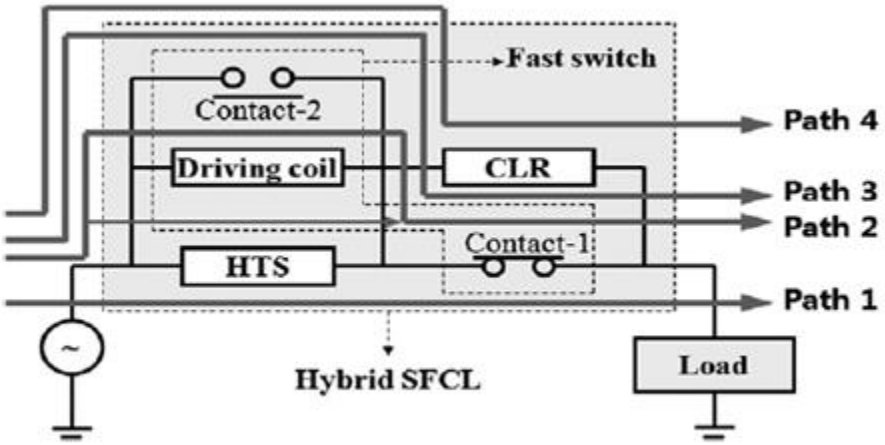

Figure 2-9: Current flow paths of the SFCL at normal and fault conditions [8]

This fast switch starts to operate after current flowing through the driving coil induces enough electromagnetic force. Contact-2 of the fast switch is then closed and most of the current flows through contact-2. At the same time, contact-1 is mechanically opened, but contact-1 is still electrically closed due to arcing. So, at this point in time, the fault current flows through contact-1 as seen in Path 3 in Figure 2-9.

Contact-1 becomes electrically open, when the fault current flowing through the contact-1 becomes zero and the electric arc on the contact is removed. The fault current then flows through the CLR and is limited by the Z_{shunt} as seen in Path 4 of Figure 2-9.

In transition from non-limiting period (i.e. Path-2 and Path-3 fault current flowing time) to limiting period (Path-4 fault current flowing time), the fast switch needs high current interrupting capacity on Contact-1. Due to this basic requirement, first peak non-limiting hybrid SFCL is installed with the main circuit breaker of the line integrated as the fast switch.

The second improved type of SFCL is a first peak limiting type that limits a fault current within a half cycle of the fault current. This type of SFCL is suitable for boosting up fault current liming capacity of an existing line CB.

The first peak non-liming hybrid SFCL still has the reclosing problem to meet requirements of utilities [8]; for EEP case, reclosing time of a line after fault is in seconds range. And, it also requires design with consideration of protection coordination of relays.

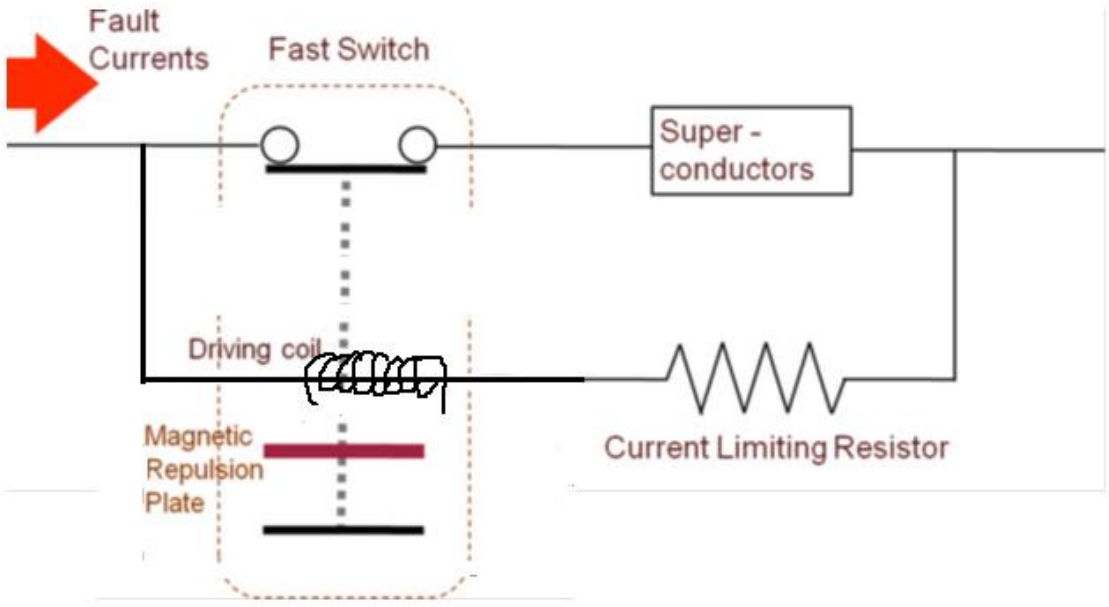

Figure 2-10: Components and circuit diagram of improved hybrid FCL

3. MODELING OF AKAKI-II SUBSTATION AND SUPERCONDUCTOR FAULT CURRENT LIMITER

3.1. Introduction

In this chapter, methods of modelling substation and modelling of SFCL are represented. The overall substation of Akaki II is represented in ETAP software by modelling each components of the substation using appropriate models. And, selectively, the problematic bus-bar is simulated with the designed SFCL to show the impact of the SFCL to limit the fault current.

3.2. Modeling of Akaki-II Substation

For the short-circuit analysis of the substation, ETAP is used as a simulating software. It is a fully graphical enterprise package that runs on Microsoft® Windows® 2003, 2008, 2012, XP, Vista, 7, and 8 operating systems.

ETAP is the most comprehensive analysis tool for the design and testing of power systems available. Using its standard offline simulation modules, it can utilize real-time operating data for advanced monitoring, real-time simulation, optimization, energy management systems, and high-speed intelligent load shedding. [12]

ETAP has been designed and developed by engineers for engineers to handle the diverse discipline of power systems for a broad spectrum of industries in one integrated package with multiple interface views such as AC and DC networks, cable raceways, ground grid, geographical information system (GIS), panels, arc flash, protective device coordination/selectivity, and AC and DC control system diagrams.

ETAP allows you to easily create and edit graphical one-line diagrams (OLD), underground cable raceway systems (UGS), three-dimensional cable systems, advanced time-current coordination and selectivity plots, schematics GIS, as well as three-dimensional ground grid systems (GGS).

The author decides to do the SC analysis of the substation network using this software. This is because, ETAP has a number of advance features related with one-line diagram for large networks. Therefore, SC analysis of the substation can be done in more clear and easy way.

Among the number properties that ETAP encompasses, the following listed ones are the most related with this paper study. [12]

i. Features

- Automatic one-line creation
- Automatic equipment connection mode
- Auto Disconnect & Reconnect
- Integrated 1-phase, 3-phase, and DC systems
- Integrated one-line diagram and underground raceway systems
- Typical data for motors, generators, transformers, reactors, governors, and exciters
- English and metric unit systems
- Export one-line diagrams to third party CAD systems via.dxf and metafile formats
- One-line templates
- Auto-update SC current

ii. AC Element, one-line Diagram

- Bus/node
- Transformer, 2-winding
- Transformer, 3-winding
- Cable
- Transmission line
- Bus duct
- Capacitor
- Panel systems
- Harmonic filter
- Remote connector
- Phase adapter
- Static Var Compensator (SVC)
- Reactor, current,-limiting
- Impedance
- Power grid (utility system)
- Synchronous generator
- Fuse
- Circuit breaker

iii. Libraries

- Motor nameplate
- Motor circuit model
- Fuse (Manufacture Published data)
- Relay (Manufacture Published Time-Current Characteristic Curves)
- HV & LV CBs (Manufacture Published Data)

iv. **Short-circuit Analysis**

- Complete compliance with ANSI/IEEE C37 series
- Complete compliance with IEC 60056, 60282, 61363, 60781, 60909, 60947
- IEEE standard 141 and 399, UL 489
- New Arc Flash analysis module (NFPA 70E-2000) for determining incident energy and access arc flash protective boundary (ANSI and IEC)
- Extensive manufacturer data for fuses, LV and HV breakers
- Automatic crest and interrupting duty comparison
- Automatic alert view to display critical and marginal limit violations
- 3-phase, line-line, line-ground, and line-line-ground faults
- Fault impedance (Z_1 and Z_0)
- CB duty calculation based on the maximum-through fault current (ANSI)
- Check making and breaking capability of protective devices against fault currents

The SC analyzer has three options of periods to represent sub-transient, transient and steady-state SC currents. These a SC fault current responses are represented in ETAP by $^1/_2$ cycle RMS value, $^1/_2$ to 4 cycles RMS value and after 30 cycles RMS value respectively. But to determine CBs' current breaking capacity, half cycle analyzer results are taken.

In the SC analysis of the substation using ETAP, there are a number of approaches taken to represent the whole power network of the substation in the software. To understand the simulation diagram, result and discussion, all the components of the substation are represented in the substation as follow.

3.2.1. The shunt reactor modeling

As it can be seen in Figure 4-4, shunt reactor of Sodo-II-line-2 incoming line is not connected. Because it is assumed that the voltage increment of Sodo-II line, due to Ferranti effect after distance from Sodo to Gellan (AkAki), is not exist in the software. Therefore, there is no need of connecting the substation shunt reactor in ETAP for SC analysis.

3.2.2. The autotransformer modeling

ETAP does not have auto-transformer as a power transformer. Therefore, the author should get a convenient SC autotransformer model that enables to represent autotransformers using available power transformers in ETAP. So, Nasser Tleis' model is used [7] pp 230 - 240. The overall derivation of the modelling is shown in below.

Three-phase autotransformers in the substation have star-star connected windings as depicted in Figure 3-1 (a). The common neutral point of the star-star connection require the two networks they interconnect to have the same earthing arrangement.

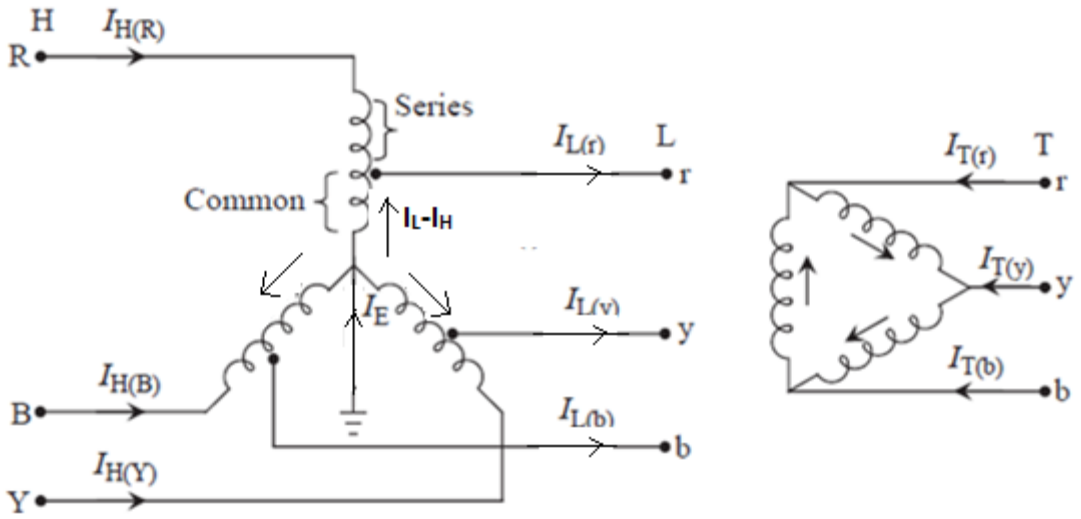

(a) 3-phase electrical diagram of the substation autotransformers

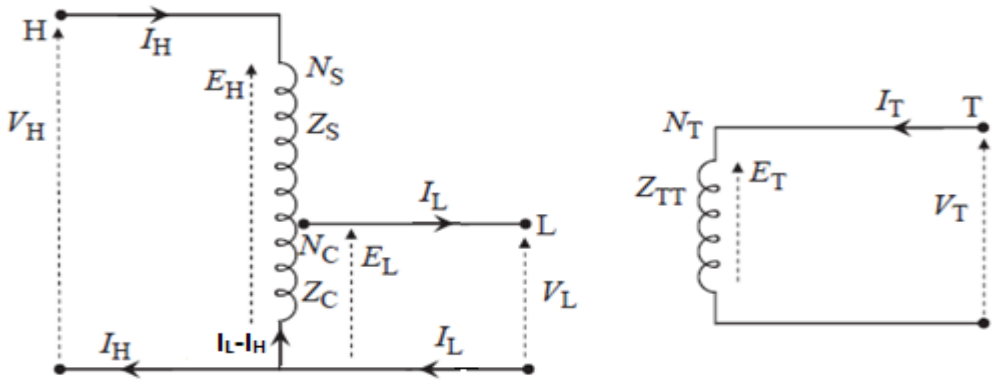

(b) Single-phase electrical representation

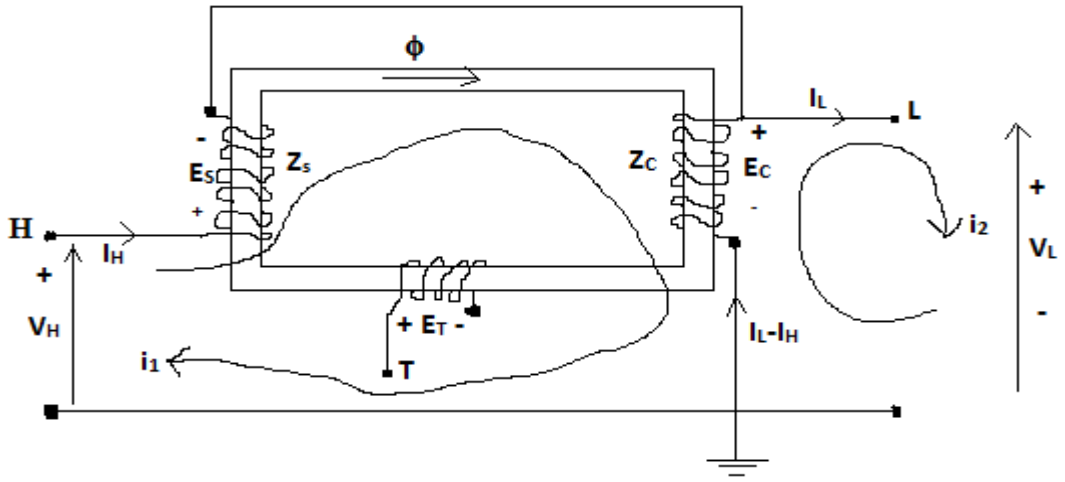

(c) Single-phase physical arrangement

Figure 3-1: Star-star autotransformer with a delta tertiary winding

Using S, C and T to denote the series, common and tertiary windings, we can write Kirchhoff's current law on both high and low voltage side in the loops shown in Figure 3-1 (c).

KCL on high voltage side,

$$-\boldsymbol{V_H + E_S + E_C + Z_S I_H + Z_C(I_H - I_L) = 0\ but, E_H = E_S + E_C} \quad \textbf{(3.1-a)}$$

$$\boldsymbol{\Longrightarrow E_H = V_H - Z_S I_H - Z_C I_H + Z_C I_L} \quad \textbf{(3.2-b)}$$

KCL on the low voltage side,

$$\boldsymbol{V_L - E_S - Z_C I_H + Z_C I_L = 0\ but, E_S = E_L} \quad \textbf{(3.2-a)}$$

$$\boldsymbol{\Longrightarrow E_L = V_L - Z_C I_H + Z_C I_L} \quad \textbf{(3.2-b)}$$

KCL on the tertiary winding side,

$$\boldsymbol{V_T - E_T = Z_{TT} I_T} \quad \textbf{(3.3-a)}$$

$$\boldsymbol{\Longrightarrow E_T = V_T - Z_{TT} I_T} \quad \textbf{(3.3-b)}$$

From the turn ration,

$$\boldsymbol{N_{HL} = \frac{1}{N_{LH}} = \frac{E_H}{E_L} \Longrightarrow E_H = N_{HL} E_L} \quad \textbf{(3.4)}$$

$$N_{HT} = \frac{1}{N_{HT}} = \frac{E_H}{E_T} \Longrightarrow E_H = N_{HT}E_T \quad \textbf{(3.5)}$$

Inserting Equation 3.2-b in Equation 3.4 and equating with Equation 3.1-b,

$$V_H - Z_S I_H - Z_C I_H + Z_C I_L = N_{HL}V_L - N_{HL}Z_C I_H + N_{HL}Z_C I_L \quad \textbf{(3.6-a)}$$

$$\Longrightarrow V_H - Z_S I_H - Z_C I_H + N_{HL}Z_C I_H = N_{HL}V_L + N_{HL}Z_C I_L - Z_C I_L \quad \textbf{(3.6-b)}$$

Inserting Equation 3.3-b in Equation 3.5 and equating with Equation 3.1-b,

$$V_H - Z_S I_H - Z_C I_H + Z_C I_L = N_{HT}V_T - N_{HT}Z_{TT} I_T \quad \textbf{(3.7)}$$

But, from MMF balance for the magnetic circuit in Figure 3-1 (c), ignoring no-load current,

$$I_H - \frac{I_L}{N_{HL}} + \frac{I_T}{N_{HT}} = 0 \quad \textbf{(3.8-a)}$$

$$\Longrightarrow I_L = N_{HL}I_H + \frac{N_{HL}}{N_{HT}} I_T \quad \textbf{(3.8-b)}$$

Inserting Equation 3.8-b in Equation 3.7,

$$V_H - Z_S I_H - Z_C I_H + Z_C N_{HL} I_H = N_{HT}V_T - N_{HT}Z_{TT} I_T - \frac{N_{HL}}{N_{HT}} I_T Z_C \quad \textbf{(3.9)}$$

Equation 3.6-b and Equation 3.9 can be represented by the star equivalent circuit, shown in Figure 3-1, containing two two-winding transformers as for a three-winding transformer.

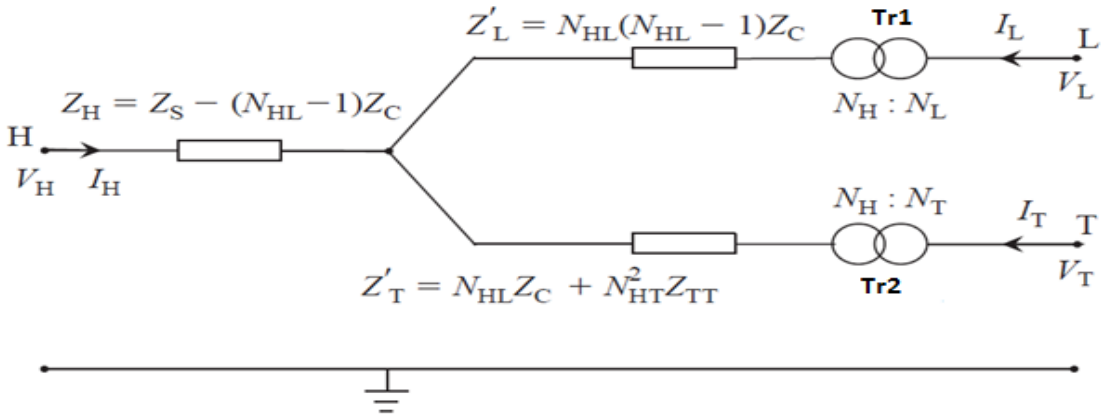

Figure 3-2: Auto-transformer's equivalent circuit in actual physical units

If similar conductor is used for common, series and tertiary winding,

$$N_{HL} = \frac{Z_S + Z_C}{Z_C} \Longrightarrow Z_S + Z_C - N_{HL} Z_C = 0 \quad \textbf{(3.10)}$$

$$N_{HT} = \frac{Z_S + Z_C}{Z_{TT}} \Longrightarrow Z_S + Z_C = N_{HT} Z_{TT} \quad \textbf{(3.11)}$$

For stabilizing autotransformers' tertiary winding, the brunched ideal transformer (N_H/N_T) should be left unconnected with other network. But, for proper representation of zero sequence impedance of the tertiary winding, its primary and secondary windings should be connected in star-star solidly grounded.

3.2.3. The feeders (incoming/outgoing) modeling

All these feeders of the substation can be categorized into three groups for good determinations of parameters for SC analysis.

- **Incoming lines:**
  - Always bring real power toward the substation. E.g. Sodo-II-line
  - They are modelled in the simulation by '*Power Grid*' component.
  - Parameters of MVA_{sc} rating and X/R ratio for the 'power grid' component are determined by considering the transmission line impedance, length and operating voltage.

$$I.e.MVA_{sc} = \frac{{V_n}^2}{Z_{TL,400KV} + Z'_G} \quad \textbf{(3.12)}$$

Where, V_n is operating voltage of the transmission line

$Z_{TL,\ 400kV}$ represents impedance of 400kV transmission line.

- **Grid connecting feeders:**
  - The real power flow either toward the substation or the reverse depends on power flow direction in ring connected power grid network. E.g. Sebeta II line, KAlity 1 L_1 (D_1), KAlity 1 L_2 (D_2), KokA L_1, KokA L_1, KAlity 1 L_1 (E_2), KAlity 1 L_2 (E_3), …

- They are modeled in the simulation by '*Composite Network'* internally having a parallel connection of '*Power Grid*' and 'Static Load' with controlling switch to bring in/out according to the operating power flow direction.
- MVA_{sc} rating of the '*Power Grid*' is determined from the upstream adjacent bus-bar MVA_{sc} rating and the connecting TL impedance. But, with no need of widened network analysis and collection of data, it would be a fair assumption that the upstream adjacent transformers have similar MVA_{sc} rating of transformers in Gellan substation at the same operating voltage.
- If once the total SC impedance of transformers in connected substations is given, we can say we have the MVA_{sc} rating after some rearrangement. And, SC impedances of all transformers are given in Appendix B.

- **Outgoing feeders:**
  - Power flows from the substation to loads.
  - P.transfo.PT_1 (E_{14}) is modeled using 'Static Load'. Because, the transformer delivers real and imaginary power to residential load around AkAki and Glean.
  - Yesu Line (E_8) cannot be modeled by a synchronous motor because when we see the complex power flow, the imaginary power flows toward the substation most of the time. Therefore, it is represented by a composite network having 'Static Load' and ''Power Grid". The MVA_{SC} for the "Power Grid" can be taken from the maximum load of the factory, 50MVA. Taking a typical synchronous motor from in ETAP with 50MVA at 94% power factor, the MVA_{sc} of Yesu is represented.

3.3. Superconductor Fault Current Limiter modeling

The selected software to get modeling of SFCL designed for the substation is Matlab/Simulink. The most convenient way to model electro-thermal-magnetic property of superconductor would be in using software of electromagnetic transient analyzer softwares like ATP/EMTP. Because of unavailability of these softwares in full version, the researcher forced to use a method of modelling superconductor behavior using combinations of blocks in Matlab/Simulink.

The YBCO superconductor material is represented in software by using its electrical and thermal behavior.

The electrical processes in YBCO superconductor are defined by the following equations. [13]

$$\boldsymbol{div(\sigma(j,T)gradV) = 0} \quad \textbf{(3.13)}$$

Where σ(j,T)*grandV = σ(j,T)*E = j; And, j is current density; σ(j,T) is electric conductance; V is electric potential; And, E is electric intensity.

And, thermal processes in superconductor are governed by the following equation. [13]

$$\boldsymbol{c(T)\rho\frac{\partial T}{\partial t} = div(\lambda(T)gradT) + \sigma(j,T)E^2} \quad \textbf{(3.14)}$$

Where, c(T) is superconductor thermal capacity per kilogram, λ(T) is superconductor thermal conductance, ρ is density of superconductor material, j is current density.

If the heat of SC current is assumed immediately distributed all over the superconductor mass through shunt silver conductor, then gradT will be zero. Therefore, this leads to the relation. [9]

$$\boldsymbol{E_{lim} = \sqrt{\frac{\rho c_p \Delta T_{max}}{\Delta t}}} \quad \textbf{(3.15)}$$

As ref. [13], electrical conductivity of superconductor can be given as:

$$\boldsymbol{\sigma(j,T) = \begin{Bmatrix} \sigma_s, (j < j_c(T)) \\ \frac{\sigma_n}{1+\alpha_\rho*(T-T_c)}, (j < j_c(T)) \end{Bmatrix}} \quad \textbf{(3.16)}$$

Where is σ_s electrical conductivity of superconductor in superconducting state, σ_n is electrical conductivity of superconductor in normal state, T_c is critical temperature of superconductor, is coefficient that defines change of electrical resistance with heating, $j_c(T)$ is critical current density of superconductor that is a function of temperature. But, since the excess fault current is the cause of temperature beyond designed cooling temperature, it the critical current density can be taken at $77K^0$.

By taking the inverse of the property given in Equation 3.16, easily relation of resistance of superconductor with temperature can be as follow.

$$R/R_0 = 1 + \alpha(T - T_0) \quad \textbf{(3.17)}$$

4. DESIGN OF SFCL AND SIMULATION STUDIES

4.1. Introduction

Simulation of SC analysis of the substation with/without SFCL is presented in this chapter using the models expressed in the previous chapter. Also, depending on SC analysis of the substation without SFCL, designing of all components of SFCL is explained detail.

4.2. Short Circuit Analysis of the Substation without Superconductor Fault Current Limiter

The following basic data are used as input for the short circuit analysis.

I. **The substation circuit diagram**
II. **Average incoming complex power through all 400kV, 230kV and 132kV lines**
III. **Transformers' Data**
   - Equivalent impedances
   - losses
   - Turn ratio
   - Voltage drop
   - SC withstand time
IV. **CB's Data**
   - Current interruption capacity
   - Rated transient recovery voltage
V. **Feeders Equivalent Parameters**
   - Impedance value of the lines
   - Sub-transient impedance of directly connected generators
VI. **Power flow data**

The data related with specification of equipment and components of the substation are shown in the tables found in Appendix B. Other data collected from the substation by the researcher are given in the following tables Table 4-1 &Table 4-2.

Table 4-1: Monthly peak load of incoming and outgoing feeders of the substation

Line name	Voltage	Date / Hour	09/06/2016		17/06/2016		1/07/2016		18/07/2016	
			P (MW)	Q (MVAR)	P (MW)	Q (MVAR)	P (MW)	Q (MVAR)	P (MW)	Q (MVAR)
Sebeta II line (C_1)	**400KV**	11:00	124	79	127	70	123	96	99	100
		13:00	187	-95	103	25	119	-34	80	88
Sodo II line 2 (C_9)	**400KV**	11:00	-405	99	-408	96	-375	83	-305	101
		13:00	-669	133	-469	82	-531	113	-315	74
Kaliti 1 L_1 (D_1)	**230KV**	11:00	66	-39	73	-29	44	-30	25	-31
		13:00	140	07	93	-15	93	02	16	-17
Kaliti 1 L_2 (D_2)	**230KV**	11:00	69	-39	74	-28	46	-30	25	-28
		13:00	146	07	98	-14	95	03	30	-18
KokA L_1 (D_{11})	**230KV**	11:00	30	-39	24	-38	41	-48	42	-45
		13:00	26	-37	24	-36	46	-50	54	-56
Koka L_2 (D_{12})	**230KV**	11:00	25	-40	20	-41	37	-49	39	-46
		13:00	21	-39	17	-39	43	-52	51	-56
Kaliti 2 L_1 (E_2)	**132KV**	11:00	11	-28	11	-27	10	-22	05	-26
		13:00	34	-06	21	-18	19	-07	10	-15
KAliti 2 L_2 (E_3)	**132KV**	11:00	11	-26	11	-27	10	-22	5	-26
		13:00	33	-06	21	-18	19	-07	10	-15
Yesu line (E_8)	**132KV**	11:00	06	-16	07	-17	06	-14	03	-16
		13:00	20	-04	13	-11	11	-05	06	-10
KokA line (E_{11})	**132KV**	11:00	07	01	09	02	06	-01	12	0
		13:00	09	04	12	03	12	-01	14	0
KokA-D.Z.line (E_{12})	**132KV**	11:00	29	15	28	15	24	07	28	08
		13:00	30	15	29	12	34	09	30	05
KokA-ILG.Z.line (E_{13})	**132KV**	11:00	08	03	11	04	08	0	13	01
		13:00	12	05	15	05	17	0	18	0
P.transfo.PT_1 (E_{14})	**132KV**	11:00	09	06	04	03	09	06	01	01
		13:00	09	05	07	04	10	06	01	01

*****Negative power flow (real and imaginary) represents power flow toward the substation. Reversely, positive values are for the opposite power flow direction.

* The time 11:00 & 13:00 hours are taken because peak-load hours of the substation are around 10:00-14:00.

*This data uses to understand the power flow direction in the entire connections of the substation so that all feeders are able to be modeled for SC analysis.

Table 4-2: Parameters of Feeders (Overhead power lines) that have connection with the substation

	Line name	Un [kV]	R_{PS}[Ω/km]	X_{PS} [Ω/km]	C_{PS}[ηF/km]	l [km]	R_{ZS} [Ω/km]	X_{ZS} [Ω /km]	C_{ZS} [nF/km]
1	Sebeta II line (C_1)	400	0.019	0.3291	11.1	33	0.2108	0.9855	7
2	Sodo II line 2 (C_9)	400	0.0206	0.3082	12.5	267	0.2215	1.0163	7.1
3	KAlity 1 L_1 (D_1)	230	0.0739	0.4142	8.9	3	0.2466	1.2614	5.9
4	KAlity 1 L_2 (D_2)	230	0.0739	0.4142	8.9	3	0.2466	1.2614	5.9
5	KokA L_1 (D_{11})	230	0.0739	0.4142	8.9	66.4	0.2466	1.2614	5.9
6	KokA L_2 (D_{12})	230	0.0739	0.4142	8.9	66.4	0.2466	1.2614	5.9
7	KAliti 2 L_1 (E_2)	132	0.1906	0.4264	8.6	3	0.3678	1.3413	5.6
8	KAlity 2 L_2 (E_3)	132	0.1906	0.4264	8.6	3	0.3678	1.3413	5.6
9	Yesu line (E_8)	132	0.1836	0.4181	8.8	1	0.3637	1.3547	5.7
10	KokA line (E_{11})	132	0.1906	0.433	8.4	61	0.3717	1.3245	5.5
11	KokA-D.Z.line (E_{12})	132	0.1906	0.4264	8.6	29	0.3678	1.3413	5.6
12	KokA-ILG.Z.line(E_{13})	132	0.1906	0.4264	8.6	29	0.3678	1.3413	5.6

Since, it is important to find equivalent of autotransformer for SC analysis, let SC specifications (the manufacturer provided) be taken.

- SC at LV side of the 500MVA autotransformers (400kV/230kV/15kV)

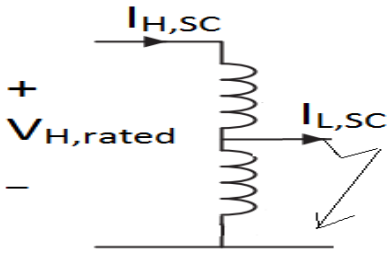

Figure 4-1: SC fault at low voltage side of the autotransformer

The SC specifications for these transformers are:

$I_{H,SC}$ = 5.77 kA, $I_{L,SC}$ = 10.04 kA, $V_{H,rated}$ = 400/√3 kV, $V_{L,SC}$ = 0, N_{HL} = 40/23 = 1.7391

and N_{HL} =80/3=26.667

Inserting these values on Equation 3.6-b and Equation 3.9,

$$\frac{400KV}{\sqrt{3}} - 5.77kA * Z_s - 5.77kA * Z_c + \frac{40}{23} * 5.77kA * Z_C = \frac{40}{23} * 10.04kA * Z_c - 10.04kA * Z_c$$

After some rearrangement,

$$\mathbf{5.77Z_S + 3.1561Z_C = 230.94\ \Omega} \quad \textbf{(4.1)}$$

And,

$$Z_S + \left(1 - \frac{40}{23}\right) Z_C = 0$$

$$\mathbf{\Rightarrow Z_S + 0.73913Z_C = 0} \quad \textbf{(4.2)}$$

Rewriting Equation 4.1 and Equation 4.2 inform of matrix,

$$\begin{bmatrix} 5.77 & 3.1561 \\ 1 & -0.73913 \end{bmatrix} \begin{bmatrix} Z_S \\ Z_C \end{bmatrix} = \begin{bmatrix} 230.94 \\ 0 \end{bmatrix} \Omega$$

$$\begin{bmatrix} Z_S \\ Z_C \end{bmatrix} = \begin{bmatrix} 5.77 & 3.1561 \\ 1 & -0.73913 \end{bmatrix}^{-1} \begin{bmatrix} 230.94 \\ 0 \end{bmatrix} \Omega = \begin{bmatrix} 23.0019 \\ 31.1203 \end{bmatrix} \Omega$$

For the tertiary winding, we use Equation 3.11 as follow.

$$Z_{TT} = \frac{Z_S + Z_C}{N_{HT}} = \frac{23.0019\Omega + 31.1203\Omega}{26.6667} = 2.0296\Omega$$

Then, all impedances in the equivalent circuit diagram shown in Figure 3-2 can be obtained as follow.

$$Z_H = Z_S - (N_{HL} - 1)Z_C = 23.0019\Omega - 0.73913 * 31.1203\Omega = 0\Omega$$

$$Z'_L = N_{HL}(N_{HL} - 1)Z_C = \frac{40}{23}\left(\frac{40}{23} - 1\right) 31.1203\Omega = 40.0034\Omega$$

$$Z_{L,pu} = \frac{Z'_L}{Z_{base,Tr1}}; where, Z_{base,Tr1} = \frac{{V_{base,Tr1}}^2}{S_{base,Tr1}} = \frac{(400kV)^2}{500MVA} = 320\Omega$$

$$\Longrightarrow Z_{L,pu} = \frac{39\Omega}{320\Omega} * 100\% = 12.5\%$$

$$Z'_T = N_{HL}Z_C + {N_{HT}}^2 Z_{TT} = \frac{40}{23} * 31.1203\Omega + \left(\frac{80}{3}\right)^2 2.0296\Omega = 1497.4\Omega$$

$$Z_{T,pu} = \frac{Z'_T}{Z_{base,Tr2}}; where, Z_{base,HV} = \frac{{V_{base,Tr2}}^2}{S_{base,Tr2}} = \frac{(400kV)^2}{150MVA} = 1066.6667\Omega$$

$$\Longrightarrow Z_{T,pu} = \frac{1486.6368\Omega}{10666.667\Omega} * 100\% = 14.04\%$$

Using the winding impedance voltage drop given in the transformers' specification, X/R ration of the transformers can be calculated. I.e.:

$$X/R = \frac{\sqrt{{Z_{W,pu}}^2 - {R_{W,pu}}^2}}{R_{W,pu}} \approx \frac{12.58}{0.00017} = 74000$$

- Similar result can be found for high voltage side SC fault analysis.
- For the 125MVA/230kV autotransformers, similar analysis has been taken to represent them by their equivalent model for the ETAP simulation.

In case of representing Sodo-II-line in the SC analysis software, the 400kV line covers the total distance from AkAki-II substation to Wallayta-Sodo. The capacitive value is assumed to be cancelled by the compensation of shunt-reactor at the substation.

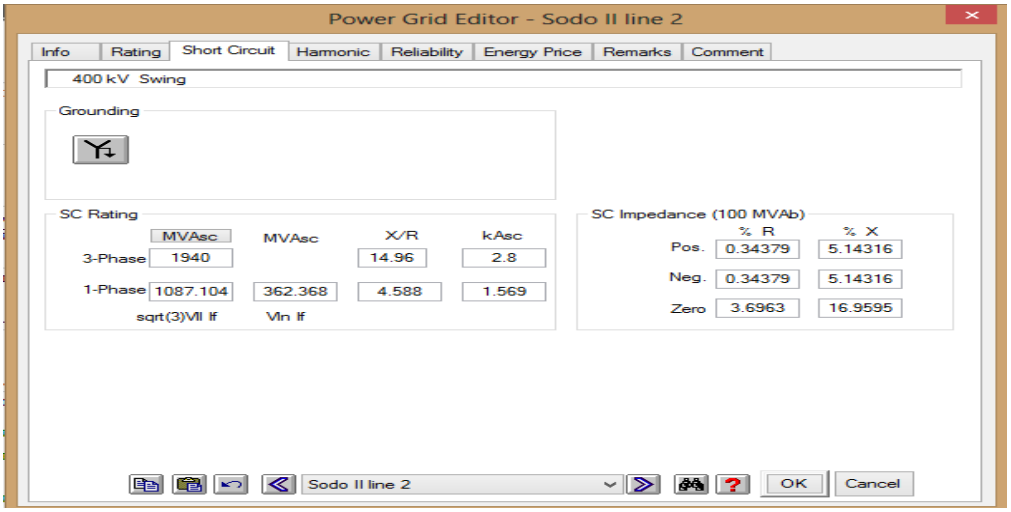

Figure 4-2: A dialogue box for feeding Power-Grid parameters

Equation 3.12 is going to be used to represent Sodo-II-line. Z'_G is equivalent generation units' impedance referred to 400kV side. But, comparatively to the total distance of the transmission line, it can be ignored.

$$Therefore, \boldsymbol{MVA_{sc}} = \frac{(\boldsymbol{400kV})^2}{\boldsymbol{267|0.0206+j0.3082|\Omega}} = 1940MVA$$

$$\text{And, } \frac{\boldsymbol{X}}{\boldsymbol{R}} = \frac{\boldsymbol{0.3082}}{\boldsymbol{0.0206}} = \boldsymbol{14.96}$$

As shown in Figure 4-2, automatically the software calculates the positive and negative impedances in percent if the MVA_{sc} and X/R ratio are fed. But, the zero-sequence should be edited to calculated value.

Another line from Sodo to AkAki is going to be connected upcoming years. Therefore, the MVA_{SC} would be double of the result in above.

The SC current rating KAlity 1-Line 1 and Line 2 are calculated as

$$\boldsymbol{MVA_{SC}} = \frac{\boldsymbol{V_n}^2}{\boldsymbol{|Z_{Tr}+Z_{TL}|}} \quad \textbf{(4.3)}$$

$$MVA_{SC} = \frac{230^2}{|j14.706 + 0.2217 + j1.2426|} = 1980.2MVA$$

The capacitive effect is ignored because it is short transmission line.

- ❖ Similarly, other grid connecting feeders can be represented.

Since, the substation is designed to distribute electrical power including power from GERD power plant; SC analysis of the substation should include the introduction of incoming line from GERD.

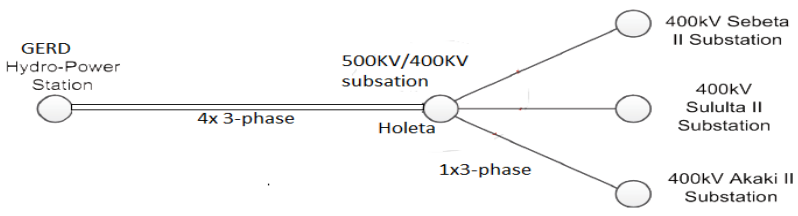

Figure 4-3: GERD-to-Holeta-AkAki II substation transmission line

As shown in the Figure 4-3, the incoming line from GERD power plant to the substation passes across Holeta substation. The lines from GERD to Holeta and Holeta to AkAki II are same with regard to their parameters. Their parameters and length are given in Table 4-3 & Table 4-4 below from the data gathered from contract agreement documents when the installer company is commissioned by EEP.

Table 4-3: GERD-to-Holeta-AkAki TL parameters

Transmission line section	**Length (km)**	**Land distance (km)**	**R_{PS} (Ω/km)**	**X_{PS} (Ω/km)**	**C_{PS} (nF/km)**
GERD to Dedesa	345	355.35	0.018627	0.269975	13.67949
Holeta to AkAki II	49.27	50.75	0.018627	0.269975	13.67949

Table 4-4: SC impedance parameter for a single 500kV/400kV, 750MVA Holeta Autotransformer

Description	**Specification**
Type	**Autotransformer**
Number of Phases	**Single**
Frequency	**50Hz**
SC impedance at nominal tap on OFAF base	**12.5**

Using the above data, the MVA_{SC} rating of the incoming line from GERD can be determined to model it in ETAP using 'Power Grid' component

$$MVA_{SC} = \frac{{V_n}^2}{|Z_{\substack{Tr@Holeta \\ equivalent}} + Z_{TL\_GERD\ to\ Holeta} + Z_{TL_{Holeta\ to\ Akaki}}|} \quad \textbf{(4.4)}$$

There is series capacitive reactance compensation at Dedesa for power transfer capacity increment. The compensation, there, reduces the total reactance by 50%. Additionally, the total shunt capacitive admittance can be ignored by the assumption that during connection to AkAki substation there would be a shunt reactor compensation to cancel the long TL capacitance effect.

Therefore, the impedance of TL from GERD to Holeta will be:

$$\boldsymbol{Z_{TL\_GERD\ to\ Holeta} = R_{TL} + j0.5X_{TL}} \quad \textbf{(4.5-a)}$$

$$\boldsymbol{\Longrightarrow Z_{TL_{GERD}to\ Holeta} = \iota_{TL} * (R_{PS} + j0.5X_{PS})} \quad \textbf{(4.5-b)}$$

$$Z_{TL\_GERD\ to\ Holeta} = \frac{345}{4}(0.018627 + \text{j}0.5 * 0.269975\ )\Omega\ Since, four\ parallel\ lines$$

$$\Longrightarrow Z_{TL_{GERD}to\ Holeta} = 1.6066 + j14.6427\Omega$$

The SC impedance for Holeta station will be one eight of a SC impedance of a transformer bay (3xsigle phase autotransformers). This is because there are eight transformer bays in parallel. The resistive impedance can be ignored when it is compared to the reactive impedance. Therefore, $Z_{tr@Holeta}$ is given as follow.

$$\boldsymbol{Z_{tr@Holeta} = \frac{1}{4} * Z_{\underset{pu}{tr}} * Z_{\underset{base}{tr}}} \quad \textbf{(4.6)}$$

$$But, Z_{\underset{base}{tr}} = \frac{(400kV)^2}{750MVA} = 213.33\ \Omega$$

$$\Longrightarrow Z_{tr@Holeta} = j\frac{1}{8} * 0.125 * 213.33\Omega = \ j3.33\ \Omega$$

And, the TL impedance from Holeta to AkAki is:

$$\boldsymbol{Z_{TL_{Holeta}to\ Akaki} = \iota_{TL} * (R_{PS} + jX_{PS})} \quad \textbf{(4.7)}$$

$$Z_{TL_{Holeta}to\ Akaki} = 49.27(0.018627 + \text{j}0.269975\ )\ \Omega$$

$$Z_{TL_{Holeta}to\ Akaki} = 0.9178 + j13.3017\ \Omega$$

During SC fault at AkAki II substation, Holeta to AkAkAi II TL becomes in parallel to the other grid network at Holeta busbar. So the equivalent impedance of $Z_{\_Holeta\ to\ AkAki}$ is smaller than the transmission line impedance due to the fact that the parallel external power grid network has finite impedance. Just by taking one fifth current ratio flowing to AkAkAi II and to the other network, the equivalent impedance will be 16% of the transmission line impedance.

$$Z_{TL_{Holeta}to\ Akaki} = 0.16 * (0.9178 + j13.3017)\Omega = \ 0.1468 + j2.1283\Omega$$

Now, calculating the MVA_{SC},

$$MVA_{SC} = \frac{400^2}{|(1.6066 + 0.1468) + j(14.6427 + 3.33 + 2.1283)|} = 7929.6917MVA$$

After all components of the substation are modeled, the whole substation one-line diagram representation looks like Figure 4-4 in ETAP software.

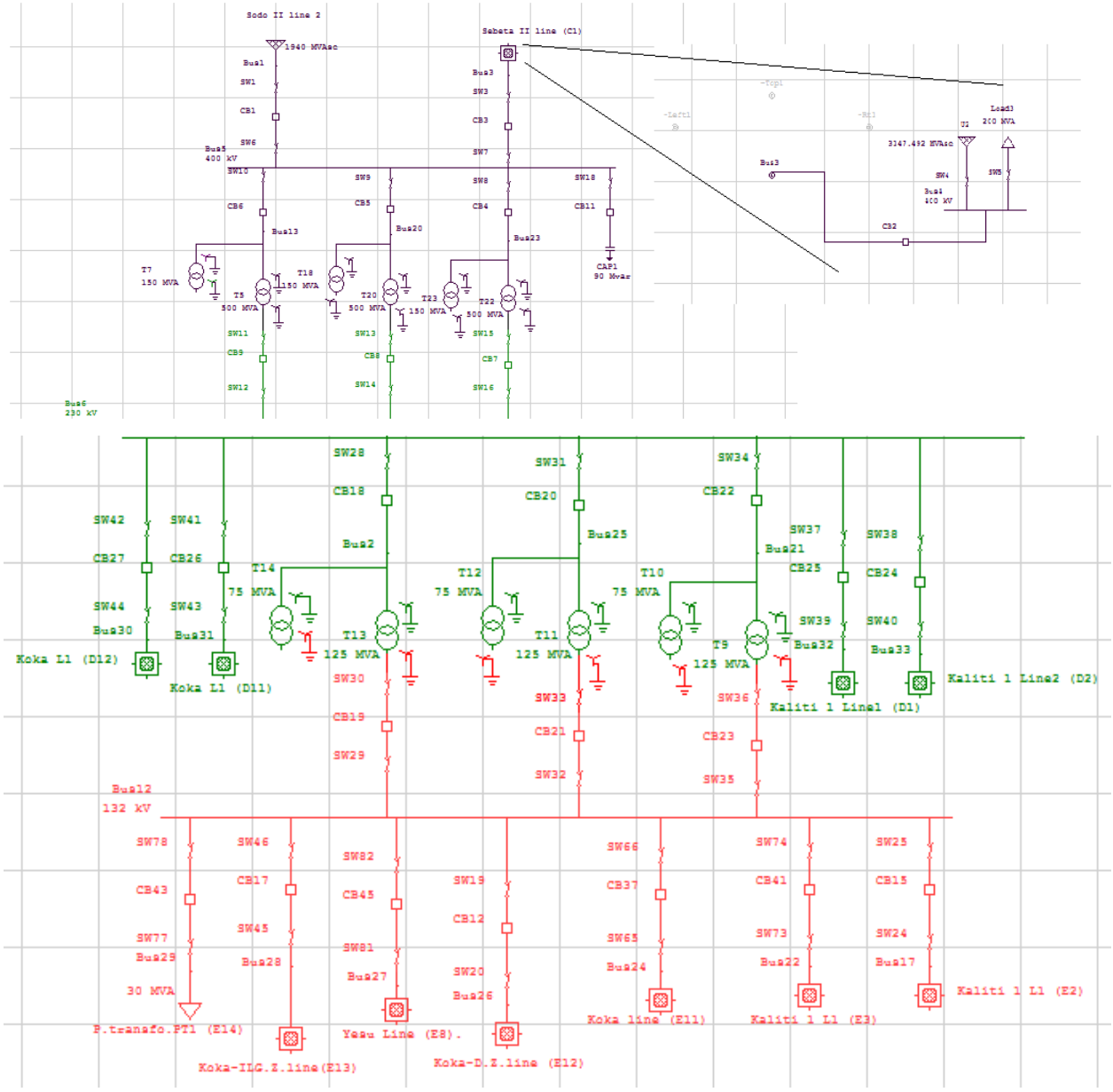

Figure 4-4: The substation one-line diagram

4.3. Design of Superconductor Fault Current Limiter

From the above SC analysis of the substation, an SFCL is needed to be installed between double bus-bars of 230kV, as shown in Figure 1-7. The maximum expected fault current at this bus-bar flowing through the CBs is obtained around 44kA. And, it is needed to bring into acceptable safety margin of the corresponding CB. So, the design SFCL aims to reduce this fault current into 35 kA.

The design of first peak limiting hybrid SFCL process includes designing of all components in the SFCL and complementary systems like cooling system. Determining of physical dimension of HT-superconductor material (YBCO CC), operating time of the fast switch, current capacity of energizing coil for the fast switch, the value of shunt resistor, cooling system, and total space requirement of the overall current limiter system should be done.

4.3.1. Determining the shunt resistor (CLR)

The SFCL superconductor module and shunt resistor together are to limit the fault current before the fast switch disconnects the superconductor. But, then, the CLR should limit the SC current to intended value (35kA, 70% of the CB breaking capacity) so that the CB can break safely.

Taking one of the line fault conditions in Figure 4-5 (let the fault is at bus-bar B),

$$\boldsymbol{I_{fault} = 2 * I_{\substack{f,contributed \\ from\ B}} \approx 44\ kA} \qquad \textbf{(4.8-a)}$$

And,

$$\boldsymbol{I_{limited} = I_{\substack{f,contributed \\ from\ B}} + I_{\substack{f,limited \\ from\ A}} = 35\ kA} \qquad \textbf{(4.8-b)}$$

$$\boldsymbol{\Rightarrow I_{\substack{f,limited \\ from\ A}} = I_{CLR} = 35\ KA - 22\ KA = 13\ kA} \qquad \textbf{(4.8-c)}$$

Figure 4-5 shows the circuit arrangement representing the substation during SC fault at one of the feeders near the connected bus-bar out of the two conductors. Where, V_a represents the voltage difference appears at the fault terminal of the bus-bars during fault. It reaches up to $^{230}/_{\sqrt{3}}$ kV per-phase. Assuming the two bas-bar conductors share equal SC rating (MVA_{SC}), two times of the positive sequence impedance of the system must be taken for each branch. (I.e. Z_{PSN}=2.84921Ω from Figure 4-13 C)

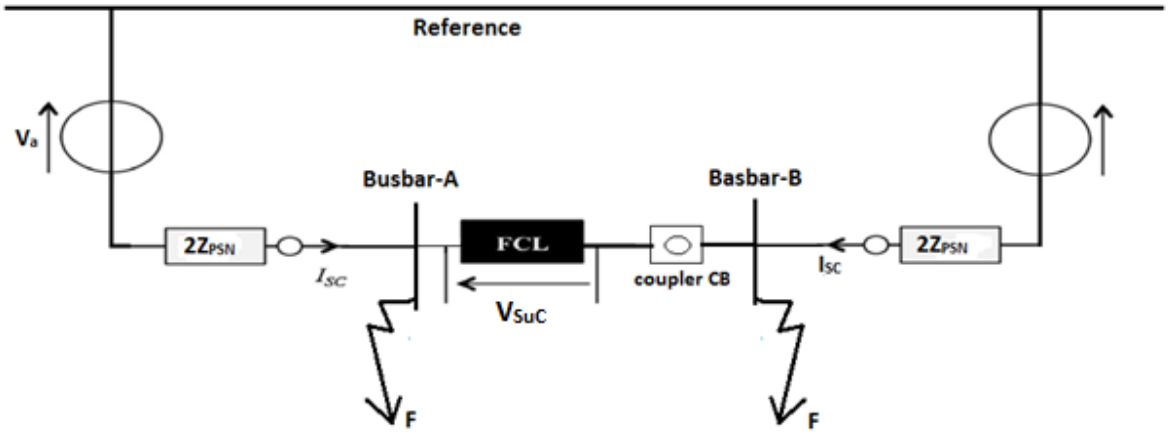

Figure 4-5: Simplified representation a clear symmetric SC fault at the bus-bar with SFCL

During quenching of the superconductor (means before shunt resistance takes over the limiting action lonely), the superconductor should develop a significant resistance to divert the SC current toward CLR.

The CLR is the only one to limit the SC for the CB after the fast switch excludes the superconductor. And if Z_{PSN} is assumed pure reactive due to its angle is approximately pure lagging (≈90^0), the value CLR to limit the SC current flowing through the bas-bar coupling is determined as follow.

$$\boldsymbol{R_{CLR}} = \sqrt{\left(\frac{V_a}{I_{f,limited\ from\ A}}\right)^2 - (2Z_{PSN})^2} = \sqrt{\left(\frac{230}{\sqrt{3}*13}\right)^2 - (2*2.85)^2}\Omega = 8.4764\Omega \qquad \textbf{(4.9)}$$

To determine voltage and power rating of the CLR,

$$\boldsymbol{V_{CLR} = I_{CLR} \times R_{CLR} = 13kA \times 8.4764\Omega = 110.1931kV} \qquad \textbf{(4.10)}$$

$$\boldsymbol{P_{CLR} = V_{CLR} \times I_{CLR} = 110.1931kV \times 13kA = 1432MW} \qquad \textbf{(4.11)}$$

Since, the shunt resistor works for a fraction of second intermittent task, the selected resistors can be overloaded ten times of the power rating. So, the design will be a CLR having ratings 143.2 MW, 4.111 kA and $8.476\ \Omega$ (one tenth of power rating on Equation 4.11).

Keeping high voltage gap requirement, CLR can be realized satisfying all the ratings. In Appendix D, the selected power resistor's specifications are given. 20 kW resistors ($\therefore$7160 resistors is optimum number) with range of 1-100 A current rating are selected to build a resistive load bank to realize the CLR.

Table 4-5: Combination of 20kW resistors to make up the CLR

I_c (A)	R (Ω)	N_p	R_p (Ω)	N_s	N_T	Equivalent CLR ratings			Remark
						I_{C_total}	R_{total}	$W_{total(W)}$	
1	20k	4111	4.865	2	9730	4111A	9.73Ω	194.6M	$\uparrow N_t$, $\cong$I, $\uparrow$R, & $\cong$W
5	800	823	0.972	9	7404	4115A	8.75Ω	148.1M	$\uparrow N_t$, $\cong$I, $\uparrow$R, & $\cong$W
10	200	412	0.485	18	7416	4120A	8.73Ω	148.3M	$\uparrow N_t$, $\cong$I, $\uparrow$R, & $\cong$W
15	88.88	274	0.324	26	7124	4110A	8.43Ω	142.5M	$\cong N_t$, $\approx$I, $\downarrow$R, & $\downarrow$W
20	50	206	0.243	35	7210	4120A	8.51Ω	144.2M	$\uparrow N_t$, $\cong$I, $\uparrow$R, & $\cong$W
25	32	165	0.194	44	7260	4125A	8.54Ω	145.2M	$\uparrow N_t$, $\cong$I, $\uparrow$R, & $\cong$W
30	22.22	137	0.162	53	7261	4110A	8.59Ω	145.2M	$\uparrow N_t$, $\approx$I, $\uparrow$R, & $\cong$W
35	16.33	118	0.138	62	7316	4138A	8.56Ω	146.3M	$\uparrow N_t$, $\cong$I, $\uparrow$R, & $\cong$W
40	12.5	103	0.121	70	7210	4120A	8.47Ω	144.2M	$\uparrow N_t$, $\cong$I, $\cong$R, & $\cong$W
45	9.88	92	0.107	80	7360	4140A	8.56Ω	147.2M	$\uparrow N_t$, $\cong$I, $\uparrow$R, & $\cong$W
50	8	83	0.096	89	7387	4150A	8.54Ω	147.7M	$\uparrow N_t$, $\cong$I, $\uparrow$R, & $\cong$W
55	6.61	75	0.088	97	7275	4125A	8.54Ω	145.5M	$\uparrow N_t$, $\cong$I, $\uparrow$R, & $\cong$W
60	5.56	69	0.081	105	7245	4140A	8.51Ω	144.9M	$\uparrow N_t$, $\cong$I, $\uparrow$R, & $\cong$W
65	4.73	64	0.074	115	7360	4160A	8.51Ω	147.2M	$\uparrow N_t$, $\cong$I, $\uparrow$R, & $\cong$W
70	4.082	59	0.069	123	7257	4130A	8.49Ω	145.1M	$\uparrow N_t$, $\cong$I, $\approx$R, & $\cong$W
75	3.556	55	0.065	131	7205	4125A	8.52Ω	144.1M	$\uparrow N_t$, $\cong$I, $\uparrow$R, & $\cong$W
80	3.125	52	0.060	142	7384	4160A	8.52Ω	147.7M	$\uparrow N_t$, $\cong$I, $\uparrow$R, & $\cong$W
85	2.768	49	0.056	152	7448	4165A	8.51Ω	149.0M	$\uparrow N_t$, $\cong$I, $\uparrow$R, & $\cong$W
90	2.469	46	0.054	157	7222	4140A	8.48Ω	144.4M	$\uparrow N_t$, $\cong$I, $\cong$R, & $\cong$W
95	2.216	44	0.050	170	7480	4180A	4.50Ω	149.6M	$\uparrow N_t$, $\cong$I, $\uparrow$R, & $\cong$W

$$N_T = N_P \times N_S \quad \textbf{(4.12-a)}$$

$$N_P = integer\left[\frac{4111}{I_c} + 1\right] \quad \textbf{(4.12-b)}$$

And,

$$N_s = integer\left[\frac{8.477}{R_p} + 0.5\right] = integer\left[\frac{8.477 \times N_P}{\frac{20KW}{I_C{}^2}} + 0.5\right] \quad \textbf{(4.12-c)}$$

In Table 4-5, the mathematical operators show how much required electrical criteria are satisfied. Where, '↑' means unnecessarily large, '↓' means unnecessarily small, '≈' means around the requirement, and '≅' means satisfying the criterion.

The economic combination of 20kW resistor is achieved at 40 A continuous current rating to satisfy all CLR ratings. Calculating space required to form the combination of 7210 resistors,

$$Sp_{required} = k_{connection}\mathbb{V}_t \quad \textbf{(4.13-a)}$$

Where, $K_{connection}$ is space factor left for connection. It is enough to be 1.2. And, V_t is the volume of the resistors that is given by,

$$\mathbb{V}_t = N_t \times \mathbb{V}_R \; and \; \mathbb{V}_R = L_3 \times D \times H \quad \textbf{(4.13-b)}$$

Where, the dimensions of a single resistor (L_3, D, & H) are given in Table D- 1.

$$\Rightarrow Sp_{required} = 1.2 \times 7210 \times 1120 \times 150 \times 260\ mm^3 = 378m^3 \quad \textbf{(4.13-c)}$$

4.3.2. Determining size of HT-superconductor

In normal operation of the grid the limitation should not be triggered by some limited over-currents. The rated current (I_a) of the grid is the maximum steady state current in RMS value but this current can be overstepped in transients for example when some large motors are starting.

Therefore it must be higher not only to the rated current (I_a) but to the peak current in the grid normal operation. This can be written($k_a * I_a$), with k_a multiplying factor taking into account all kind of possible transient increase of current and square root to change RMS value into amplitude.

The rated load current (I_a) is obtained from the maximum apparent power flowing through the bus-bar (230kV). Roughly, this apparent power is taken as equal as the total apparent rating of the three 400kV/230kV transformers.

Hence,

$$I'_a = \frac{3 \times 500MVA}{\sqrt{3} \times 400KV} = 2.165\ kA \quad \textbf{(4.14)}$$

Under equal load sharing between the two conductors of the bus-bar,

$$\frac{I_a = I'_a}{2} = 1.083\ kA \quad \textbf{(4.15)}$$

Considering starting currents (i.e. up to 20% above the rating) of rotating machines in the system and inrush current of distributing transformers, K_a is good to be taken 1.35 factor. The multiple of K_a and I_a will be the critical current (I_c) that the superconductor needed to have.

The thickness of the YBCO layer is fixed by the elaboration process of the manufacturer. So, the critical current rating of a single YBCO CC tape is, always, given in rate of its width (I c-w). So we get the conductor width:

$$W_{SC} = \frac{I_c}{I_{c-w}} = \frac{K_a I_a}{I_{c-w}} \quad \textbf{(4.16-a)}$$

Inserting the selected YBCO CC specification in Appendix C into Equation 4.16-a,

$$W_{SC} = \frac{1.35 \times 1.08KA}{300A/1.2cm} = 5.832cm \quad \textbf{(4.16-b)}$$

To find that much width of superconductor, it needs to have the following number of pieces of superconductor in parallel. These pieces will be laminated together to be wound as a single conductor.

$$N_{pieces} = \frac{5.832cm}{1.2cm/piece} \approx 5pieces \quad \textbf{(4.17)}$$

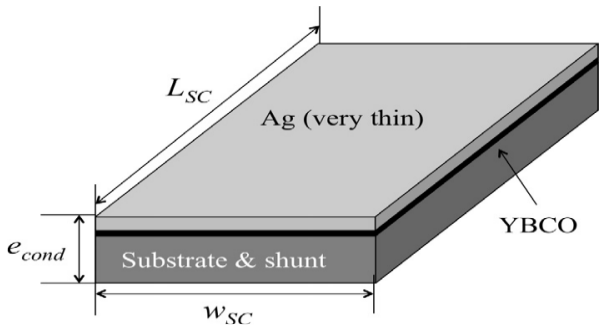

Figure 4-6: a typical YBCO CC material physical dimension [3]

$I_{c\text{-}w}$ depends on the tape performances and on the temperature. Already high (200–300 A/cm-w at 77 K^0) $I_{c\text{-}w}$ YBCO CC are available as shown in Appendix C. The capacity of YBCO CC will still rise in the following years. It increases by lowering the cooling temperature. The advantage of reducing amount of superconductor material is in trade-off with more complexes and costlier cooling system.

After the fast switch exclude the superconductor with CLR, all current limiting action is done by CLR. But, if the superconductor material is applied to quench fault current to the extent it warms up to 400K^0, the resistance of the superconductor developed during normal state can be calculated from the relation in Equation 3.17.

Here, T is the temperature and R is the resistance of CC. T_0 stands for a particular temperature and R_0 is the resistance of CC at T_0. 'α' is a constant. For selected YBCO CC, the constant is measured as 0.004.

Then the resistance at 400$K^0$of CC estimated to be

$$R_{SuC} = R_0[1 + \alpha(T - T_0)] \quad \textbf{(4.18-a)}$$

$$R_{SuC} = 0.4[1 + 0.004 * (400 - 283)]\ \mathrm{m\Omega}/cm = 0.5872\ m\Omega/cm \quad \textbf{(4.18-b)}$$

If superconductor and CLR share the SC current during period, they have equivalent resistance. So, the length of the superconductor will be

$$\iota_{SuC} = \frac{5R_{CLR}}{R_{SuC}} = \frac{5*8.4764\Omega}{0.5872\ m\Omega/cm} \approx 721.76m \quad \textbf{(4.19)}$$

This much long superconductor is not available in large scale size, commercially, even though plot projects are being done in different world companies to avail large scale (up to 2km) superconductors on the market. [14]

By using bifilar coils wound in two-in-hand configuration as shown in Figure 4-7 (b), a number of single superconductor pieces are combined and make a required length of superconductor material. Wire of 10 m and 5.83 cm axial length of 2G YBCO is wound on a circular rail, as shown in Figure 4-7 (c). Each end of the superconducting line was connected to a copper block by soldering. To minimize the resistance, the copper block was sufficiently large, and the lines were soldered carefully. And, there would be 73 plates are required to make up the total module coil.

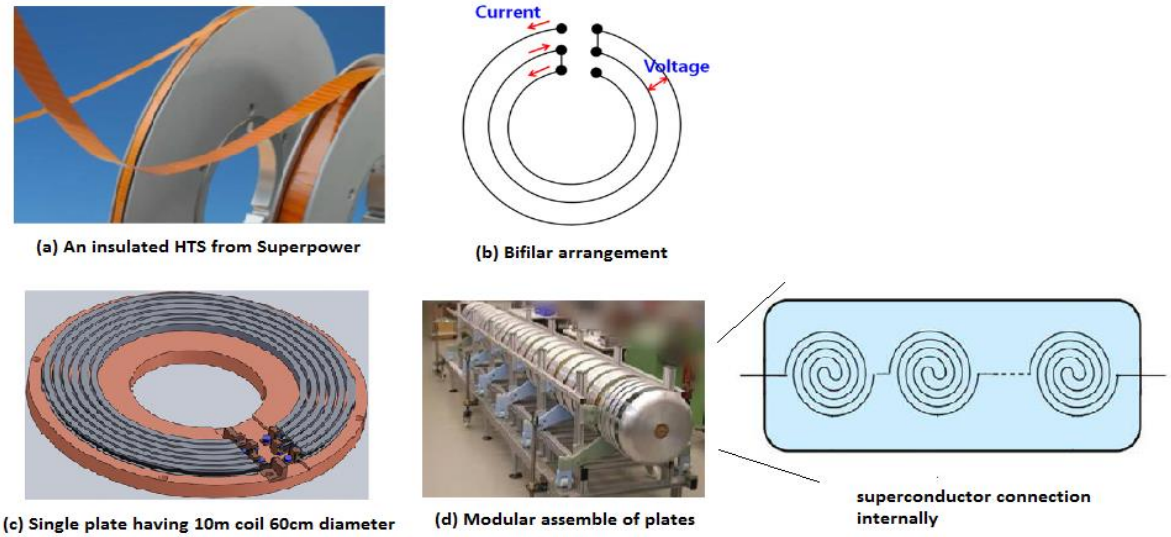

Figure 4-7: Arranging superconductor for current limiting application

The voltage gradient that is assigned that superconductor to bear has a limit. This voltage constraint gives the minimum length requirement when it's computed with V_{sc}. Voltage gradient of an YBCO CC materials is the value of E_{lim} given in Appendix C.

The voltage across the superconductor quenching (i.e. V_{SuC}) depends on the superconductor quenching resistance. Since, the maximum quenching resistance is designed to be equal with CLR and as well as the superconductor and the CLR are in parallel up to the fast switch disconnects, the maximum voltage appears across the superconductor will be half of V_{CLR} on Equation 4.10.

$$\boldsymbol{V_{SuC} = \frac{V_{CLR}}{2} = \frac{110.193\text{KV}}{2} = 55.0966kV} \quad \textbf{(4.20)}$$

To check the voltage gradient of the design is less than the rating,

$$\boldsymbol{\frac{V_{SuC}}{\iota_{SuC}} = \frac{55.0966kV}{721.76m} = 76.34V/m < 145V/m = E_{lim}} \quad \textbf{(4.21)}$$

The total volume of the resistive superconductor module (V_{module}) is calculated as:

$$\boldsymbol{\mathbb{V}_{module} = A_{cross-section} \times \iota_{module}} \quad \textbf{(4.22-a)}$$

$$\boldsymbol{A_{cross-section} = A_{plate} = r^2\pi = 30^2\pi cm^2 = \frac{0.283m^2}{phase}} \quad \textbf{(4.22-b)}$$

$$\boldsymbol{\iota_{module} = N_{plates} \times thickness_{plate} = 73 \times 10cm = \frac{7.3m}{phase}} \quad \textbf{(4.22-c)}$$

$$\boldsymbol{Hence, \mathbb{V}_{module} = 0.283m^2 \times 7.3m = \frac{2.07m^3}{phase}} \quad \textbf{(4.22-d)}$$

Therefore, land area occupied by the module,

$$\boldsymbol{A_{land} = 0.6m \times 7.3m \approx 4.38m^2/phase} \quad \textbf{(4.23)}$$

4.3.3. The fast switch

The total time delay taken by the fast switch to separate the superconductor and divert all the SC current (i.e. 35 kA at maximum) toward the shunt resistor can be determined by two factors. And, there is a trade-off between these two factors.

The first factor is that as much as the more fast switching time is selected the more reduction cost in cooling system of the superconductor.

And, the second one will be the fault current flowing through the superconductor and needed to be interrupted by the fast switch. The resistance of superconductor needs time delay to develop sufficient resistance. This factor also has to be optimized; otherwise, it requires more cost in regarding large current breaking capacity rating of fast switch.

To optimize the above two factors, the fast switch can operate after half of the SC current is limited by the superconductor. During this, CLR and the superconductor are in parallel and having equal resistance. Therefore, the SC current flowing through the superconductor (i.e. the fast switch breaking capacity) is calculated as follow.

$$\boldsymbol{I_{SuC} = \frac{1}{2} * I_{SFCL} = \frac{1}{2} * \frac{V_a}{\sqrt{(2*Zpsn)^2+\left(R_{CLR}/_2\right)^2}}} \quad \textbf{(4.24-a)}$$

$$\boldsymbol{\Rightarrow I_{SuC} = \frac{1}{2} * \frac{132.79kV}{\sqrt{(2*2.849)^2+\left(8.476/_2\right)^2}} = 9.35kA} \quad \textbf{(4.24-b)}$$

And, the operating time of the fast switch is determined from the relation in Equation 3.15.

$$\boldsymbol{\Longrightarrow \Delta t(time\ delay) = \frac{\rho c_p \Delta T_{max}}{E_{lim}{}^2}} \quad \textbf{(4.25-a)}$$

$$\boldsymbol{\Delta t = \frac{1.25\Omega m*10^{-6}*\frac{2.5J}{m^3K^0}*10^6*(400-77)K^0}{(145V/m)^2} = 48ms} \quad \textbf{(4.25-b)}$$

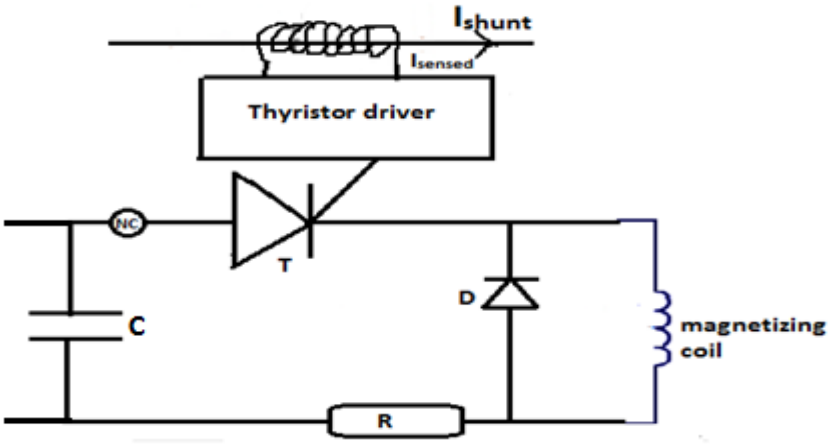

Figure 4-8: Control circuit of the fast switch

In Figure 4-8, controlling part of the fast switch is depicted how it would look like to be. When current develops to flow in the CLR line during fault occurrence in a line, a current sampling device such as a CT detects the current and makes a comparator in the driver to give HIGH output.

But this HIGH output of the comparator is connected to the pulse generator after a timer takes sufficient delay that is the superconductor material subjected to stay in limiting action; i.e. on Equation 4.25-b.

The thyristor (T) is ON, when it is fired with the driver pulse generator. Mostly, pulse generator acts according to gate which detects rising edge of the comparator.

The other components in the control circuit are DC power source (Capacitor), resistor and freewheeling diode. Where, NC is a normally series combination of all closed switch from the four outgoing/incoming line of the 400 kV busbar.

There is 400V rectified controlling DC power is already available in the substation to charge the capacitor when it is at the minimum voltage level. And, this voltage value is one of the basic design parameter of fast switch. The capacitor is needed to discharge large amount of current for fraction of seconds to actuate the switch coil with sufficient force.

To determine the power rating of the capacitance, the magnitude of current should be determined from relation of electro-magnetic-mechanical system. If the switch's electro-mechanical operation is shown as in Figure 4-9, the repulsion force created in the coil is related with opponent force due to inertia of the overall moving part (contact, magnetic disc and connecting rod), stiffness of spring (to restore the contact at NC state), and damping mechanism.

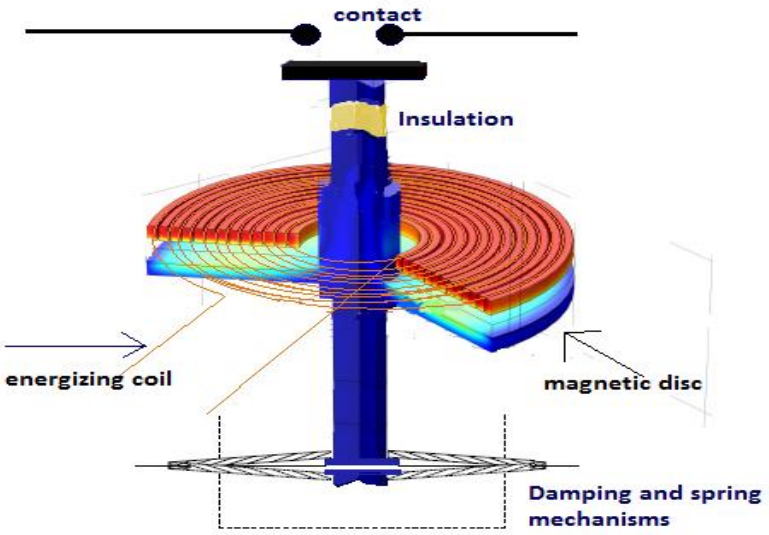

Figure 4-9: Electro mechanical part of the fast switch

The mechanical equation that describe this force will be

$$F = M\frac{d^2\chi}{dt} + B\frac{d\chi}{dt} + K\chi \quad \textbf{(4.26)}$$

Where; M – Is total mass of movable part.

It can reach up to 1kg for kA range current interruption in (4.24).

B – Is damping constant of mechanical holding system.

– I.e. 5N-s/m is enough for I_{SuC} in (4.24).

K – Is stiffness constant of spring.

– A spring with 500N/m would fit for I_{SuC} in (4.24).

X – Displacement of the moving part.

– 4mm separation is enough for medium voltage.

Rearranging Equation 4.26, its electrical analogy will give the following differential equations (ODE). [15]

$$0 = M\frac{d\dot{\chi}}{dt} + B\dot{\chi} + K\int\dot{\chi} - F \quad \textbf{(4.27-a)}$$

$$0 = L\frac{di}{dt} + Ri + \frac{1}{c}\int i - V \quad \textbf{(4.27-b)}$$

The voltage of the capacitor can be assumed constant due to large time gap comparing the capacitor discharging time and the fast switch separating duration. The solution function of the energizing current will be exponentially decaying sum of sine and cosine functions.

The boundary conditions are

- **i.** At the moment when the thyristor is about to connect, the flow of energizing current starts from zero value. I.e. $i(0^-) = 0$
- **ii.** When the magnetic force is able to disconnect the superconductor, it satisfies the ODE in Equation 4.27. (means at t=48s)

Finally, determined value of the maximum current flowing through the controlling circuit is not more than 8 A RMS. The overall components of the designed fast switch are shown in Appendix E with their specifications to afford from market.

4.3.4. The cooling system

The SFCL must be cooled to below the critical temperature of high temperature superconductor modules. In general, they are submerged in sub-cooled liquid nitrogen (LN_2) for their stable thermal characteristics.

The heat dissipation during the fault current-limiting process generates bubbles by vaporization of the liquid nitrogen, resulting in the deterioration of the electric insulation. The use of the sub-cooled LN2 at elevated pressure can suppress the generation of bubble and evade the occurrence of the cavitation in the cooling system.

The heat load of cryogenic system is relatively smaller than the available cooling capacity of cryo-cooler. This excessive cooling capacity can cause the frost of sub-cooled nitrogen at below the conduction cooling plate. But this freezing wouldn't be more expanded because of self-regulatory. Self-regulatory means that the frozen liquid nitrogen prevents the sub-cooled nitrogen from circulating the liquid nitrogen vessel and finally this effect will cause the advance on temperature of liquid nitrogen.

The heat produced by dissipation due to resistance of the superconductor during quenching is calculated as

$$P_{heat}(t) = I_{SC}(t)^2 * R_{SC}(t) \quad \textbf{(4.28)}$$

Using the experimental approximate for quenching resistance of the superconductor vs. time (milliseconds) in [6] as shown on Equation 4.29, the power dissipation will vary as the graph in Figure 4-11.

$$R_{SC}(t) = [e^{\frac{t}{110}} - 1]\ m\Omega/cm \quad \textbf{(4.29)}$$

For 721.76 meters of five superconductors in parallel,

$$R_{SC}(t) = \left[14.44e^{\frac{t}{110}} - 14.44\right]\ \Omega \quad \textbf{(4.30)}$$

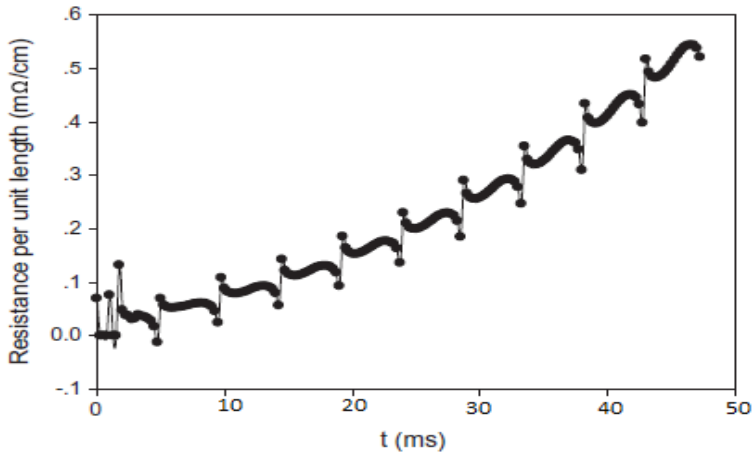

Figure 4-10: Resistance of YBCO material during quenching period with 77K^0-400K^0 temperature range [16]

The total resistance of SFCL will be as follow.

$$R_{SFCL}(t) = \frac{122.36e^{t/110} - 122.36}{14.44e^{t/110} - 5.96}\ \Omega \quad \textbf{(4.31)}$$

According to the resistor, SFCL SC current magnitude (versus milliseconds) varies as follow.

$$I_{SFCL}(t) = \frac{230\sqrt{\frac{2}{3}}}{\sqrt{(R_{SFCL}(t))^2 + 5.698^2}} sin(100\pi t + \alpha) kA \qquad \textbf{(4.32-a)}$$

$$\Rightarrow I_{SC}(t) = \frac{8.476}{R_{SC}(t) + 8.476} \times \frac{230\sqrt{\frac{2}{3}}}{\sqrt{(R_{SFCL}(t))^2 + 5.698^2}} sin\,(100\pi t + \alpha) kA \qquad \textbf{(4.32-b)}$$

If 'α' is selected equivalent to the system impedance angle (i.e. ≈89^0, almost reactive) so that the decaying exponential DC component is removed, it would be appropriate to design regarding symmetrical component magnitude, since the design is based on the regarding comparison of the CB symmetrical SC current breaking capacity.

This current dissipates heating power on the superconductor. Using the superconductor current and resistance time functions, the heating power dissipating on the superconductor can be drawn as shown below.

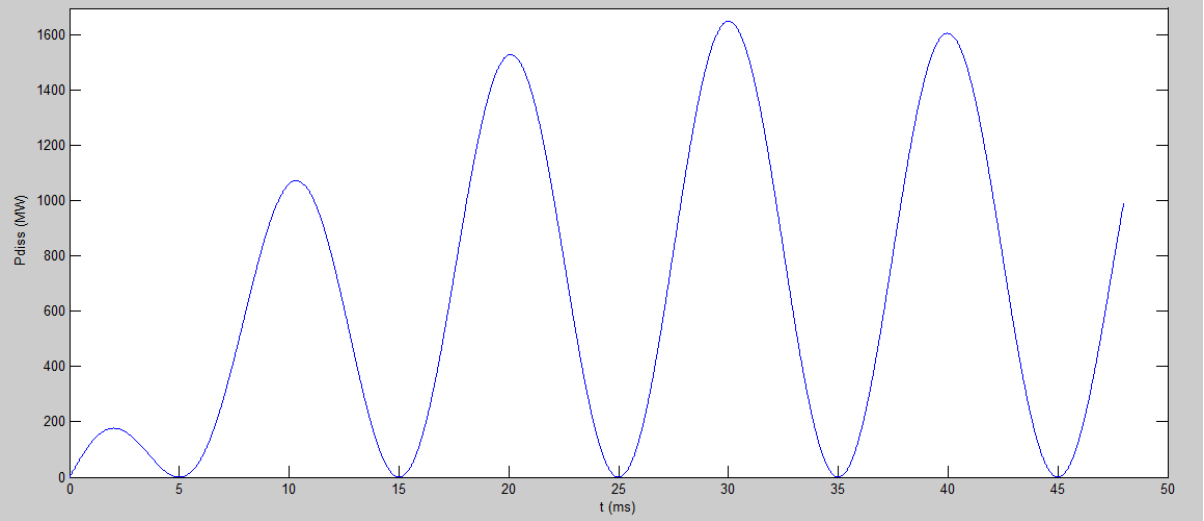

Figure 4-11: Heating power dissipated on the superconductor during quenching

The area of the above graph is total heat energy exerted on the superconductor during fault limiting. Therefore, this amount of energy should be removed by the cooling system. That is,

$$Q_{dissip} = \int_0^{t_{max}} P_{dissip}(t)dt \approx \sum_{\Delta t_{i=1}}^{\Delta t_{i=N}} P_{dissip}(t_i) = 30.73 MJ/phase \qquad \textbf{(4.33)}$$

The heat energy removed by the cooling system is given as the heat absorbed by LN_2.

$$\boldsymbol{Q_{cooling} = 30.73MJ = C_p \times \rho_d \times V \times \Delta T} \quad \textbf{(4.34)}$$

Where, C_p is the specific heat, ρ_d is the density, V is the volume, and ΔT is the difference of temperature of the sub-cooled nitrogen. The value of specific heat is 2,000 J Kg^{-1} K^{-1}, density is 860 Kg m^{-3}, is 223 K.

Therefore, the minimum amount of LN_2 required will be

$$\boldsymbol{V = \frac{30.73 \times 10^6}{2000 \times 860 \times 223} m^3 \approx 80\ liters/phase} \quad \textbf{(4.35)}$$

The cooler should cool away the heat energy received by the pressurized liquid nitrogen within required reclosing time for next fault occurrence. If this delay is taken to be even two minutes, the cooler will have the following power rating.

$$\boldsymbol{P_{cooling} = \frac{Q_{cooling}}{t_{recolsing}} = \frac{30.73MJ}{120s} = 256kW} \quad \textbf{(4.36)}$$

As the volume of cooling liquid nitrogen increases, the speed of heat transfer increases. So, the superconductor could achieve shorter recovery time. Extra volume of nitrogen liquid needs pumping to circulate to cool the superconductor. This pumping power is related with the volume of nitrogen and pressure requirement.

4.4. SC analysis with Superconductor Fault Current Limiter

Only the part of the SC current at busbar B, in Figure 4-5, coming from busbar A is going to be reduced by the SFCL. So, the SFCL model is going to be inserted between the busbar A and B through coupling line.

The linearly approximated relation of resistance increment of the superconductor with temperature given in Equation 3.17 is modelled using variable resistor as controlling input variable of temperature.

From Equation 4.18-a inserting the particular value and taking the length from Equation 4.19, resistance of the five superconductors in parallel during quenching will be as follow.

$$\boldsymbol{R_{SuC} = 0.0231T - 0.762\Omega} \quad \textbf{(4.37)}$$

From Equation 4.25, temperature can be arranged to be a function of time (ms),

$$\boldsymbol{T(t) = [77 + 6.73t]K^0} \quad \textbf{(4.38)}$$

Where, t is in ms and runs 0-48 to keep the superconductor below $400K^0$. The above equation is simulated Matlab/Simulink using a ramp time signal generator with 6728 slope and a constant with 77 magnitude so that the temperature goes up to $400K^0$; finally that are summed up together and fed to the controlling input of the variable resistance to have the property of superconductor quenching behavior as shown in Figure 4-12 circled part.

To introduce SC fault, a CB is used to shunt the equivalent load resistor and inductor into the ground. To analyze the result in terms of symmetrical maximum expected SC current criteria for the main CB of the line, the SC must be introduced at interruption angle (α) same as the impedance angle of the positive-sequence-network.

The solver for the circuit in Simscape models of Simulink is typically preferred to be one of ode23t, ode15s or ode14x (fixed-step). Otherwise, the simulation for half of a second takes a couple of days to give a single output. For this case, ode23t solver type is selected.

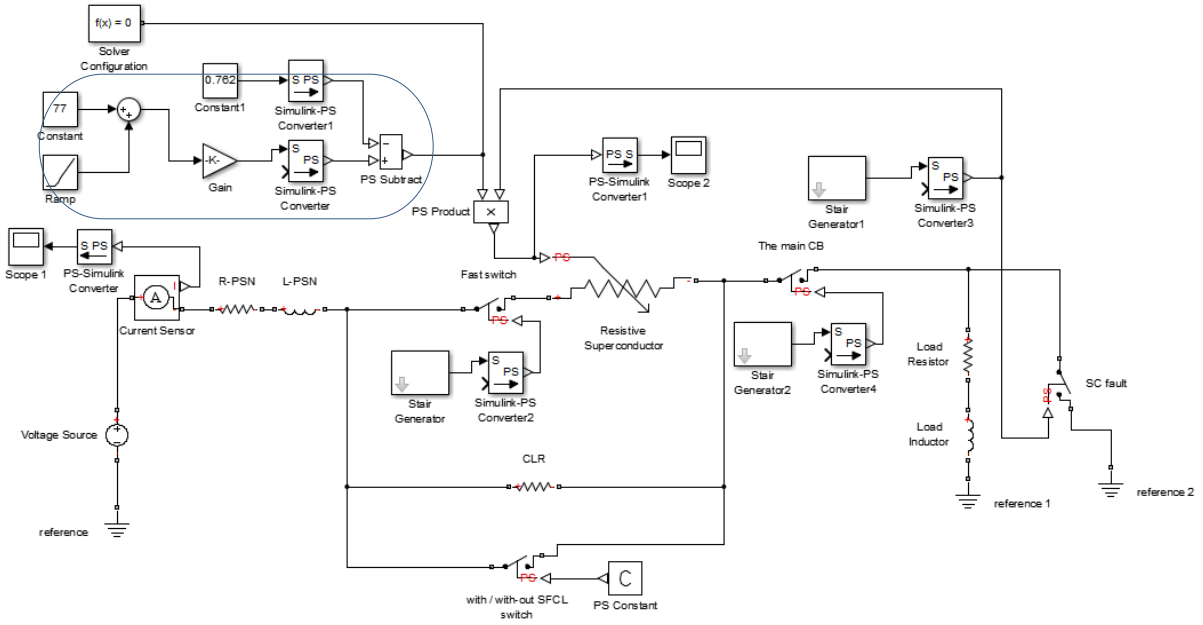

Figure 4-12: SC simulation with SFCL using Matlab

As it is seen from, Figure 4-12, Scope-2 shows the resistance value of variable resistor representing a superconductor. And, Scope-1 shows current in the circuit in normal load condition, fault condition and finally after the CB opens.

To simulate before and after using the SFCL, one can shunt using 'with/without' switch by the controlling constant, 'C'. This controller change the switch when it's constant is -1 or 1; because the threshold is 0. The results in **Figure 4-15** and **Figure 4-16** are obtained in this way.

4.5. Results and Discussions

4.5.1. SC analysis of the substation without superconductor fault current limiter

ETAP SC analyzer has its own result reporting feature. It produces report in PDF, MS Word and MS Excel formats. The following detail result is taken from ETAP SC result report manager. The results are based on ½ cycle SC analysis of the software to obtain sub-transient SC current under loaded condition.

Power Grid Input Data

Power Grid	Connected Bus	Rating		% Positive Seq. Impedance 100 MVA Base			Grounding	% Zero Seq. Impedance 100 MVA Base		
ID	ID	MVA sc	kV	X/R	R	X	Type	X/R	R0	X0
Holeta up comming line	Bus18	7929.691	400.000	14.96	0.08411	1.25828	Wye - Solid	4.59	3.696300	16.95950
Sodo II line 2	Bus1	3880.000	400.000	14.96	0.17190	2.57158	Wye - Solid	4.59	3.696300	16.95950
U1	Bus7	3316.689	230.000	204.46	0.01475	3.01502	Wye - Solid	121.15	0.139850	16.94300
U2	Bus4	6674.954	400.000	80.82	0.01854	1.49802	Wye - Solid	16.18	0.434770	7.03259
U4	Bus8	3316.689	230.000	204.46	0.01475	3.01502	Wye - Solid	121.15	0.139850	16.94299
U5	Bus10	1276.894	132.000	9.10	0.85575	7.78461	Wye - Solid	7.13	6.186471	44.08421
U6	Bus11	1244.947	230.000	14.61	0.54855	8.01372	Wye - Solid	1.99	16.374200	32.53700
U7	Bus14	1244.947	230.000	14.61	0.54855	8.01372	Wye - Solid	1.99	16.374180	32.53698
U9	Bus16	412.016	132.000	5.53	4.31679	23.88393	Wye - Solid	6.91	13.012900	89.88970
U10	Bus15	1276.894	132.000	9.10	0.85575	7.78461	Wye - Solid	7.13	6.186471	44.08421
U11	Bus35	322.472	132.000	9.10	3.38851	30.82476	Wye - Solid	7.13	6.186475	44.08424
U12	Bus19	1093.136	132.000	30.64	0.29841	9.14313	Wye - Solid	67.63	0.633260	42.82941
U13	Bus51	1093.136	132.000	30.64	0.29841	9.14313	Wye - Solid	67.63	0.633259	42.82930

Total Power Grids (= 13) 33082.465 MVA

(a) Parameters fed into the 'Power Grid' component to represent the feeders

Short-Circuit Summary Report

1/2 Cycle - 3-Phase, LG, LL, & LLG Fault Currents

Prefault Voltage = 100 % of the Bus Nominal Voltage

Bus		3-Phase Fault			Line-to-Ground Fault			Line-to-Line Fault			*Line-to-Line-to-Ground		
ID	kV	Real	Imag.	Mag.	Real	Imag.	Mag.	Real	Imag.	Mag.	Real	Imag.	Mag.
Fault1	400.00	1.361	-35.038	35.064	1.397	-14.647	14.713	30.343	1.179	30.366	-30.854	3.445	31.046
Fault2	400.00	1.361	-35.038	35.064	1.397	-14.647	14.713	30.343	1.179	30.366	-30.854	3.445	31.046
Fault3	400.00	1.361	-35.038	35.064	1.397	-14.647	14.713	30.343	1.179	30.366	-30.854	3.445	31.046
Fault4	230.00	1.029	-46.595	46.606	1.988	-23.539	23.623	40.352	0.891	40.362	-41.183	6.969	41.769
Fault5	230.00	1.029	-46.595	46.606	1.988	-23.539	23.623	40.352	0.891	40.362	-41.183	6.969	41.769
Fault6	230.00	1.029	-46.595	46.606	1.988	-23.539	23.623	40.352	0.891	40.362	-41.183	6.969	41.769
Fault7	230.00	1.029	-46.595	46.606	1.988	-23.539	23.623	40.352	0.891	40.362	-41.183	6.969	41.769
Fault8	132.00	2.055	-36.724	36.781	1.559	-23.362	23.414	31.804	1.780	31.853	-32.418	6.784	33.120
Fault9	132.00	2.055	-36.724	36.781	1.559	-23.362	23.414	31.804	1.780	31.853	-32.418	6.784	33.120
Fault10	132.00	2.055	-36.724	36.781	1.559	-23.362	23.414	31.804	1.780	31.853	-32.418	6.784	33.120
Fault11	132.00	2.055	-36.724	36.781	1.559	-23.362	23.414	31.804	1.780	31.853	-32.418	6.784	33.120
Fault12	132.00	2.055	-36.724	36.781	1.559	-23.362	23.414	31.804	1.780	31.853	-32.418	6.784	33.120
Fault13	132.00	2.055	-36.724	36.781	1.559	-23.362	23.414	31.804	1.780	31.853	-32.418	6.784	33.120
Fault14	132.00	2.055	-36.724	36.781	1.559	-23.362	23.414	31.804	1.780	31.853	-32.418	6.784	33.120

All fault currents are symmetrical momentary (1/2 Cycle network) values in rms kA

* LLG fault current is the larger of the two faulted line currents

(b)SC currents at each feeders

Short-Circuit Summary Report

Bus		Positive Sequence Imp. (ohm)			Negative Sequence Imp. (ohm)			Zero Sequence Imp. (ohm)		
ID	kV	Resistance	Reactance	Impedance	Resistance	Reactance	Impedance	Resistance	Reactance	Impedance
Fault1	400.000	0.25573	6.58128	6.58625	0.25573	6.58128	6.58625	3.95832	33.71359	33.94517
Fault2	400.000	0.25573	6.58128	6.58625	0.25573	6.58128	6.58625	3.95832	33.71359	33.94517
Fault3	400.000	0.25573	6.58128	6.58625	0.25573	6.58128	6.58625	3.95832	33.71359	33.94517
Fault4	230.000	0.06288	2.84852	2.84921	0.06288	2.84852	2.84921	1.29373	11.10707	11.18216
Fault5	230.000	0.06288	2.84852	2.84921	0.06288	2.84852	2.84921	1.29373	11.10707	11.18216
Fault6	230.000	0.06288	2.84852	2.84921	0.06288	2.84852	2.84921	1.29373	11.10707	11.18216
Fault7	230.000	0.06288	2.84852	2.84921	0.06288	2.84852	2.84921	1.29373	11.10707	11.18216
Fault8	132.000	0.11576	2.06876	2.07200	0.11576	2.06876	2.07200	0.41847	5.60569	5.62129
Fault9	132.000	0.11576	2.06876	2.07200	0.11576	2.06876	2.07200	0.41847	5.60569	5.62129
Fault10	132.000	0.11576	2.06876	2.07200	0.11576	2.06876	2.07200	0.41847	5.60569	5.62129
Fault11	132.000	0.11576	2.06876	2.07200	0.11576	2.06876	2.07200	0.41847	5.60569	5.62129
Fault12	132.000	0.11576	2.06876	2.07200	0.11576	2.06876	2.07200	0.41847	5.60569	5.62129
Fault13	132.000	0.11576	2.06876	2.07200	0.11576	2.06876	2.07200	0.41847	5.60569	5.62129
Fault14	132.000	0.11576	2.06876	2.07200	0.11576	2.06876	2.07200	0.41847	5.60569	5.62129

(c)Sequence network impedances calculated from each feeders

Figure 4-13: SC analysis report generated from ETAP for the substation

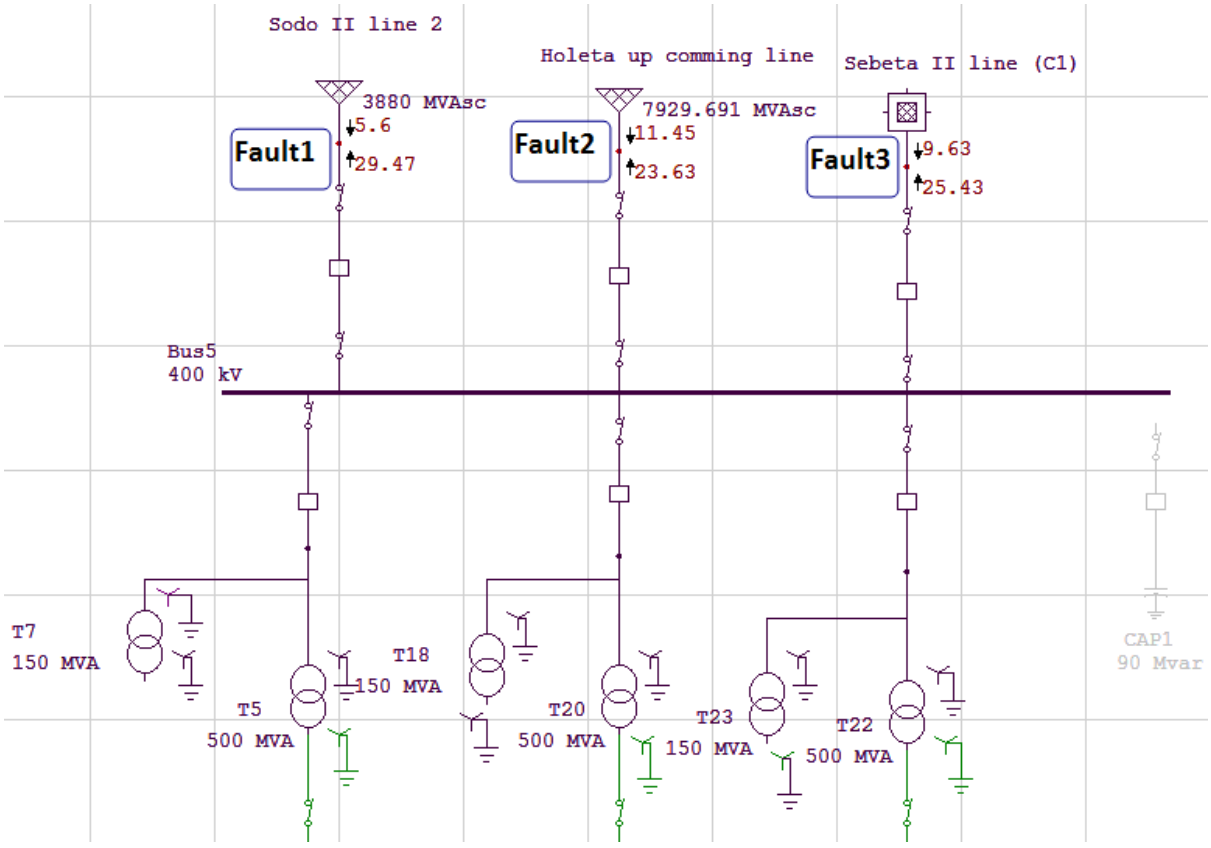

(a) 400kV feeders SC current

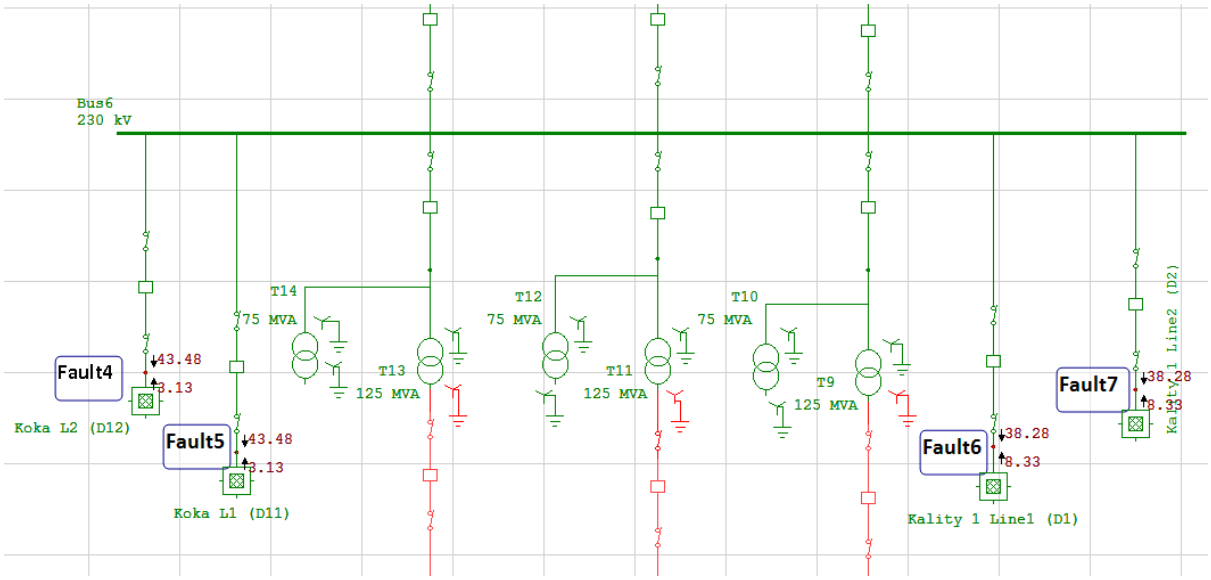

(b) 230kV feeders SC currents

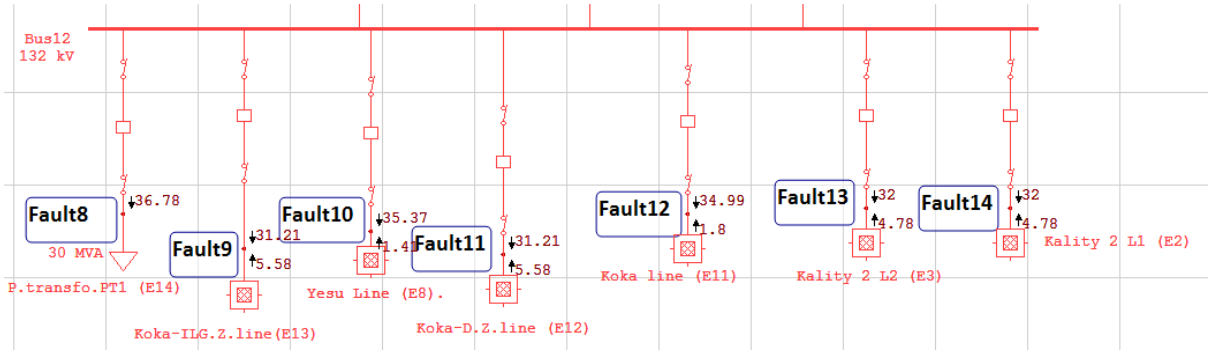

(c) 132kV feeders SC currents

Figure 4-14: The fault current distribution during fault at each feeder

In the SC analysis, all lines (feeders) of the substation are selected to be faulted. The results shown in Figure 4-13 & Figure 4-14 represent phenomena of fault at each feeder during different time. But, we can get the maximum SC current at each feeder simultaneously. In other word, if only one line (feeder) of the substation was selected to be faulted and SC analysis was taken, the same result would be obtained as the result shown in Figure 4-13 & Figure 4-14 for that particular line.

At the substation, besides the bas-bar coupler switch, there is left gap enough to install a bay as a reserve. This gap is around 20 meter wide per phase. To allocate this available space to install the SFCL, it can be compared with the volume of CLR (it's almost the total volume of the SFCL). Therefore, the CLR's volume on Equation 4.13-c can use 10 meter wide leaving the other free width for enough high voltage spacing; 20 m length and 1.8 m height.

4.5.2. SC analysis at 230kV bus-bar with the Superconductor fault current limiter

Figure 4-15 shows graph of SC current waveform in the case of no use of SFCL. The current has about 32 kA peak amplitude (or 22 kA RMS). This current will be reduced into 13 kA RMS current as shown in Figure 4-16 after using the designed SFCL.

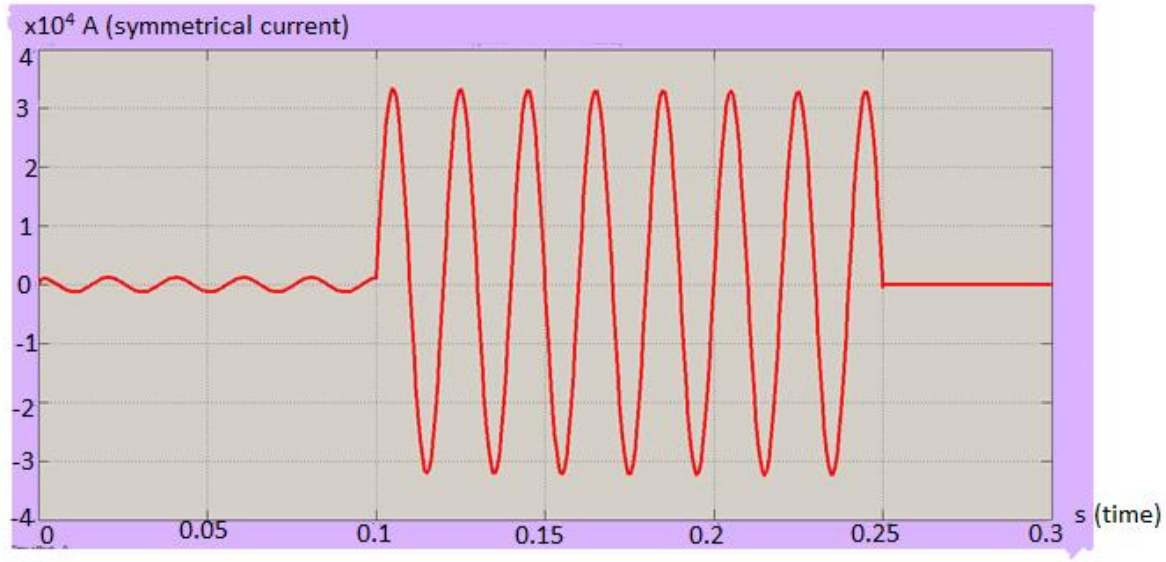

Figure 4-15: SC current contributed from busbar without SFCL

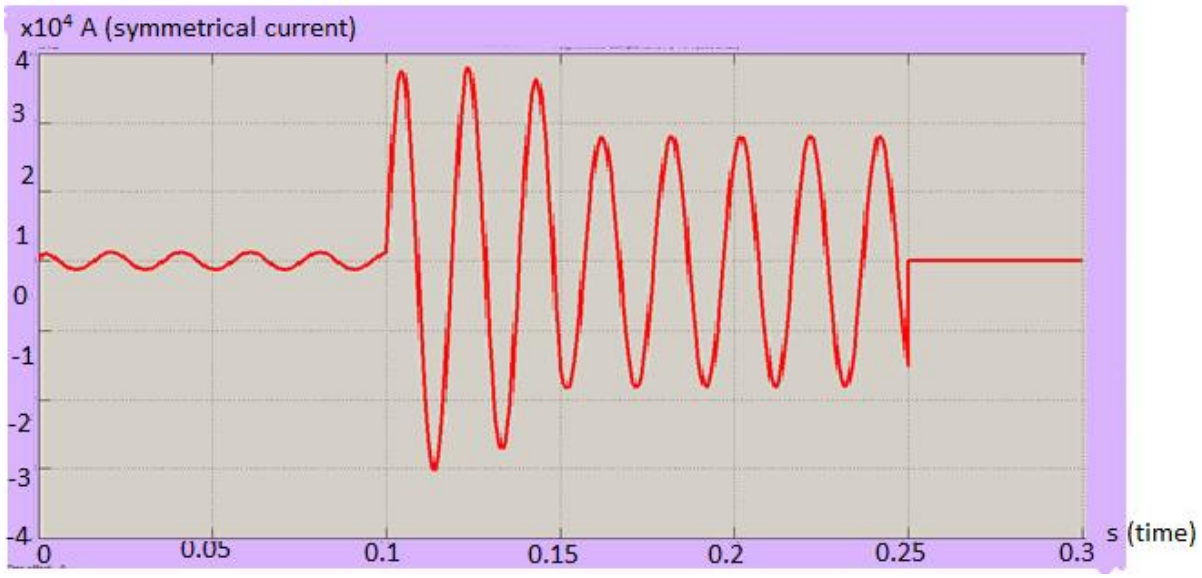

Figure 4-16: The reduced SC current without SFCL

In Figure 4-16, the first part of the graph (0 - 0.1s), it is normal load current of the 230 kV bus-bar. Assuming, the fault occurs at 0.1s, immediately the current rises. The response from 0.1s to 0.15s is the fault current under the limiting action of SFCL. During this time, the fast switch yet doesn't disconnect the superconductor. As the result, the limiting action is being done by the parallel combination of the rising superconductor's quenching resistance and the CLR. That is why it goes decreasing. But, when the fast switch disconnects the superconductor, the whole limiting action becomes by only the CLR. Therefore, it remains reduced to 13kA RMS value until the main CB breaks.

This means the total fault current at the bus-bar doesn't exceeds beyond 35 kA. Therefore, the CB will have 15kA safety margin from its breaking capacity. Due to the SFCL, the substation CB's safety margin with regarding its breaking capacity by reducing the maximum SC current from **44kA** to **35kA.** Therefore, the substation can integrate with other incoming line coming having **3585 MVA** from power generation site.

The fast switch designed for the SFCL disconnects the superconductor after two and half cycle of SC. So, if a nearby CB adjusted to operate after three cycles, it will face a maximum of 35 KA fault current. Practical the substation's CBs operate starting from three cycles, according to the magnitude of the SC current.

On Equation 4.25-c, time is very huge elapse for most fast switch to make separation of contacts. Ones their coil gets excited, they don't even take a millisecond to interrupt a line.

Therefore, after they detect superconductor branch current, there should be a timer or delay mechanism for the pulse generator to switch on the thyristor after fifty milliseconds, almost.

4.6. Cost Analysis of Implementing Superconductor Fault Current Limiter

Material cost per-phase to afford this SFCL system is the sum of cost of the superconductor material (≈$180,000) [17], cost of CLR (≈$144,200) [18], taking cost of 15 KA CB for electro-magnetic-mechanical part the fast switch $1,500 [19]. Adding the three main costs, the total cost of the SFCL will be around $320,000 per-phase.

With this cost, the substation is going to be able to break the maximum expected SC current after the power from GERD dam is integrated to the substation with around thirty percent safety margin.

Even though the total cost (based on current commercial) of superconductor project is above three fold times than that of conventional solution, the cost of 2G superconductor wire is already able to decrease from ≈$200/kA-m to $36/kA-m in R&D level [20]. The commercial cost increase with increment superconductor materials so that companies can yield in mass production.

The other important point should be noticed is that the SC rating of substations' continues to increase for sake of reliability, but the capacity of CBs' is limited. Therefore, it is inevitable to look other solution than the conventional methods. That is why, most recently, SFCL becomes the most primary preferable alternative method in the world.

5. CONCLUSIONS, RECOMMENDATIONS AND FUTURE WORK

5.1. Conclusions

In this thesis, the design and modeling of SFCL to increase the safety margin of high voltage substation CB by reducing maximum expected SC current has been attempted. It includes all works from SC capacity problem investigation up to the study of cost effectiveness and space requirement calculation. All the necessary data are collected to do SC analysis of the substation. Depending on the results of the SC analysis and with consideration of transient behavior of the system, the hybrid-resistive SFCL is designed.

The designing of the SFCL takes into account the determining of the rating of CLR, the rating and operation time of the fast switch, the size and rating of the superconductor material, and the cooling system to keep the superconductor at 77 K^0. After the design, commercially available appropriate components have been selected.

With the designed SFCL using Matlab/Simulink model, it has been observed that the maximum SC current of the substation is minimized at the 230 kV bas-bar of the substation, by limiting the maximum expected fault current from **44 kA** to **35 kA**. This means that the substation can be integrated to extra power coming from a generation having SC rating of **3585 MVA** at 50kA CB due to the insertion of the designed SFCL.

The question cost regarding implementation of SFCL is being addressed by improving the manufacturing process of superconductors in mega sale range. As the result, for future, application of SFCL increases throughout the world electrical power systems.

This work clearly and completely demonstrates SFCL designing steps and related concepts. Therefore, this document can be used as a guide to show overall SFCL design steps and procedures for academic or project purpose.

From the overall work, it can be concluded that a resistive-SFCL is a good solution to increase SC capacity of high-voltage substations. Especially, in a rapidly growing electric power system like that of Ethiopia, increasing SC capacity of substations enables us to increase capacity of power delivering and reliability by connecting a number of generation units in ring system.

5.2. Recommendations

It is recommended that Ethiopian Electric Power (EEP) may try to increase breaking capacity of substation CBs by using superconductor fault current limiters in series with CB rather than replacing the existing one as usual.

It is also recommended that reducing of blackout cases in Ethiopia can be incorporated with implementation of different types of SFCL.

5.3. Suggestions Future Work

1. The design and implementation of SFCL ma be investigated for the future power system of the Ethiopia by forecasting the generation growth and interconnection of the transmission lines of the country. So that the improvement can work for several years for the future.
2. The same objective of increasing of the safety margin of the CB may be investigated by minimizing the maximum SC current using different types of SFCLs, such as saturable-core transformer in substations.

References

[1] Y. Y. H. S. a. T. M. E. Calixte, "Theoretical expression of rate of rise of recovery voltage across a circuit," *EPRI,* vol. 75, pp. 1-8, 2005.

[2] B. C. P. Y. T. J. Y. J. K. S. E. Y. W. S. K. H. R. K. H. I. D. S. W. Yim, "Improvement in operational characteristics of KEPCO's," *Physica C,* vol. 484, pp. 267-271, 2013.

[3] N. K. Kiran V. Natkar, "Short Circuit Analysis of 220/132 KV Substation by Using ETAP," *International Journal of Advanced Technology in Engineering and Science,* vol. 4, no. 03, March 2016.

[4] J. Y. B. L. S.Lee, "Analysis Model Development and Specification Proposal of Hybrid Superconducting Fault Current Limitter (SFCL)," *Physica C,* vol. 470, pp. 1615-1620, 2010.

[5] A. S. E. I. A. a. G. M. B. Jennifer Kincaid, "Evaluating the Impact of Superconducting Fault Current Limiters on Distribution Network Protection Schemes," in *46th International Universities' Power Engineering Conference*, Soest,Germany, 2011.

[6] B. L. J. S. J. X. Z. Z. H. D. W. H. Z. X. S. a. C. S. J. Wen, "Maximum Permissible Voltage of YBCO Coated Conductor," *Physica C 501,* pp. 14-15, 2014.

[7] N. Tleis, "Power Systems Modelling and Fault Analysis: Theory and Practice," Elsevier Ltd., 2008, pp. 43-60, 230-242.

[8] "Fault Current Limiters-Basic Concept and Associated Technologies," EPRI EL-6275, 1989.

[9] A. B. Pascal Tixador, "Superconducting Fault Current Limiter optimized design," *Physica C,* vol. 518, pp. 130-133, 2015.

[10] P. Alto, "Superconducting Fault Current Limiters: Technology Watch," EPRI, CA: 2009.1017793.

[11] Palo Alto, "Superconducting Power Equipment: Technology Watch 2012," EPRI, CA: 2012.1024190.

[12] *ETAP 12.6 User Guide, Operation Technology Inc.,* March 2014.

[13] S. P. Fedasyuk D., "Simulation of Superconducting Fault Current Limiter Behavior in Matlab/Simulink," in *Proceedings of the International Conference on Computer Science and Information Technologies*, Ukraine, 2006.

[14] T. B. A. R. Alexander Usoskin, "Long-length YBCO coated conductors," in *ICEC/ICMC Conference*, Invited talk, WA4, ID 293, Jul 8,2014.

[15] H.-Y. Yao, "Design and Analysis of A Recoil-Type Vibrotactile Transducer," *Acoustical Society of America),* no. paris, 2010.

[16] *2G Wire Spec Sheet,* Newyork, USA: SuperPower, Furukawa Electric Group, 2014.

[17] "YChart," AMS, [Online]. Available: https://ycharts.com/companies/AMSC?__hstc=753710.a0ee106c024a0d5d95d50a0222e6e54b.1496613543924.1496613543924.1496613543924.1&__hssc=753710.1.1496613543925&__hsfp=2412431773..

[18] "Alibaba.com," [Online]. Available: https://www.alibaba.com/product-detail/High-Quality-100K-ohm-20KW-Ceramic_60326476074.html. . [Accessed 2016 December 26].

[19] Ethiopian Electric Power (EEP) and Shanghai Electric Group, *Contract agreement and equipment specification for Gellan (Akaki II) substation construction,* 2011.

[20] V. Selvamanickam, *Recent Advances in HT Superconductor and Application,* Housten: university of Houston, 2014.

[21] "Data sheet: DR Wirewood Power Resistor," ZENITHSUN RESISTOR, 2007.

[22] "China-made-in.com," Yueqing Heyi Electrical Co., Ltd., [Online]. Available: http://chendechina.en.made-in-china.com/product/IeCnBcGVlOpw/China-Power-Capacitor-Single-Phase-440V-15kvar-50Hz-60Hz-Cylinder-Type-CE-Certificate.html. [Accessed October 2016].

[23] Datasheet of Power thyristors, Semicondctor Components Industries LLL., January, 2015.

[24] K. A. S. K. S. Meenu Kanwar, "Comparison of Simulation Tools ATP-EMTP and MATLABSimulink," *IJRSCSE,* vol. 1, no. 3, pp. 50-56, July 2014.

Appendix A

Hybrid Resistive Versus Saturable-Core Superconductor Fault Current Limiter

Table A-1: Detail Comparison of Hybrid Resistive and Saturable-Core SFCL [9]

Specification	**Superlimiter™**	**SI-SFCL**
Type	Resistive SFCL module	Inductive SFCL using saturable-core transformer
Operating voltage	138 kV	220 kV
Rated current	1.2 kA	800 A
Expected fault current	63 kA	50 kA
Current limiting capacity	~37%	~40%
Limiting action delay	Less than 1 cycle	Immediate
Max limiting duration	As long as required, can limit continuously	Limited: until the temperature of SFCL transformer reaches the max rating.
Peak max voltage drop	Unavailable	<1.25%
Let-through current	40 kA	30 kA
Recovery time	15s	<500msec
HTS material	YBCO fault current limiting tape	unavailable
HTS operating temperature	71-72 K^0	unavailable
Size	8m long by 3m diameter per phase	8x8x9 m^3
Weight	40,000 Kg per phase (including the cooling system)	120 ton

Appendix B

Important Specifications of the Substation's Components

Table B-1: Some specifications of single phase 166.67 MVA, [(400/√3)/ (230/√3)] kV Autotransformer of the substation [19]

Description	**Specification**
Manufacturer	China
Type	Auto-Transformer
Standards applied	IEC 76
Method of cooling	ONAN/ONAF/OFAF
Number of phases	Single
Rated voltage	
a) 400KV winding, kV	400
b) 230KV winding, kV	230
c) Stabilizing winding, kV	15
Rated continuous power on all taps at OFAF (Max, rating)	
a) 400KV winding, 1-phase rated power, MVA	166.67
b) 230KV winding, 1-phase rated power, MVA	166.67
c) Stabilizing winding, 1-phase rated power, MVA	50
Voltage regulation by on-load taps changer on 400 kV winding,	±8 taps @1%
Number of tap positions of on load tap changer	17
Vector group (connection symbol)	YNa0 + d
No-load losses at rated voltage, frequency and, kW	
Load losses at maximum tap position and @ ONAN base, kW	≈60
Load losses at nominal tap position and @ ONAN base, kW	≈63
Load losses at minimum tap position and @ ONAN base, kW	≈70
No-load current at nominal tap position @ ONAN base:	
a) At 90% voltage, % of rated current	<0.12
b) At 100% voltage, % of rated current	<0.2

c) At 110% voltage, % of rated current	<1.2
Content of harmonics current at 100% rated voltage	
a) 3rd harmonics, % of no-load current	40-50
b) 5th harmonics, % of no-load current	10-25
c) 7th harmonics, % of no-load current	5-10
Voltage drop at 75 ^{0}C for maximum tap position at ONAN, %	≈6.4∟90^0
Voltage drop at 75 ^{0}C for nominal tap position at ONAN, %	≈6.5∟90^0
Voltage at drop 75 ^{0}C for minimum tap position at ONAN, %	≈6.7∟90^0
RMS SC current withstand for 3 sec, kA	
a) At 400kV terminal, kA	≈5.77
b) At 230 kV terminal, kA	≈10.04
Weights:	
a) Core and windings, kg	≈74500
b) Oil, kg	≈54600
c) Tank without heat exchanger, kg	≈7000
Total weight of transformer with oil and including all accessories, Kg	≈180100

Table B-2: Some specifications of three phase 125 MVA, 230/132 KV Autotransformer of the substation [19]

Description	**Specification**
Manufacturer	Arstom China
Type	Auto-Transformer
Standards applied	IEC 60076.1-2000
Method of cooling	ONAN/ONAF/OFAF
Number of phases	Three
Rated voltage	
a) 230kV winding, kV	230
b) 132kV winding, kV	132
c) Stabilizing winding, kV	15
Rated continuous power on all taps at OFAF (Max, rating)	

a) 230kV winding, 1-phase rated power, MVA	125
b) 132kV winding, 1-phase rated power, MVA	125
c) Stabilizing winding, 1-phase rated power, MVA	75
Voltage regulation by on-load taps changer on 230 kV winding, range (%)	±10 taps @1%
Number of tap positions of on load tap changer	21
Vector group (connection symbol)	YNaO + d11
No-load losses at rated voltage, frequency and at nominal tap position, kW	28.63
Load losses at maximum tap position and @ ONAN base, KW	249
Load losses at nominal tap position and @ ONAN base, KW	272.6
Load losses at minimum tap position and @ ONAN base, KW	313.8
No-load current at nominal tap position as percent of rated current @ ONAN base and 100% voltage, %	<0.35
Content of noise level as percent of no-load current at 100% rated voltage	70 dB(A)
Impedance voltage at 75 ^{0}C for maximum tap position at OFAF, %	11.43
Impedance voltage at 75 ^{0}C for nominal tap position at OFAF, %	11.92
Impedance voltage at 75 ^{0}C for minimum tap position at OFAF, %	12.46
RMS SC current withstand for 3 sec, kA	
a) At 230kV terminal, kA	3.01
b) At 132 kV terminal, kA	5.24
Weights:	
Active part, Kg	≈46500
Oil, Kg	≈38100
Tank, Kg	≈17500
Total weight of transformer with oil and including all accessories, Kg	≈1258000

Table B-3: Three phase power transformer 132KV/15KV, 125MVA of the substation [19]

Description	**Specification**
Manufacturer	Arstom China
Type	SFZ -50000/132
Standards applied	IEC 60076.1-2000
Method of cooling	ONAN/ONAF
Three phase rating, MVA	50
Rated voltage	
a) Primary winding, kV	132
b) Secondary winding, KV	15
Voltage regulation by on-load taps changer on 230 KV winding, range (%)	±10 taps @1%
Number of tap positions of on load tap changer	21
Vector group (connection symbol)	YN + d11
No-load losses at rated V, frequency and at nominal tap, kW	24.6
Load losses at maximum tap position and @ ONAN base, kW	226.3
Load losses at nominal tap position and @ ONAN base, kW	191.4
Load losses at minimum tap position and @ ONAN base, kW	191.2
No-load I at nominal tap @ ONAN base and 100% voltage, %	0.06
noise level	63
Impedance voltage at 75 ^{0}C for maximum tap position at OFAF, %	10.51
Impedance voltage at 75 ^{0}C for nominal tap position at OFAF, %	10.88
Impedance voltage at 75 ^{0}C for minimum tap position at OFAF, %	11.34
RMS SC current withstand for 3 sec, kA	
c) At 400kV terminal, kA	
d) At 230 kV terminal, kA	
Weights:	
Oil, Kg	≈13000
Tank, Kg	≈3900
Total weight of transformer with oil and including all accessories, Kg	≈62000

Table B-4: Some specifications of 400kV circuit breakers of the substation [19]

	Line bay	**Transformer bay**
Manufacturer	China	China
Type	Three chambers (vertical mover)	Three chambers (vertical mover)
Installation	Outdoor	Outdoor
Rated voltage (kV)	400	400
Maximum system voltage (kV)	420	420
Rated nominal current, (kA)	4	4
Rated frequency (Hz)	50	50
Rated operating sequence	O-0.3s-CO-3min-CO	O-0.3s-CO-3min-CO
Rated SC withstand current:		
a) 1 second, kA RMS	63	63
b) 3 second, kA RMS	50	50
Rated SC breaking current		
a) Symmetrical, kA RMS	63	63
Rated SC making current, kA peak	≥80	≥80
Rated lightning impulse withstand voltage, kV		
a) To earth	1450	1450
b) Across open contact	1450+400	1450+400
Rated switching impulse withstand voltage		
a) To earth, kV	1050	1050
b) Across open contact, kV	900+345	900+345
Power frequency withstand voltage, 1min, kV		
a) To earth	520	520
b) Across open contact	610	610
Standard applied	IEC 60056	IEC 60056

Table B-5: Some specifications of 230kV circuit breakers of the substation [19]

	Line bay	**Transformer and reactor bays**
Manufacturer	China	China
Type	Three chambers (vertical mover)	Three chambers (vertical mover)
Installation	Outdoor	Outdoor
Rated voltage (kV)	230	230
Maximum system voltage (kV)	245	245
Rated nominal current, (kA)	≥3.15	3.15
Rated frequency (Hz)	50	50
Rated operating sequence	O-0.3s-CO-3min-CO	O-0.3s-CO-3min-CO
Rated short time withstand current:		
c) 1 second, kA RMS	40	40
a) 3 second, kA RMS	31.5	31.5
Rated SC breaking current		
a) Symmetrical, kA RMS	50	50
Rated SC making current, kA peak	≥80	≥80
Rated lightning impulse withstand voltage, kV		
a) To earth	1050	1050
b) Across open contact	1200	1200
Power frequency withstand voltage, 1min, kV		
a) To earth	460	460
b) Across open contact	530	530
Standard applied	IEC 60056	IEC 60056

Table B-6: Some specifications of 132kV circuit breakers of the substation [19]

	Bus-bar bay
Manufacturer	China
Type	3pole live tank
Model	LW25-145
Installation	Outdoor
Rated voltage (kV)	≥132
Maximum system voltage (kV)	145
Rated nominal current, (KA)	3.15
Rated frequency (Hz)	50
Rated operating sequence	O-0.3s-CO-3min-CO
Rated short time withstand current:	
d) 1 second, kA RMS	40
b) 3 second, kA RMS	31.5
Rated SC breaking current	
b) Symmetrical, kA RMS	50
Rated SC making current, kA peak	≥80
Rated lightning impulse withstand voltage, kV	
c) To earth	650
d) Across open contact	750
Power frequency withstand voltage, 1min, kV	
c) To earth	275
d) Across open contact	325
Operating time from trip contact to primary contact separation (microsecond)	≤60
Interrupting time (opening time plus maximum arc interrupting time) (microsecond)	≤30
Closing time from moment the coil becomes energized to	≤100
Rated TRV at 100% rated SC breaking current (kV)	145
Weight of breaker (Kg)	1400
Standard applied	IEC 60056

Table B-7: Some specifications of 400kV disconnectors of the substation [19]

	Line bay	**Busbar bay**
Manufacturer	China	China
Type	Pantograph	Pantograph
Installation	Outdoor	Outdoor
Rated voltage (kV)	400	400
Maximum system voltage (kV)	420	420
Rated nominal current, (kA)	3.15	3.15
Rated frequency (Hz)	50	50
Rated operating sequence	O-0.3s-CO-3min-CO	O-0.3s-CO-3min-CO
Rated short time withstand current:		
a) 1 second, KA RMS	50	50
b) 3 second, KA RMS	≥40	≥40
Grounding blades peak current (kA)	≥80	≥80
Rated lightning impulse withstand voltage, KV		
a) To earth	1425	1425
b) Across open contact	1425+240	1425+240
Rated switching impulse withstand voltage		
a) To earth, kV	1050	1050
b) Across open contact, kV	900 +345	900 +345
Power frequency withstand voltage, 1min, kV		
a) To earth	520	520
b) Across open contact	610	610
Standard applied	IEC 60129	IEC 60129

Table B-8: Some specifications of 230kV disconnectors of the substation [19]

	Line bay
Manufacturer	China
Type	
Installation	Outdoor
Rated voltage (kV)	230
Maximum system voltage (kV)	245
Rated nominal current, (kA)	≥1.25
Rated frequency (Hz)	50
Rated short time withstand current:	
a) 1 second, kA RMS	40
b) 3 second, kA RMS	≥31.5
Rated lightning impulse withstand voltage, kV	
a) To earth	1050
b) Across open contact	1200
Power frequency withstand voltage, 1min, kV	
a) To earth	460
b) Across open contact	530
Standard applied	IEC 60129

Table B-9: Some specifications of 132kV disconnectors of the substation [19]

	Bus-bar bay
Manufacturer	China
Type	Center break
Model	GW4-145
Installation	Outdoor
Rated voltage (kV)	132
Maximum system voltage (kV)	145
Rated nominal current, (kA)	2
Rated frequency (Hz)	50
Rated short time withstand current:	

a) 1 second, kA RMS	40
b) 3 second, kA RMS	31.5
Grounding blades peak current (kA)	50
Rated lightning impulse withstand voltage, kV	
a) To earth	650
b) Across open contact	750
Power frequency withstand voltage, 1min, kV	
a) To earth	275
b) Across open contact	315
Weight of breaker (Kg)	300
Standard applied	IEC 60129

Table B-10: Some specifications of 400KV lightning arrestors of the substation [19]

Description	**Specification**
Place of manufacture	China
Model	ZnO, gapless
Installation	Outdoor
System nominal voltage (kV)	400
System continuous max. voltage (kV)	420
Rated voltage of arrestor, Ur, (kV)	342 (since, it is per-phase)
TOV capability: for 1 second, kV RMS	411
For 10 second, KV RMS	394
Power frequency withstand voltage, 1min, KV	630
Impulse voltage (1.2/50 microsecond) (KV)	1425
Rated discharge current (kA)	20
Max. discharge current (kA)	≥40
Overall weight (Kg)	1020
Standard applied	IEC 600994

Table B-11: Some specifications of 230kV and 132kV lightning arrestors of the substation [19]

	230kV	**132kV**
Place of manufacture	China	
Model		ZnO, gapless
Installation	Outdoor	Outdoor
System nominal voltage (kV)	230	132
System continuous max. voltage (kV)	245	145
Rated voltage of arrestor, Ur, (kV)	198	120
TOV capability: for 1 second, kV RMS	≥228	≥138
For 10 second, kV RMS	≥214	≥130
Power frequency withstand voltage, 1min, kV	≥460	315
Impulse voltage (1.2/50 microsecond) (kV)	1050	650
Rated discharge current (kA)	10	10
Max. discharge current (KA)	≥40	≥40
Overall weight (Kg)		175
Standard applied	IEC 600994	IEC 600994

Table B-12: Some specifications of YN-connected shunt reactor used for Sodo incoming line into the substation for MVAR compensation [19]

Description	Specification
Manufacture	China
Type	BKS-90000/550
Standards applied	IEC
Installation	Outdoor
Rated voltage (kV)	500
Method of cooling	ONAN
Number of phases	Three
Frequency, Hz	50
Rated power, MVAR	90
Load losses at 75 c^0 and rated voltage, KW	240

Flux density at rated conditions, W/mm^2	1.33
Lightning impulse test voltage of winding, full wave 1.2/50 µs	1425
switching impulse test voltage of winding, full wave 1.2/50 µs	1050
Power frequency withstand voltage of winding 1 min, KV	570
Noise level at rated conditions (distance of 3m), dB	<75

Table B-13: Some specifications of MVAR compensation unit capacitor in the substation at 400kV-busbar [19]

Description	**Specification**
Manufacturer	China/Cooper
Type	EX-TL
Standards	IEC 60871-1&2
Unit capacitor	
a) Rated voltage, V	15155
b) Rated reactive output power, kVAr	517 leading
c) Frequency, Hz	50
d) Rated capacitance, µF	7.17
e) Actual capacitance, µF	7.22
f) Number of elements connected in series and/or parallel per unit capacitor	Series 8/Parallel 2
Number of unit capacitors in a bank (per phase)	64
Connection	YN (neutral point is grounded)

Appendix C

Commercially Available YBCO CC Superconductors

Table D- 1: SuperPower® 2G HTS Wire Specifications [16]

	Minimum Ic measured by continuous direct current	Width	Total Wire Thickness	Critical Axial Tensil Strain at 77K	Critical Bend Diameter in Tension (40µm) @ room temp	Critical Bend Diameter in Compression (40µm) @ room temp
SF = Stabilizer Free *(standard 2µm of silver)*						
SF2050	50 amp	2 mm	0.055 mm	0.45%	11 mm	11 mm
SF3050	75 amp	3 mm	0.055 mm	0.45%	11 mm	11 mm
SF4050	100 amp	4 mm	0.055 mm	0.45%	11 mm	11 mm
SF6050	150 amp	6 mm	0.055 mm	0.45%	11 mm	11 mm
SF12050	300 amp	12 mm	0.055 mm	0.45%	11 mm	11 mm
SF12100*	300 amp	12 mm	0.105 mm	0.40%	25 mm	25 mm
SCS = Surround Copper Stabilizer *(standard 2µm of silver and 40µm of copper; critical tensile stress of >550MPa at 77K)*						
SCS2050	50 amp	2 mm	0.1 mm	0.45%	11 mm	11 mm
SCS3050	75 amp	3 mm	0.1 mm	0.45%	11 mm	11 mm
SCS4050	100 amp	4 mm	0.1 mm	0.45%	11 mm	11 mm
SCS6050	150 amp	6 mm	0.1 mm	0.45%	11 mm	11 mm
SCS12050	300 amp	12 mm	0.1 mm	0.45%	11 mm	11 mm

* 2G HTS wire type SF12100 with highly resistive substrate, flexibility in wire stabilization options and very tight currentuniformity is suitable for fault current limiter (FCL) applications.

Table C- 2: SF12100 detail specifications [16]

Dimension (L x W)	10mx12mm
Critical current (I_c)	300A
Cost ($/m)	100
$E_{lim.}$ (V/m)	145
ρ (superconducting state)	1.25mΩ-m
$E_{cond.}$ (mm)	285
T_{max}	750K^0 recommended less than 400K^0
C_p (specific heat per unit volume)	2.5 $MJ/m^3/K^0$
α	0.004
R_{SC} (quenching resistance)	0.4mΩ/cm at 283K^0
Substrate	Hastelloy

Appendix D

Selected Commercially Available Power Resistor

Table D- 1: A 20kW ZENITHSUN RESISTOR's DR series wire-wound power resistors (China top resistors) [21]

Description		**Specification**
Made of		A tubular ceramic wound with copper wire
Application		Educational modeling, load testing, industrial electric power distribution, UPS, …
Short time overload		1000% rated power, 5sec
Temperature coefficient		±350PPM/^{0}c
Insulation resistance		100MΩ
Dielectric withstanding voltage		1000 V DC for 1 minute
Humidity		40 ^{0}c 90% RH 240 hours
Continuous current capacity		1-100A
Cost		20*
Dimension (mm)	D	150
	L1	1000
	L2	1040
	L3	1120
	h	100
	H	260
	N	30
	d	8
	q	10
	Q	152

***** The price is obtained from Alibaba.com, on 26-Dec-16, https://www.alibaba.com/product-detail/High-Quality-100K-ohm-20KW-Ceramic_60326476074.html.

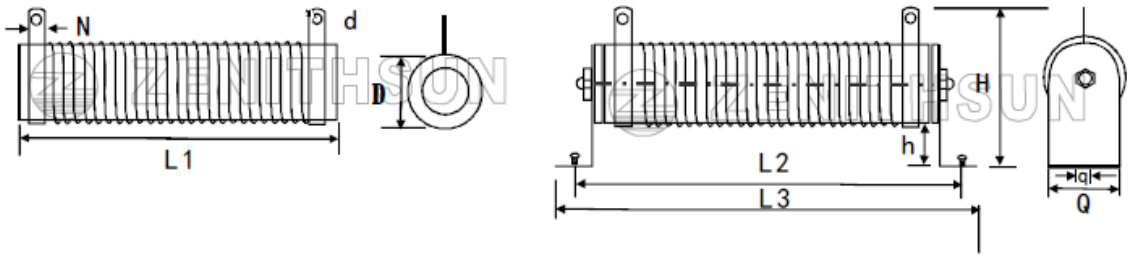

(a) Different dimensions expressing the physical appearance of the resistor

(b) Photo of the resistor

Figure D- 1: 20kW Power Resistor produced by China Company [21]

Appendix E

Some Components of the Fast Switch

Table E- 1: Power capacitor [22]

Description	Specification
Manufacturer	Yueqing Heyi Electrical Co., Ltd. Zhejiang, China
Model No.	BSMJ0.3KVAR-1
Type	Polypropylene Capacitor
Electrolyte	Air Medium
Phase	Single Phase
Voltage Rating	440V
Price	15USD

Table E- 2: Power Thyristor [23]

Description	Specification
Identification no.	MCR72-6
Rated Average On-State Current	8A
Type	SCR
Repetitive non-peak reverse voltage	100A
Peak non-repetitive surge current	1490A
Forward peak gate voltage	±5V
Forward peak gate current	1A
Price	5USD

Appendix F

A Matlab Code to Calculate Power Dissipation on the Superconductor

```
>> t=0:0.01:48;% to integrate with 0.01 ms resolution
for i=1:4801
Rsc(i)=14.44*exp(t(i)/110)-14.44;
end
for i=1:4801
Rsfcl(i)=8.4764*Rsc(i)/(8.4764+Rsc(i));
end
for i=1:4801
Isfcl(i)=(230*sqrt(2/3))/sqrt(5.698^2+(Rsfcl(i))^2)*sin(0.1*pi*t(i)+1.57);
% 0.1 is 2*frequency(50)/1000(since t is in ms) and 1.57rad = ~89degree
end
for i=1:4801
Isc(i)=Isfcl(i)*8.4764/(8.4764+Rsc(i));
end
for i=1:4801
Pdissip(i)=Isc(i)*Isc(i)*Rsc(i);
end
>> plot(t,Pdissip)
Qfinal=0;
for i=1:4801
Qprevious=Qfinal;
Qiteration=0.01*Pdissip(i);% integration with 0.01 ms resolution (energy in Mega Watt-ms)
Qfinal=Qprevious+Qiteration;
end
Qdissip=Qfinal;
Qfinal=Qdissip/1000;% energy in Mega Joule
>> Qfinal
```